Cucurbit[8]uril Assisted Vesicle Formation by Viologen Amphiphiles: A Systematic Analysis and Application

by

Julfikar Hassan Mondal

Department of Chemistry
Indian Institute of Technology Guwahati
Guwahati, Assam, 781039
India

A Thesis Submitted in Partial Fulfillment of the Requirements for the degree of

Doctor of Philosophy
In
Chemistry

IIT Guwahati, January 2015

Dedication

To my parents, brother and my sisters

Declaration

I hereby declare that the matter embodied in this thesis is result of investigations carried out by me in the Department of Chemistry, Indian Institute of Technology Guwahati, India under the guidance of Dr. Debapratim Das. In keeping with the general practice of reporting scientific observations, due acknowledgements have been made wherever the work described is based on the findings of other investigators.

Julfikar Hassan Mondal

भारतीय प्रौद्योगिकी संस्थान गुवाहाटी
INDIAN INSTITUTE OF TECHNOLOGY GUWAHATI

Dr. Debapratim Das
Assistant Professor
Department of Chemistry
Ph: + 91 361 258 3301
Fax: + 91 361 258 2349
E-mail: ddas@iitg.ernet.in

14th January, 2015.

To whom it may concern

This is to certify that the thesis entitled **"Cucurbit[8]uril Assisted Vesicle Formation by Viologen Amphiphiles: A Systematic Analysis and Application"** submitted by Julfikar Hassan Mondal (Roll No. 11612217) for the award of PhD degree to IIT Guwahati, is absolutely based on his own research work and that neither this thesis nor any part of it has been submitted for any degree/diploma or any academic award anywhere before.

(Dr. Debapratim Das)

Contents

Abstract

This thesis entitled "**Cucurbit[8]uril Assisted Vesicle Formation by Viologen Amphiphiles: A Systematic Analysis and Application"** deals primarily with supramolecular host-guest chemistry based on Cucurbit[8]uril. The research has been focused on the understanding of self-assembly of viologen amphiphiles in absence and presence of Cucurbit[8]uril and construction of stimuli sensitive self-assembled system.

Chapter 1 is a brief introduction to the Cucurbituril host family, its discovery, synthesis and host-guest interaction with viologen amphiphiles, an up to date review on this field along with brief introduction to the present thesis.

Chapter 2 describes the different physicochemical parameters of a viologen surfactant DDEV in pure and mixed state with three tetraalkylammonium bromide surfactants. The molar ratio varied from 0-100% and we found that doping of 1% DDEV does not imparts any change in the physicochemical parameters of Tetraalkylammonium bromide surfactants.

Chapter 3 is the extension of previous chapter. Here we have shown how Mutual Sharing of Properties of Individual Surfactants in the 1% DDEV Doped Systems occurs to construct vesicle and w/o-microemulsion which is not possible in absence of one.

Chapter 4 describes the mechanism of micelle to vesicle transformation by viologen amphiphiles in presence of Cucurbit[8]uril and DHN. In this chapter we have also shown two types of self-sorting parallely occurs during the transformation.

Chapter 5 describes the vesicle formation ability of different amino acids in presence of Cucurbit[8]uril and DHN. We have developed supramolecular peptide amphiphile which eventually transformed to vesicle. Lastly we have shown its multi-stimuli responsiveness.

Acknowledgements

First, I would start with thanking God for all the blessings that have been given to me, like having the most supportive and loving people around me. One of them is my supervisor Dr. Debapratim Das. He is one of the most kind, supportive, patient and helpful supervisor that I ever had. It is an honour to be one of his group members. Moreover, I would like to give my special thanks to my committee members: Prof. Gopal Das, Dr. Bhubaneswar Mondal, and Dr. Lal Mohan Kundu for their supports and suggestions.

I will never be able to thank my parents Imdadul Haque Mondal and Hasina Bagum enough for all the love, encouragement, help, guidance and prayers that they provided me. You have always been there for me. To my brother and sisters, thank you for helping, guiding, and supporting me.

I would like to thank IIT Guwahati and Department of Chemistry for financial support and all the facilities that were made available to me. I thank CIF, IIT Guwahati for providing the instrumental facility.

I must thank my lab mates Sahnawaz, Titli, Bapan and Nilotpal for their help and support and also sincere thanks to my seniors, friends and other research scholars in the department, especially Dr. Ziyauddin Khan, Md. Palashuddin Sheikh, Ashim Paul, Sukhamoy Gorai, Sameer Hussain, Samir Gorai, Prasenjit Barman, Anup Bhunia, Hridesh Agarwal, Surajit Ghosh, Sanat Ghosh, Jaydeb Mandal, Md. Belal and Md. Ashraful Haque.

I would like to thank all others who are associated with my work directly or indirectly at IIT Guwahati for their help.

LIST OF ABBREVIATIONS

ABBREVIATIONS

A_{min}	Minimum area per molecule at the air/solution interface at the CMC
Azo-AA	4-((4-aminophenyl)diazenyl)benzoic acid
CDs	Cyclodextrins
CB[*n*]	Cucurbit[*n*]uril
CV	Cyclic Voltametry
CF	5-(6)-carboxyfluorescein
CT	charge transfer
CMC	critical micelle concentration
DDEV	N-ethyl-N'-dodecylviologen dibromide
DTAB	Dodecyltrimethylammonium bromide
DTEAB	Dodecyltriethylammonium bromide
DTPAB	Dodecyltripropylammonium bromide
DEV	Diethylviologen
DOSY	Diffusion Ordered Spectroscopy
DHN	2,6-dihydroxy naphthalene
ESI-MS	Electrospray ionization-mass spectrometry
FESEM	Field Emission Scanning Electron Microscope
Gly	Glycine
ΔG_m^0	Standard Gibbs free energy, enthalpy, entropy of micellization, respectively
ΔH_m^0	
ΔS_m^0	
ΔG_{ad}^0	Standard Gibbs free energy of adsorption
HLB	Hydrophilic-lipophilic balance
ITC	Isothermal Tritration Calorimetry
MV^{2+}	Dimethylviologen dication
K_a	Association constant
κ	Specific Conductance
MWCNT	Multiwall carbon nanotube
N_A	Avogadro's number
n	Aggregation number of a surfactant micelle
π_{CMC}	CMC surface pressure at the CMC
Phe	Phenylalanine
SPA	Supramolecular peptide amphiphile
TEM	Transmission Electron Microscopy
Tyr	Tyrosine
Trp	Tryptophan
Γ_{max}^{tot}	Maximum surface excess at the air/solution interface at CMC
TMV	N-Tetradecyl-N'-methylviologen
T	absolute temperature in kelvins
w/o	Water-in-Oil
Xcmc	CMC expressed in mole fraction unit
W_0	water-to-surfactant mole ratio
γ	surface tension at the air/solution interface

CHAPTER 1

Introduction

1.1 Prelude

Though the existence of intermolecular forces was first proposed by Johannes Diderik van der Waals in 1873,[1] it was Emil Fischer, who developed the philosophical roots of supramolecular chemistry in 1894 by postulating the famous "lock and key" model for enzyme-substrate interactions.[2] The essential principles of molecular recognition and host-guest chemistry was thus introduced. The use of these principles eventually paved the way to a growing understanding of protein structure and other biological processes. The milestone breakthrough about the elucidation of the double helical structure of DNA occurred with the realization of the involvement of hydrogen bonds between two separate strands of nucleotides.[3] Concurrently, chemists began to recognize and study synthetic structures based on non-covalent interactions, such as micelles and microemulsions.

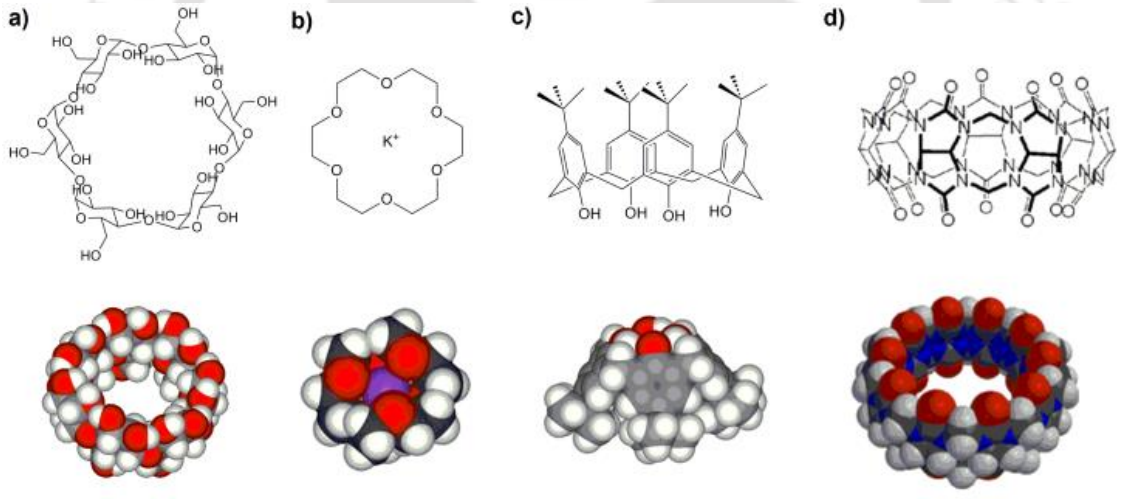

Figure 1.1 Various supramolecular hosts and their 3D arrangements: a) α-cyclodextrin; b) 18-Crown-6-ether with potassium ion; c) calixarene; d) cucurbit[7]uril.

In the long run, chemists were able to take the concepts of non-covalent bonding and utilize them to synthetic systems. Charles J. Pedersen provided the breakthrough in the 1960s with the synthesis of the crown ethers (Figure 1.1).[4] The crown ethers were the first of its kind, macrocyclic synthetic hosts, capable of incorporating guests through non-covalent bonding. Active research began toward synthesizing shape- and ion-selective receptors, and throughout the 1980s research in this area gathered a rapid

pace with emerging concepts such as mechanically-interlocked molecular architectures.[5-7] This era produced several macrocyclic structures like cryptands, synthetic hosts, rotaxanes, pseudorotaxanes *etc.* It was Jean-Marie Lehn who finally provided a name to this rapidly expanding area of research, "Supramolecular Chemistry".[7,8] Over the years, supramolecular chemistry and especially the host-guest chemistry have grown as an independent sub-branch of chemistry.

1.2 Cucurbiturils

1.2.1 Brief History, and Synthesis

The present thesis is primarily based on the host-guest chemistry of Cucurbituril with amphiphiles. Here is a brief introduction about the origin of the work described in this thesis.

Supramolecular chemists have designed, synthesized, and appraised the recognition properties of a wide variety of macrocyclic hosts. These include cyclodextrins, calixarenes, cyclophanes, crown ethers, and many others that display remarkable affinity and selectivity.[9–11] Among the common synthetic receptors, commercial availability and low cost of cyclodextrins (CDs, Figure 1.1) made them the receptor of choice for industrial applications. However, several limitations arising from their low affinity and low selectivity also exist. To this end, as a potential replacement for the cyclodextrins and other known supramolecular hosts, a new family of host molecules emerged, cucurbit[*n*]uril (CB[*n*]).[12-14] The association constants (K_a) of their host–guest complexes are typically several orders of magnitude higher than those of CDs in aqueous systems.[12,13] The highest K_a recorded so far is 3×10^{15} M^{-1} for CB[7] binding with ferrocene derivatives, reaching that of the well known avidin–biotin complex.[15]

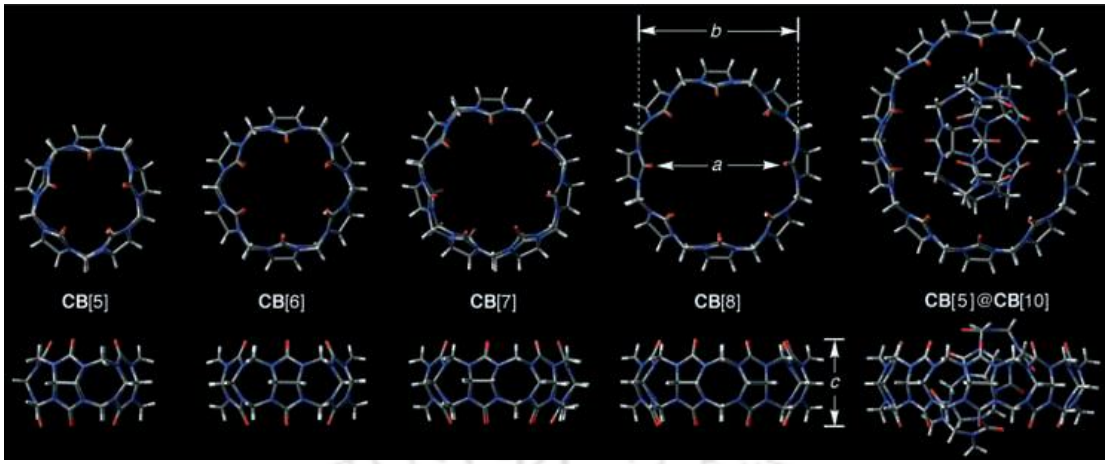

Figure 1.2 Top and side views of the X-ray crystal structures of CB[5], CB[6], CB[7], CB[8], and CB[5]@CB[10].The various compounds are drawn to scale (taken from ref. 12)

Mock et al. in 1981, first confirmed the macrocyclic structure of CB[6] (Figure 1.2) consisting of six glycoluril units and twelve methylene bridges and named it "cucurbituril" owing to its resemblance of a pumpkin, a prominent member of the *Cucurbitaceae* family.[16] It was synthesized (Figure 1.3) following a report first published by Behrend[17] in 1905 using condensation reaction of glycoluril and formaldehyde in concentrated hydrochloric acid. The research groups of Kim and Day, almost two decades later, performed the same reaction under milder and kinetically controlled conditions and reported the crystal structures of three other members of the cucurbituril family (CB[5,7,8]).[18,19] The crystal structure of CB[10] was reported by Day et al. in 2002 (as the CB[5]@CB[10] complex)[20] and in 2005 by Isaacs et al. (cucurbit[5]uril-free CB[10]),[21] whereas those of CB[9] and CB[11] are yet to be isolated.

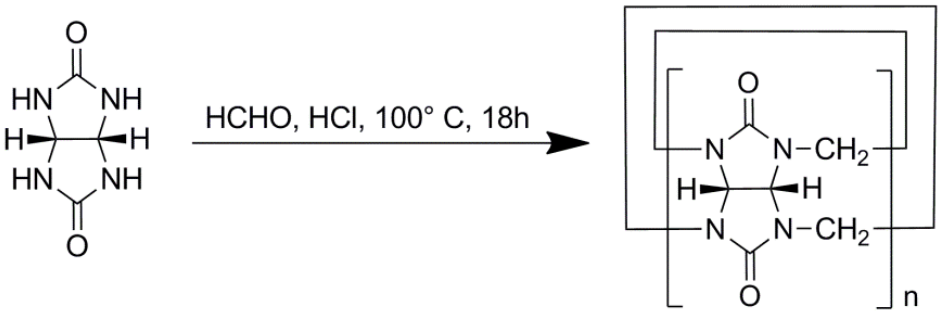

Figure 1.3 Synthesis of CB[*n*].

1.2.2 Properties

The pumpkin shaped CB[*n*] are cyclic methylene-bridged glycoluril oligomers. The X-ray crystal structures of different members of CB[*n*] are shown in Figure 1.2.[12] Like cyclodextrins, the various CB[*n*] have a common depth (*c*) (9.1 Å), while their equatorial widths (*b*) , annular widths (*a*), and cavity volumes vary systematically with increasing number of glycoluril units present (Table 1.1). The portals, constituted with carbonyl groups are narrower than the cavity by ~ 2 Å resulting in constrictive binding that produces significant steric barriers to guest association and dissociation.[12,22-25] The portals are hydrophilic in nature while the interior of the cavity is hydrophobic.

Although the structural rigidity and excellent thermal stability (Table 1.1)[13,23] make CB[*n*] a better choice over CDs as a host, the major limitation for CB[*n*] comes from their poor solubility in aqueous medium. CB[6] and CB[8] are essentially insoluble, whereas CB[5] and CB[7] possess modest solubility in water (Table 1.1).[12,13,22] The solubility of CB[5]–CB[8] noticeably increases in concentrated aqueous acid (e.g., 61 mM for CB[6] in HCO_2H/H_2O (1:1), about 60 mM for CB[5], about 700 mM for CB[7], and about 1.5 mM for CB[8] in 3M HCl).[26-28]

Table 1.1 Dimensions and physical properties of CB[*n*]

CB[*n*]	M_r	*a*[Å][a]	*b*[Å][a]	*c*[Å][a]	V [Å^3]	S_{H_2O} [mM]	Stability [° C]	pK_a
CB[5]	830	2.4[13]	4.4[13]	9.1[13]	82[13]	20-30[13]	>420[13]	
CB[6]	996	3.9[13]	5.8[13]	9.1[13]	164[13]	0.018[22]	425[23]	3.02[24]
CB[7]	1163	5.4[13]	7.3[13]	9.1[13]	279[13]	20-30[13]	370[13]	
CB[8]	1329	6.9[13]	8.8[13]	9.1[13]	479[13]	<0.01[13]	>420[13]	
CB[10][b]	1661	9.0-11.0	10.7-12.6	9.1	-	-	-	-

[a] The values quoted for *a, b,* and *c* for CB[*n*] take into account the van der Walls radii of the relevant atoms. [b] Determined from the X-ray structure of the CB[5]@CB[10] complex.[20]

It is worth mentioning that CB[*n*] are remarkably inert both *in vitro* and *in vivo*. The IC_{50} value of CB[7] toward Chinese hamster ovary CHO-K1 cells after 48 h is determined as 0.53 mM.[29] Concentrations as high as 1.0 mM were found viable at shorter incubation time (3 h) and no cytotoxic effects were detected at concentrations of 0.5 mM or less. CB[7] is also inert at 1.0 mM towards human kidney HEK293, human hepatocyte HepG2 and murine macrophage RAW264.7 cells after 48 h of incubation as

estimated by Fedin and co-workers.[30] A similar result was obtained with CB[5]. Similar inert behaviour was also observed in various other mammalian and human cell lines.[31] Oral doses of 600 mg/kg of equimolar mixture of CB[7] and CB[8] also showed no adverse effect.[29] Owing to the poor solubility of CB[8], monitoring the toxicity is more problematic yet, at 20 μM, no sign of *in vitro* toxicity was observed.

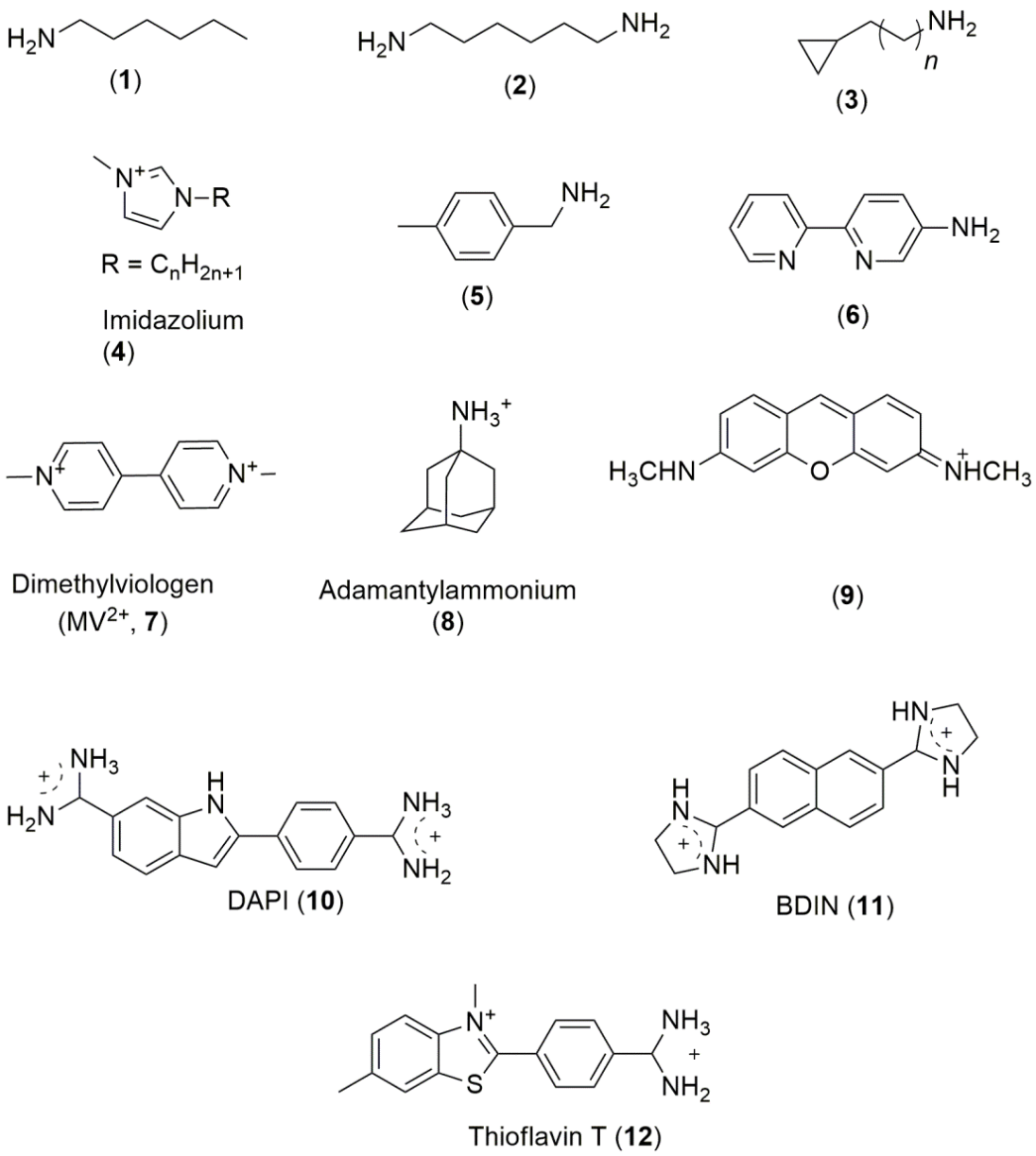

Figure 1.4 Various types of charged organic species as guests for CB[6] and CB[7].

1.2.3 Host-Guest Chemistry of CB[5], CB[6] and CB[7]

The rigid hydrophobic cavity and two hydrophilic portals make CB[*n*] an interesting host for a plethora of molecules. Some excellent reviews covering all the different types of molecules tested as probable guests for CB[*n*] are available in literature.[12-14,32-34] CB[5] can encapsulate small molecules such as N_2 in the cavity and binds cations such as NH_4^+ and Pb^{2+} strongly at the portals. Two NH_4^+ ions can completely seal both the openings of CB[5].[13,24,35-37] Though the interest in studying the higher analogues are increasing, CB[6] is still studied on account of its economical and simpler synthesis and purification. Despite the resemblance to α-cyclodextrin (α-CD) in terms of cavity size, its highly symmetrical structure with two identical openings and a vastly different electronic structure distinguish CB[6] from α-CD.

The binding of CB[*n*] with different guest molecules primarily occur involving two different supramolecular interactions, ion-dipole interaction at the portal region as well as hydrophobic interaction inside the cavity. The rigidity of CB[*n*] and the close proximation of two binding regions that favour positively charged groups.[12,13] Among the various types of guests studied for binding with CB[*n*], positively charged organic species were found to be most preferred.[12] CB[6] forms especially stable complexes with protonated diaminoalkanes ($^+NH_3(CH_2)_nNH_3^+$, n = 4-7, $K_a > 10^5$ M^{-1}, Figure 1.4) while protonated aromatic amines such as *p*-methylbenzylamine ($K_a \sim 3 \times 10^2$ M^{-1}) binds with CB[6] relatively lesser affinity.[13] CB[6] has the ability to encapsulate neutral molecules such as tetrahydrofuran, Xe, diethylether, and benzene in aqueous solution.[12,13] CB[6] is also able to bind alkali-metal, alkaline-earth, transition-metal, and lanthanide cations in homogenous solution.[13,14,24,35-39] On the other hand, CB[7] forms complexes with larger guest molecules like, 2,6-bis(4,5-dihydro-1*H*-imidazol-2-yl)naphthalene (BDIN, **11,** Figure 1.4).[13] It binds protonated adamantylamine (**8**, Figure 1.4) as well as methyl viologen dication (*N*,*N*'-dimethyl-4,4'- bipyridinium, MV^{2+}, **7**, Figure 1.4) in a 1:1 ratio.[13] Neutral molecules such as ferrocene and carborane get easily encapsulated in CB[7] in aqueous solution. K_a recorded for ferrocene@CB[7] is 3×10^{15} M^{-1}.[40] A variety of dyes, ionic liquids, neurotransmitters etc. also form inclusion complexes with CB[6] and CB[7]. Apart from all these guests mentioned above, plenty

of other guests were found to bind with CB[6] and CB[7]. It is beyond the limit of this thesis to include all the examples. For comprehensive accounts, see the Cucurbituril special edition of Israel Journal of Chemistry, 2011, pp 487-678 and reviews therein.

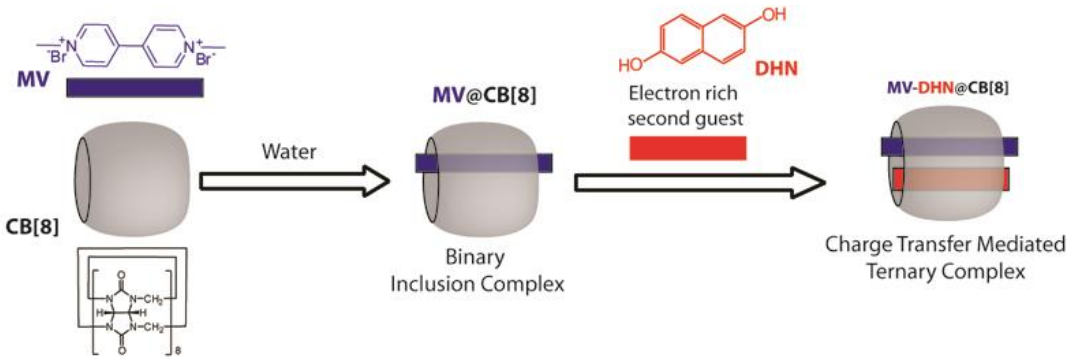

Figure 1.5 Pictorical presentation of the formation of MV-DHN@CB[8] ternary complex.

1.2.4 Host-Guest Chemistry of CB[8]: The Ternary Complexation

The smaller analogues of CB family can bind only one guest inside the cavity whereas the larger analogue, CB[8] can host two guests inside and that makes it unique among all the various synthetic hosts available. The larger cavity volume of CB[8] (Table 1.1) compared to the smaller analogues of CB[*n*], can provide enough space to accommodate two guests inside the hydrophobic cavity.[12] For example, it can include two BDIN molecules to form a 1:2 complex.[13] Similarly, the one electron reduction product of MV^{2+} i.e., the monocation radical $MV^{+\cdot}$ can form a 2:1 ternary complex with CB[8].[41] The dimerization constant of $MV^{+\cdot}$ in the presence of equimolar CB[8] is estimated to be 2×10^7 M^{-1}, which is about 10^5 times higher than that of $MV^{+\cdot}$ alone in aqueous media.

In one of their path-breaking works, Kim et al. have shown the ability of CB[8] to form hetero ternary complexes.[42] Typically an electron deficient acceptor molecule like MV^{2+} binds to CB[8] as the first guest as shown in Figure 1.5. Upon addition of an electron rich donor, 2,6-dihydroxy naphthalene (DHN), the binary complex MV@CB[8] incorporates DHN through charge transfer (CT) complexation and forms a ternary complex, MV-DHN@CB[8] (Figure 1.5). The ternary complexation can be studied using UV-visible spectroscopy by tracing the appearance of a CT band as well as by the formation of an intense color (Figure 1.6). Further analysis can be done using

Isothermal Titration Calorimetry (ITC), NMR and fluorescence spectroscopy as well as by ESI-MS. The solution binding constant for this ternary complexation was observed to be $5.9 \times 10^5\ M^{-1}$.[43]

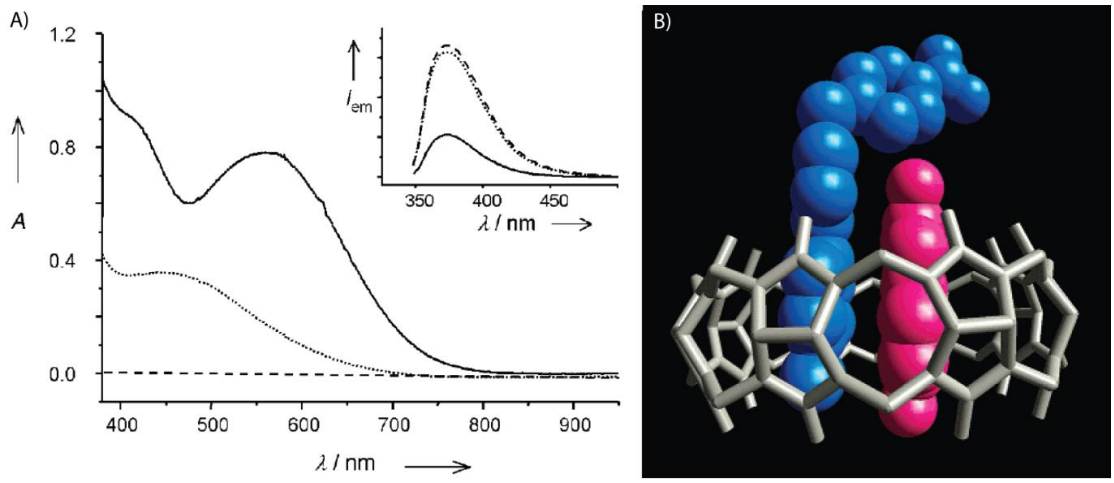

Figure 1.6 (A) Absorption and emission (inset) spectra obtained in H_2O of DHN (dashed line), a 1:1 mixture of DHN and MV. (dotted line), and DHN-MV@CB[8] (solid line). (B) Crystal structure of 1:1:1 complex of DHN(magenta)-a MV containing molecule (blue)-CB[8](magenta).[42]

A detailed study involving 32 probable second guests for MV@CB[8] by Scherman et al. showed a wide range of binding constants from 10^2 to $10^6\ M^{-1}$ (Figure 1.7). Both solution phase ITC and gas phase ESI-MS measurements were applied for the study and hydrophobic aromatic compounds were found to be the best guests for this system in solution but polar electron-rich aromatic compounds with multiple functionalities bound most strongly in the ESI-MS experiments. When free energies of solvation were taken into account, an excellent agreement between solution-based titrations and gas-phase studies was found.[43] In separate studies, Kim et al. and Urbach et al. have shown that aromatic amino acids like, tryptophan, tyrosine, and phenylalanine can also form such ternary complexes with tryptophan showing the highest affinity.[44,45] Interestingly, peptides containing N-terminal tryptophan were found to be binding more strongly than peptides with tryptophan at any other position.[45] Peptides with the N-terminal sequences like Trp-Gly-Gly and Phe-Gly-Gly could form dimers inside the CB[8] cavity.[46]

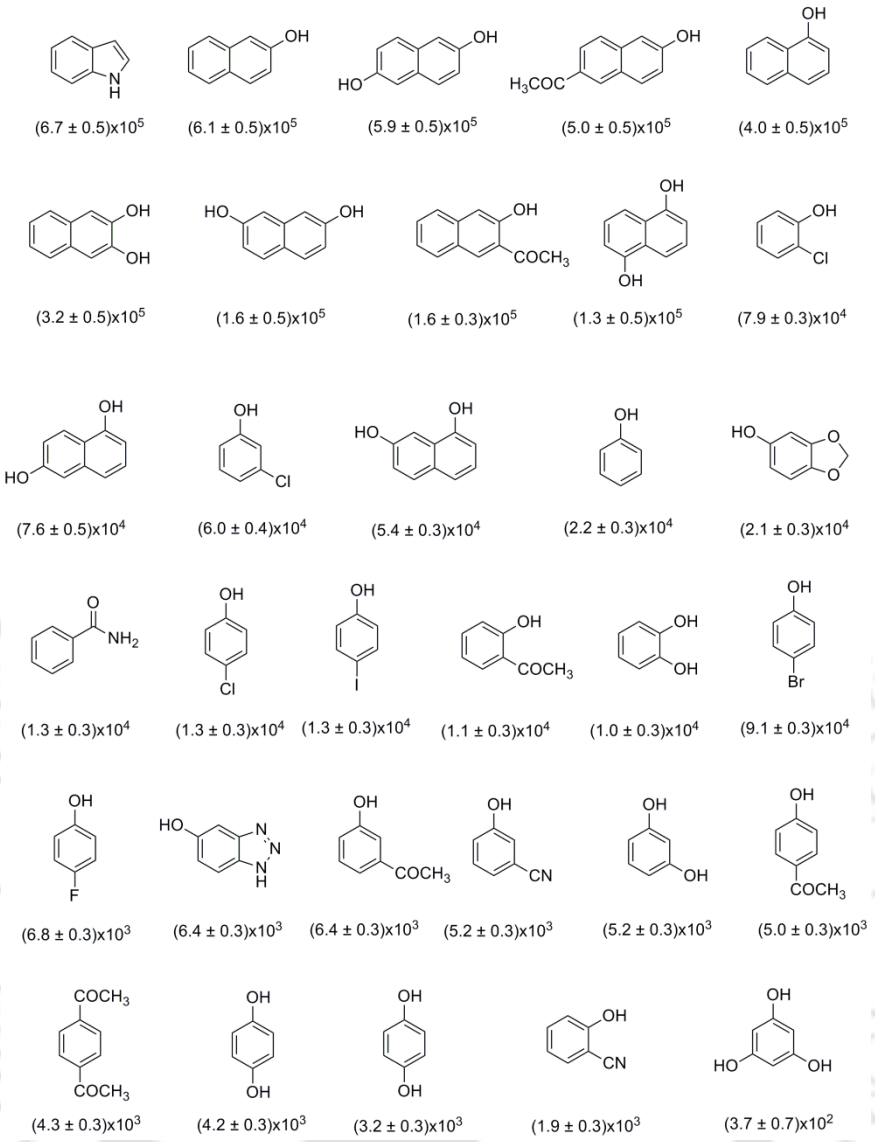

Figure 1.7 Chemical structures of the aromatic guests in decreasing order of their solution binding constants (ITC) in water (K_a values given in M^{-1})[43]

This unique characteristic of CB[8] has been extensively exploited as a "molecular handcuff" to prepare various kinds of soft-materials. Brunsveld et al. have demonstrated protein-dimerization[47,48] using ternary complexation of CB[8] while Scherman et al. have prepared protein-polymer conjugates utilizing the same technique.[49] Two different polymers were supramolecularly conjugated using the ternary complexation to create a linear polymer (Figure 1.8).[50] The same mechanism was also used to prepare crosslinked polymer using two different polymeric units

containing pendant first and second guests for CB[8].[51] The naphthalene–MV@CB[8] complexation was also exploited in preparing polymer-nanoparticle conjugates[52] as well as multistimuli responsive polymeric nanocontainer.[53] The ternary complexation by N-terminal tryptophan residue was used for sensing and separation of peptides from a mixture of peptides.[54] Recently Scherman et al. have also shown the preparation of light responsive hybrid raspberry like colloids.[55] In another context, the ternary complexation was exploited by Sivaguru et. al. where the 1:2 complex of CB[8] with coumarine was used for selective *syn* or *anti* cycloaddition and CB[8] acted as a nano- reaction container.[56] A comprehensive review on the application of the ternary complexation can be found in ref. 57.

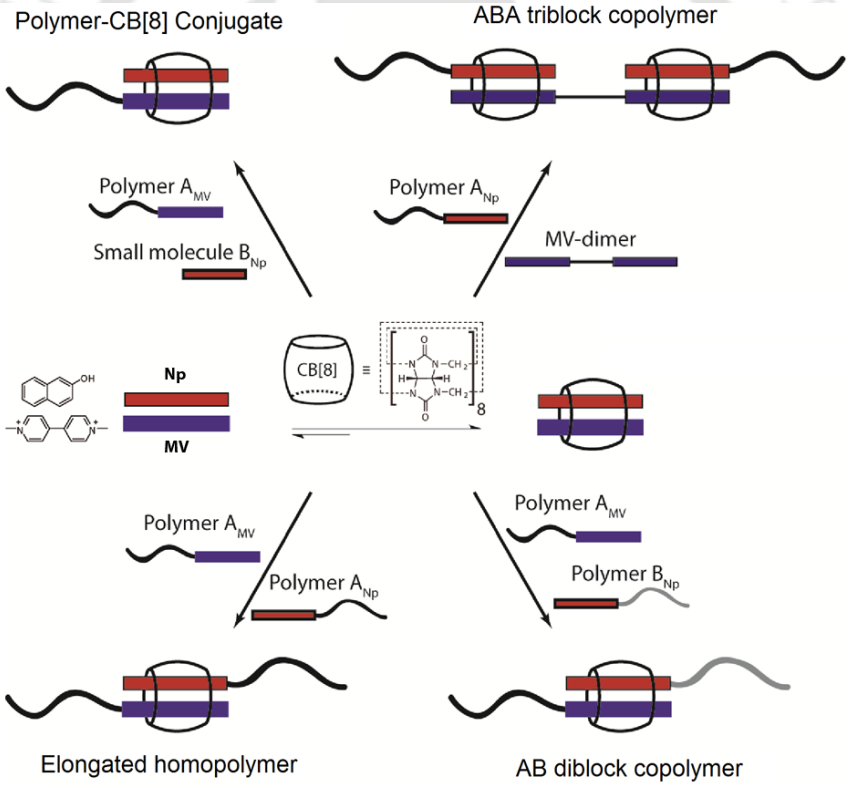

Figure 1.8 A variety of polymeric structures can be formed in aqueous medium via host-guest interaction of CB[8] by interconnecting complementary end-groups such as electron-rich 2-naphthol (Np) and electron deficient methyl viologen (MV) attached onto polymers.[50]

1.3 Surfactants and their Self-assembly

1.3.1 Surfactant

Surfactant is an abbreviation for surface-active agent, which literally means active at surface.[58-68] Surfactants consist of at least two parts, one, which is soluble in water (hydrophilic head group), and another, which is not (hydrophobic tail) (Figure 1.9). As a combined result of solvophobic and solvophilic interactions, these molecules form a structurally rich variety of self-organized assemblies including micelles, microemulsions, vesicles, monolayers, etc. The hydrophobic part of the surfactant can be of various chain length (typically 8-20 carbon atoms), which may contain multiple bonds, or can be made of two or more hydrocarbon chains. Aggregation behaviour depends on the nature and the concentration of surfactants, the nature of the solvent, and the method of preparation.

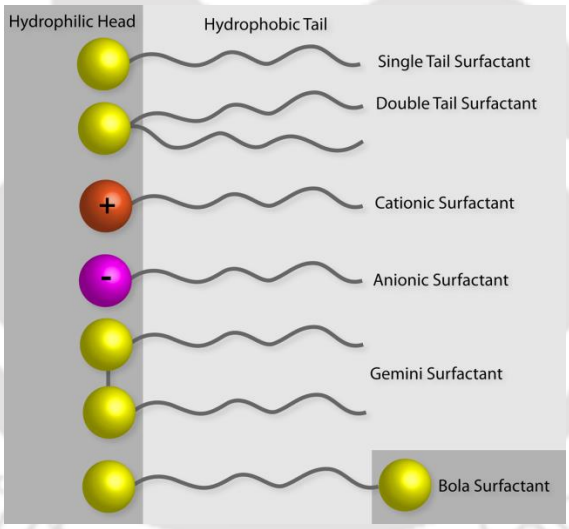

Figure 1.9 Cartoon pictures of various types of surfactant molecules.

1.3.2 Various types of Self-assemblies formed by surfactants

1.3.2.1 Micelle: When dispersed in water, surfactant molecules orient themselves in such an organized way so that the polar heads get solubilized in water and the hydrophobic tails are directed away from water thus forming an interface with high air/water curvature (Figure 1.10) and the self-assembly thus formed is coined as

"micelle".[58-68] The minimum surfactant concentration at a particular temperature above which micelle forms, termed as critical micelle concentration (CMC), is the intrinsic characteristic of each surfactant.

Below the CMC, surfactants are mono-dispersed in aqueous solution and act as normal electrolyte. When the monomers of surfactants get aggregated, i.e. at CMC, the physical properties of surfactant solution such as surface tension, viscosity, conductivity, etc. exhibit abrupt changes, which are attributed to the formation of micelles.[58-68]

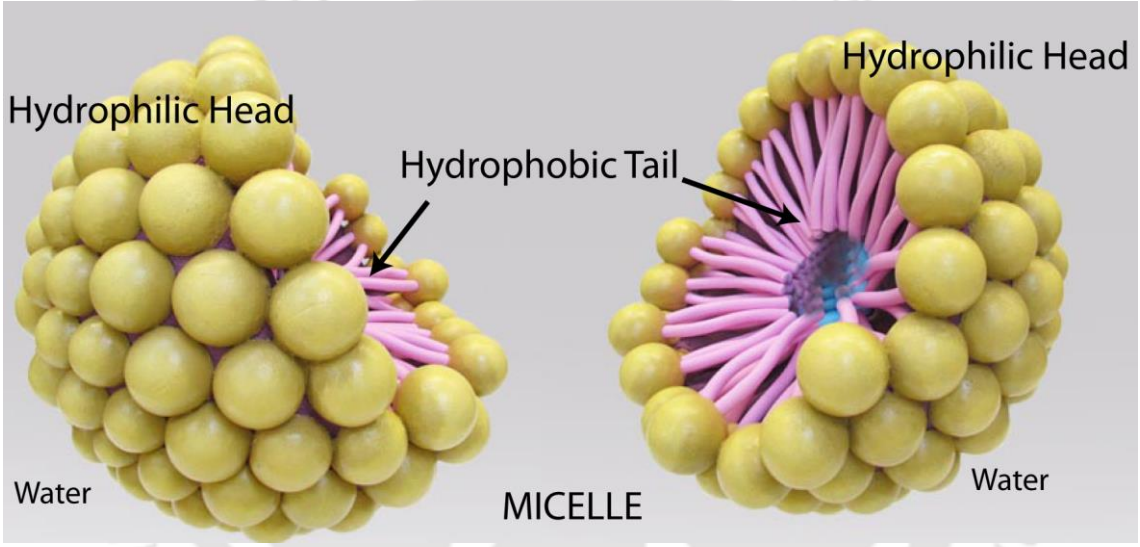

Figure 1.10 Pictorial presentation of a typical spherical micelle showing the arrangement of the surfactants.

1.3.2.2 Bilayer/Vesicles: One of the most sophisticated models of the biological membrane[69,70] is the closed bilayer aggregate formed by twin-chain surfactants in aqueous medium. When added to water, single chain amphiphiles form both monolayers on the surface of the water and micelles whereas double chain amphiphiles form bilayers instead of micelles (Figure 1.11).[58-68] Such bilayer when assumes the form of a closed spheres is popularly known as vesicles or liposomes. They offer the investigator a feature, unavailable in single-molecule chemistry: an inside and an outside separated by a physical barrier. Such double-chain amphiphiles are the basic building blocks of all biological membranes.[58,69,70] Like micelles, their self-organization in water is the result of hydrophobic effect,[58,59] and depends on the

hydrophilic-lipophilic balance (HBL) of the lipid, as well as on its geometry.[58,59] The kinetic stability of vesicles is considerably greater than that of micelles. Like micelles and reverse micelles, vesicles also have the ability to solubilize both hydrophobic and hydrophilic molecules.

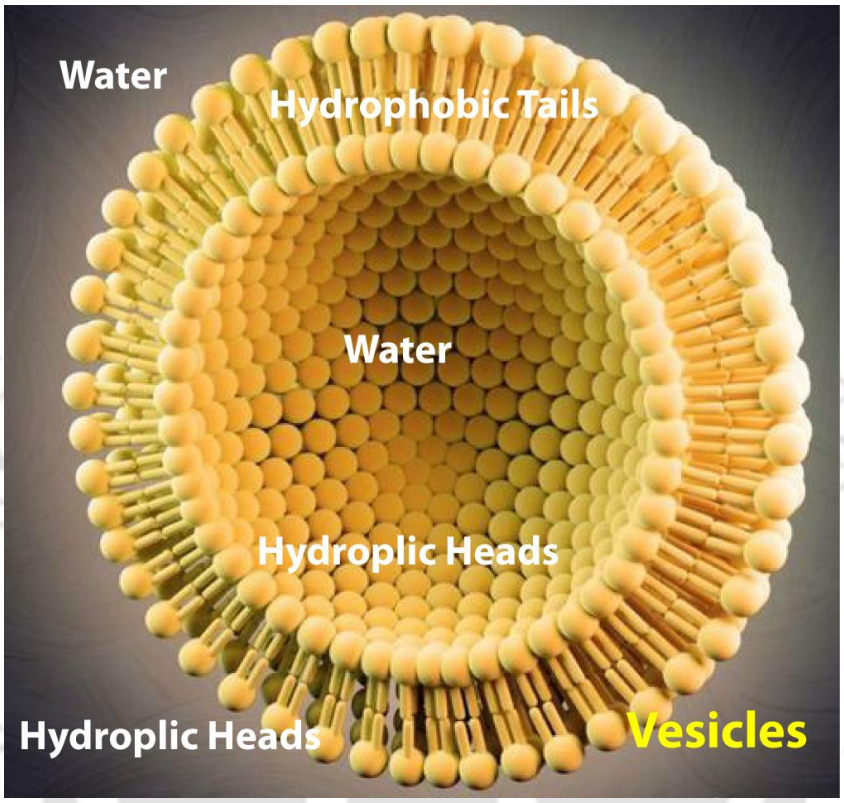

Figure 1.11 Pictorial presentation of a vesicle showing the lipid bi-layer and the arrangement of surfactant molecules.

1.3.2.3 Water-in-Oil (w/o) Microemulsions: Microemulsions are transparent dispersion of oil and water made with surfactant molecules. When oil-content is low, small oil droplets get surrounded by surfactant molecules and dispersed into water, known as oil in water microemulsion.[60,61] With increase in volume fraction of oil, the structure can invert without any apparent discontinuity in the physical properties from an oil-in-water to a w/o microemulsion.[60,61] w/o microemulsions, also termed as reverse micelles, are optically transparent nanometer scale aggregates of water and surfactants in an apolar bulk solvent.[60,61,67,68] Structurally, water forms a microdroplet surrounded by a monolayer of surfactant molecules organized with their polar heads toward the aqueous core, known as the water-pool, and the hydrophobic tails in

contact with the bulk apolar solvent, thus forming an anisotropic interface separating the polar aqueous part from the nonpolar oily region (Figure 1.12).[58-68] Technological and biotechnological potentials of thermodynamically stable w/o microemulsions are wide-ranging due to their increased interfacial area, as well as improved ability to solubilize otherwise immiscible substrates.[67,68]

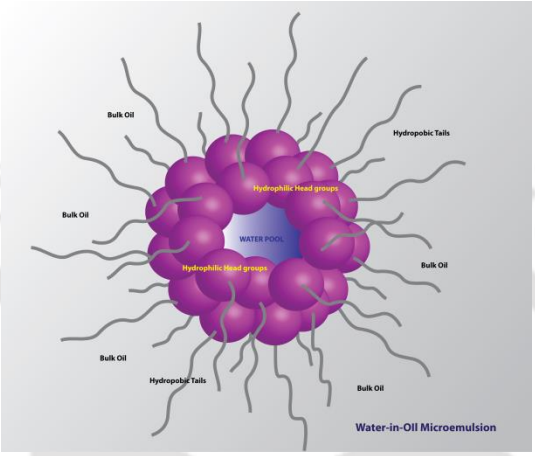

Figure 1.12 Arrangement of surfactants in a typical w/o-microemulsion showing the water pool and the bulk oil.

1.4 Viologen and Viologen Amphiphiles

Viologens are bipyridinium derivatives of 4,4'-bipyridyl (1,1′-dialkyl-4,4′-bipyridinium salts).[71] The best-known viologen is paraquat (MV, **7**, Figure 1.4), which is one of the world's most widely used herbicides. Apart from their well-known herbicidal activity, viologen and its derivatives have quite extensively been studied owing to their ability to function as electrochromic systems. Viologens are easily reduced to form the radical mono-cation which is intensely colored (Figure 1.13). Viologens can reversibly change color upon reduction and oxidation and act as an electron mediator. A variety of studies, including electron transfer to various biological molecules, photochemical solar energy conversion, and active materials in electrochromic displays have been reported in literature.[72-82] Viologens have extensively been incorporated in many systems as an electron acceptor from electron rich aromatic donors such as naphthalene,[83] pyrene,[84] coronene,[85] phenothiazine[86] etc. The charge transfer

mediated binding of viologens with various nucleosides as well as with DNA has also been reported by various groups.[87-89]

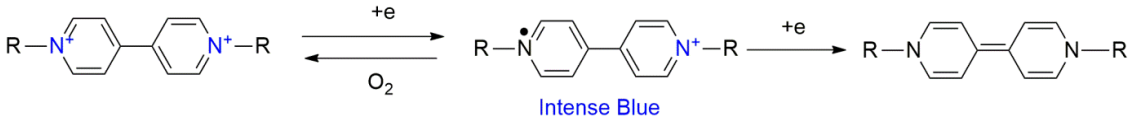

Figure 1.13 The reduction process of viologens generating intense blue colored monocation radical.

The asymmetric viologen amphiphiles have also been utilized in many studies especially in the area of electrochemistry. Kaifer et. al. have used asymmetric viologen surfactants for the modification of electrode surface.[90] Almgren and coworkers studied the electrochemical properties of *N*-tetradecyl-*N*′-methylviologen (TMV) in differently charged micelles with a glassy carbon electrode using electrochemical techniques and observed that the redox potential varies depending on the charge of the surrounding surfactants.[91] Similar studies were also reported earlier for other micellar systems.[92] Recently, Qian et al. prepared a multi-walled carbon-nanotube (MWCNT)–viologen surfactant composite and studied their morphology and electrochemistry in Langmuir-blodgett (LB) film. Cyclic voltammograms of the LB films revealed one or two couples of one electron transfer process corresponding to the viologen–MWCNT hybrids with the cathodic and anodic potentials closely related to the alkyl chains of the viologens.[93]

Although the ability of viologens and their amphiphiles to act as an acceptor in these charge transfer process is known for a long time, it has recently gained interest to form such self-assemblies and utilizing them as new soft-materials for variety of applications. The charge transfer complex mediated supramolecular conjugation of two linear polymers as well as cross-linked polymers were reported by Scherman et al.[50,51] George et al. have used an asymmetric viologen-surfactant toward the development of charge transfer mediated high-aspect ratio nanofibres exhibiting high field effect mobility while operating under ambient condition.[94,95]

Nevertheless, till now the main focus of utilizing the viologen surfactants were on their electrochemical properties and in this regard, it is essential to know the self-

aggregation behaviour of these surfactants. The micellization behaviour and the properties of viologen surfactants are important parameters which need to be analyzed in order to efficiently use these classes of amphiphiles for the construction of new assemblies. Unfortunately no effort in this regard has so far been made. One of the probable reasons behind lack of such information is the poor amphiphilic characters of these surfactants. The planar doubly charged head group presumably leads to inappropriate hydrophilic-lipophilic balance (HLB) for these surfactants to efficiently self-organize. The poor solubility is another reason behind such ignorance. Mixing with other surfactants to get mixed micellar systems could be a way out for studying and utilizing these important surfactants.

1.5 Host-Guest Interaction of CB[*n*] with Surfactants

Though significant progress has been made in utilizing the ternary complexation by CB[8] to develop various soft-materials, not much effort have been devoted in understanding the interaction of CB[8] with amphiphilic molecules.[96] Kim and his co-workers have shown that tetramethylammonium surfactants form U-shaped pseudo-ternary inclusion complexes inside the CB[8] cavity (Figure 1.14A). Similar U-shaped binding is also observed in case of a bolaamphiphile, dodecane-1,12-diammonium salt, inside CB[8] cavity (Figure 1.14B).[97] Interestingly, CB[7] was found to form inclusion complex with similar surfactants but it binds near the polar head groups while CB[5] sits at the head group from outside but no inclusion complexation occurs in that case (Figure 1.14D).[96,98] In another recent study on the interaction of trimethylalkylammonium surfactants of varying alkyl chain length with CB[7], Garcia-Rio et al. have shown that the binding constant values for the 1:1 complexation are effectively independent of the alkyl chain length and the CB[7] complexed monomers are not involved in the micelle formation.[99,100] The same group also demonstrated the 2:1 binding between a bolaamphiphile and CB[7] where the host binds at both terminals of the surfactants (Figure 1.14C).[100] Although viologens are the most studied guest for CB[*n*], no work has so far been reported on the binding of CB[*n*] with viologen surfactants alone.

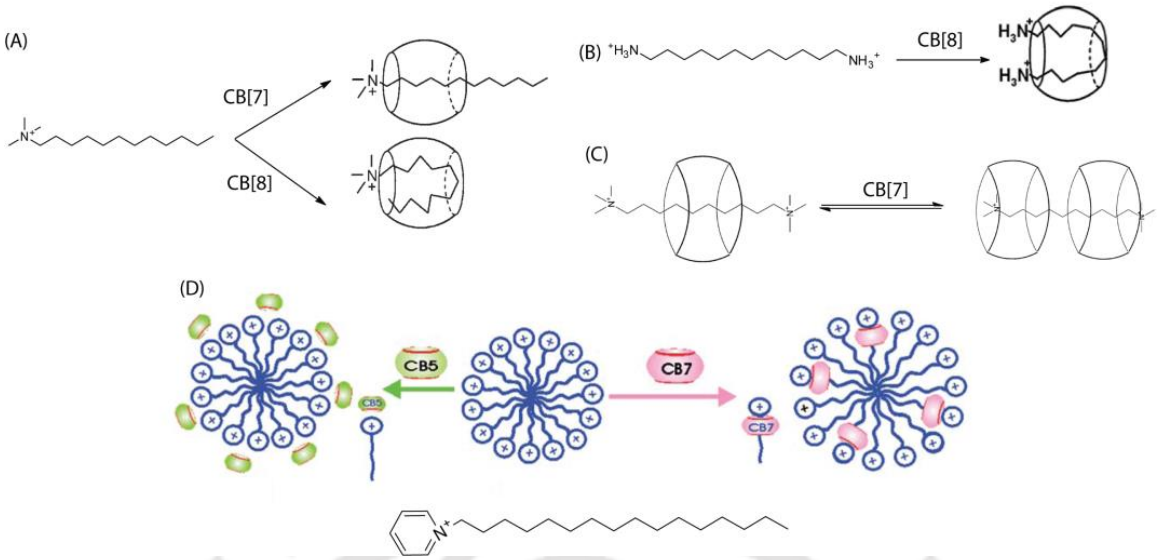

Figure 1.14 Different modes of binding of CB[5], CB[7], and CB[8] with various surfactants and their micelles.[96-98,100]

1.5.1 Viologen Amphiphiles with CB[8]: Vesicle Formation Through Ternary Complexation: In one of their pioneering works, Kim et al. have showed that aqueous solutions of asymmetric viologen surfactants get transformed into vesicles upon addition of CB[8] and DHN (Figure 1.15).[101] The transformation is aided by the ternary complex formation. Utilizing this concept, Scherman et al. have demonstrated the construction of a supramolecular peptide-amphiphile (Figure 1.16).[102] The vesicle formed by this peptide-amphiphile was used as a stimuli responsive delivery vehicle.[102] The same group have also recently showed the formation of a polymeric peptide-amphiphile based vesicle to encapsulate basic fibroblast growth factor.[103] Recently, Zhang and co-workers have shown similar ternary complexation mediated vesicle formation by a supramolecular glycolipid.[104] Surprisingly, no work has so far been reported on the mechanistic detail of such micelle to vesicle transformation by ternary complexation.

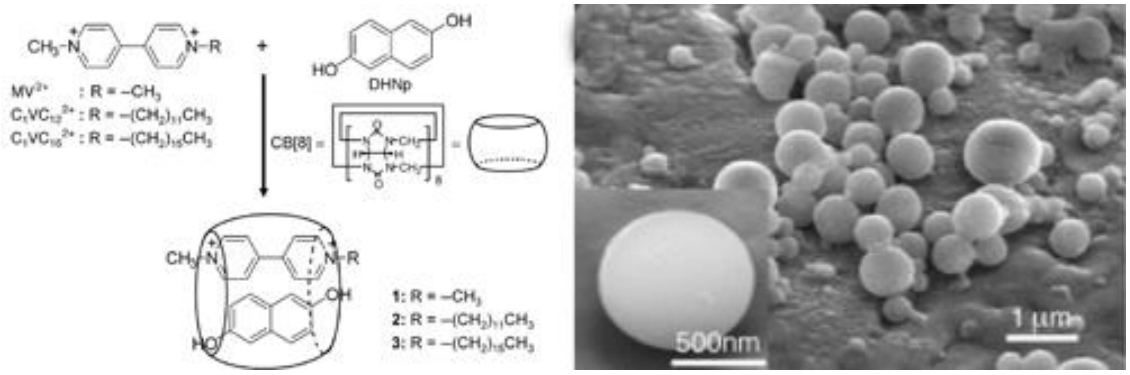

Figure 1.15 Pictorial presentation of the CB[8] assisted ternary complexation of a viologen surfactant and the FESEM image of the vesicle formed by one of those ternary complexes. [picture taken from 101]

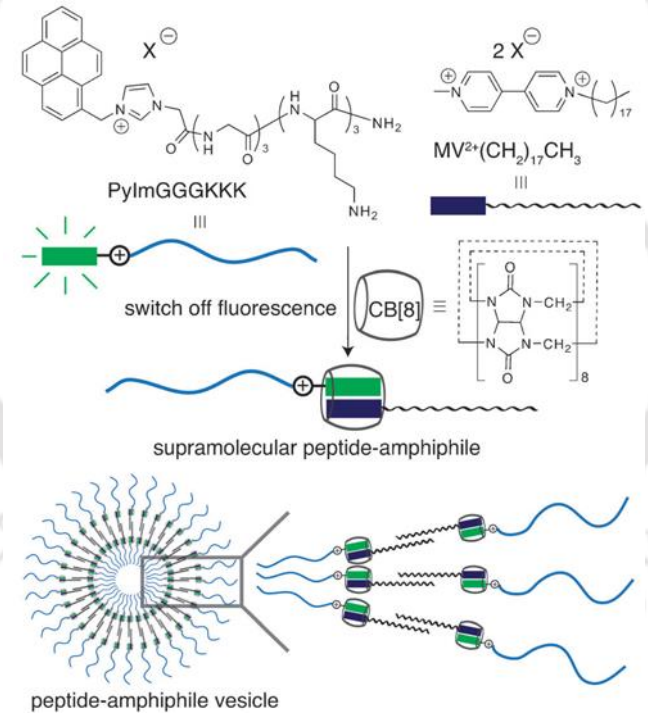

Figure 1.16 Pictorial presentation of supramolecular peptide amphiphile and its vesicle prepared by ternary complexation of a viologen surfactant, CB[8] and a peptide molecule.

1.6 Objectives of the Present Thesis

As discussed in the previous sections, the vesicle formation by viologen amphiphiles through ternary complex formation with CB[8] and DHN made us curious to

understand the mechanism behind such transformation. Viologen surfactants are poor amphiphiles owing to their planar head group which leads to their poor solubility in water as well as moderate self-assembling tendency when compared to other cationic surfactants with similar tail length. Although the asymmetric viologen surfactants are unable to form w/o-microemulsions as well as vesicles or liposomes, they can still self-assemble to form micelles in aqueous medium. The observation of vesicle formation by viologen surfactants through ternary complexation with CB[8] and DHN is quite surprising considering the poor self-assembling ability of viologen surfactants. We are in particular interested in understanding the inherent mechanism behind such a transformation. In the present thesis we aimed to address the following specific objectives,

- Whether the ternary complexation leads to "micelle to vesicle" transformation or it is a different mechanism which depends on the process of mixing.
- The binding of CB[8] with the viologen surfactants at various stages of the stepwise preparation of the vesicles.
- Whether this transformation can be achieved in presence of other surfactants (mixed micellar system).
- If there is any self-sorting mechanism involved.
- Whether the transformation is possible when other second guests are used such as aromatic amino acids.
- Development of stimuli sensitive vesicles using the ternary complex mediated vesicle formation by viologen surfactants.

In order to ascertain a detail understanding behind such a transformation, we have systematically studied the self-assembly process of viologen surfactants in pure and mixed conditions. The complexation with CB[8] and DHN with viologen surfactants were studied thoroughly at various stages to reveal some of the underlying features of such micelle to vesicle transformation. Further, the ability of different aromatic amino acids to affect such vesicle formation have been screened and eventually prepared a

multi-stimuli sensitive vesicle as controlled release system using the ternary complexation.

1.7 Present Thesis

1.7.1 Physicochemical Analysis of Mixed Micelles of a Viologen Surfactant

In order to understand the mechanistic detail of the CB[8] assisted vesicle formation by viologen surfactants, it is important to know the self-assembly behaviour of the viologen amphiphiles. We envisioned that a thorough study of the physicochemical properties related to the micellization of these viologen amphiphiles in pure and mixed conditions could be useful in this regard.

A systematic study on the micellization of a viologen surfactant (DDEV, dodecyl-ethylviologen) in pure and mixed conditions with tetraalkylammonium surfactants were carried out. The viologen surfactant was doped in various molar ratio (0-100%) with DTAB (dodecyltrimethylammonium bromide) and various physicochemical parameters related to the self-assembly of these surfactants were derived from the experimental results and compared. From the comparative study of these parameters, it revealed that the viologen amphiphile is a poor self-assembling surfactant. It was observed that in case of 1% viologen surfactant doped DTAB system, all the physicochemical properties remained unaltered. Similar experiments and analysis were also carried out with other tetraalkylammonium surfactants and found that the 1% doping of viologen surfactants cannot impart any significant change in these systems as well.

1.7.2 Mutual Sharing of Properties of Individual Surfactants in the 1% DDEV Doped systems

The prospect of mutual sharing of properties of individual surfactants in these DDEV doped systems were evaluated. Viologen amphiphiles due to their planar head group they are unable to form w/o microemulsion on the other hand tetraalkylammnium surfactants cannot form vesicles. The formation of vesicles by hexadecyl or dodecyl viologens through ternary complexation in presence of a well-known synthetic

macrocyclic host, CB[8] and DHN, made us curious to evaluate the prospect of introducing the vesicle formation ability into the tetraalkylammonium surfactants by only 1% doping of viologen surfactants. Interestingly, addition of CB[8] and DHN into the mixed micellar system of 1% DDEV doped DTAB also transformed the solution into vesicles. Similar results were also obtained with other tetraalkylammonium surfactants as well.

In addition to the vesicle formation, we also have checked the possibility to construct water-in-oil (w/o) microemulsions with this 1% DDEV doped systems. Though DTAB is well known to form such w/o microemulsions, it is impossible to prepare such self-assemblies with DDEV. The new 1% DDEV doped systems were also found to be able to form w/o-microemulsions in 9:1 isooctane-hexanol system. The phase boundaries were observed to be very much similar to that of the pure tetraalkylammonium surfactants. These newly constructed w/o-microemulsions certainly open up the possibility to utilize these redox-active viologen units at the oil/water interfaces of w/o-microemulsions which was not possible without the mutual sharing of the properties of the surfactants.

1.7.3 Dual Self-sorting by Cucurbit[8]uril to Transform a Mixed Micelle to Vesicle

Toward elucidating the mechanistic detail of the CB[8] mediated vesicle formation by viologen amphiphiles, we have utilized various spectroscopic and microscopic techniques. A thorough study was performed using a 1:1 mixed micellar system of a viologen surfactant and a tetraalkylammonium surfactant. It was observed that the vesicle formation process is a micelle to vesicle transformation and independent of the order of addition of the components. In absence of DHN, CB[8] forms U-shaped pseudoternary inclusion complex with the aliphatic tail of the surfactants and in the 1:1 mixed system, no preferential binding was observed. Toward forming the ternary complex and consequently the vesicles, two kinds of self-sorting mechanisms were observed where one is within the viologen amphiphile and another between the tetraalkylammonium surfactant and the viologen amphiphile.

1.7.4 Aromatic Amino Acids as a Second Guest for CB[8] Induced Vesicle Formation : Development of a Multi-Stimuli Sensitive Vesicle

In this section, we have demonstrated the formation of a multi-stimuli responsive vesicle formation by a supramolecular peptide amphiphile through the ternary complexation of CB[8]. While screening the aromatic amino acids for their ability to transform the solution of viologen surfactants through ternary complexation with CB[8], it was observed that though Tyrosine and Phenylalanine can form ternary complexes with methylviologen (**7**) inside the CB[8] cavity, they failed to do so with viologen amphiphile probably due to lower binding constant for the ternary complexation than that of CB[8] toward the hydrophobic tail of the surfactants. Interestingly Tryptophan was found to be able to convert the solutions to vesicle via the ternary complexation. While tested, an Azo group containing amino acid was also found to be able to form vesicles under such conditions. Utilizing the Azo-amino acid, we have constructed a peptide and through ternary complexation with CB[8] and a viologen amphiphile, this peptide formed a supramolecular peptide amphiphile and its corresponding vesicles.

The obtained vesicles were observed to be sensitive toward UV light (365 nm) as the *trans-cis* isomerization of the Azo-group leads to the disruption of the ternary complex. The formation and deformation as well as the release of an entrapped dye inside the vesicle can be manipulated by controlled irradiation of the vesicle solution with UV light. The obtained vesicles were also found to be sensitive to two other chemical stimuli. Adamantylamine, a stronger guest for CB[8] displaces both the guests from CB[8] cavity and thereby destroys the vesicular structure. Another competitive guest in the form of DHN replaces the Azo-peptide and occupies its position in the CB[8] cavity and retains the structure but releases the peptide. Such multi-stimuli responsive vesicles can be utilized as a controlled release system for various future applications.

CHAPTER 2

Physicochemical Analysis of Mixed Micelles of a Viologen Surfactant

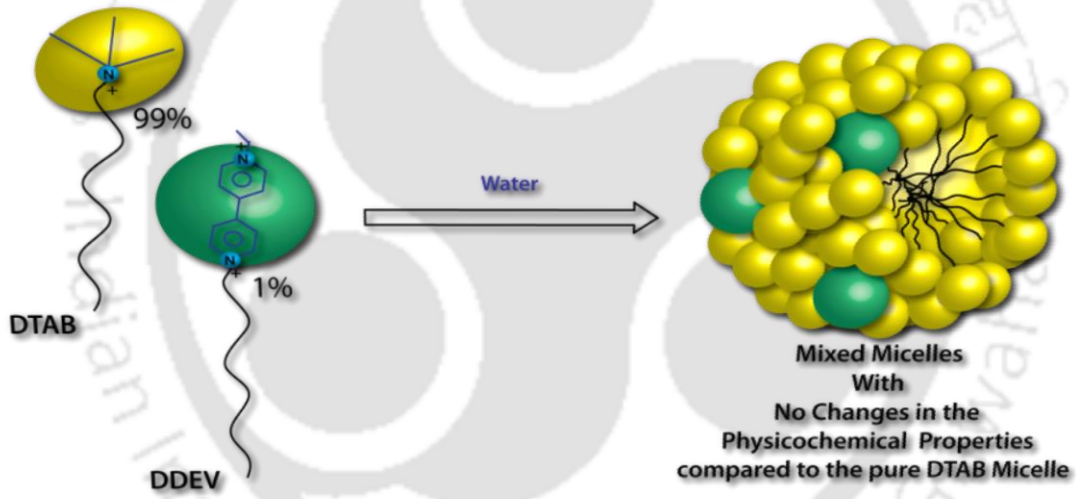

2.1 Introduction

Amongst the viologen containing components of the supramolecular assemblies mentioned in the previous chapter (section 1.2.4), the asymmetric viologen surfactants are the most common owing to their ability to facilitate the assembly process by providing the hydrophobic interactions. Though the interest to utilize the charge transfer complex formation of viologen amphiphiles is growing, till now the self-aggregation of such amphiphiles is poorly understood. Not much effort have been made to characterize and understand the self-assembly and micellization of viologen containing surfactants. Moreover, the reported studies were primarily focused on the electrochemical behavior of pure viologen amphiphiles in self-aggregated condition.[105-107] In order to utilize the self-assemblies of such amphiphiles, it is important to understand the self-assembly and related behaviour. Toward the application prospects of a surfactant, thermodynamics of formation, counterion binding (for ionic surfactants), etc., are important physicochemical aspects that need detailed attention. To the best of our knowledge, no such effort has been made for this important class of surfactants.

To this end, mixed amphiphiles have found great importance because of fundamental interests as well as extensive scientific and technological applications. In this regard, Lee et al. have reported the electrochemical behaviour of *N*-methyl-*N*'-hexadecylviologen in pure and mixed micellar systems.[92] Although a significant change in the redox behaviour was observed when the surfactant was mixed in anionic system, in cationic and non-ionic systems negligible variations were recorded.[92] Similarly, the reduction potential of the vesicle bound viologen surfactants were also found to be unaffected by cationic environments.[108] These observations clearly signify the fact that the electrochromic properties of the viologen unit at the interface is not affected by the positive charges at its surroundings.

These observations prompted us to study this particular class of surfactants. One of the major disadvantages of viologen surfactants is the low solubility and hence the inability to form robust self-assemblies. We envisioned that mixing viologen containing surfactants with other tetraalkylammonium surfactants could be of interest as that will

allow us to encounter these drawbacks. Finding a suitable binary combination will also permit us to prepare other types of membrane mimetic systems such as water-in-oil (w/o) microemulsions, and vesicles with specific features which are otherwise not possible to obtain in absence of one of the components.

In this chapter, we report a systematic study on the micellization of a viologen surfactant in pure and mixed condition with tetraalkylammonium surfactants. The aim of this study is to formulate a micellar system incorporating viologen at the air/water interface while the micellar and thermodynamic properties of the tetraalkylammonium surfactants remain unaltered.

2.2 Results and Discussion

For the current study, *N*-ethyl-*N*'-dodecylviologen dibromide (DDEV, Scheme 2.1) was selected in the view of its higher water solubility (1.19 M) compared to its methyl analogue (0.062 M). Dodecyltrimethylammonium bromide (DTAB, Scheme 2.1) was taken as the tetraalkylammonium surfactant in order to keep the chain length similar for both the amphiphiles.

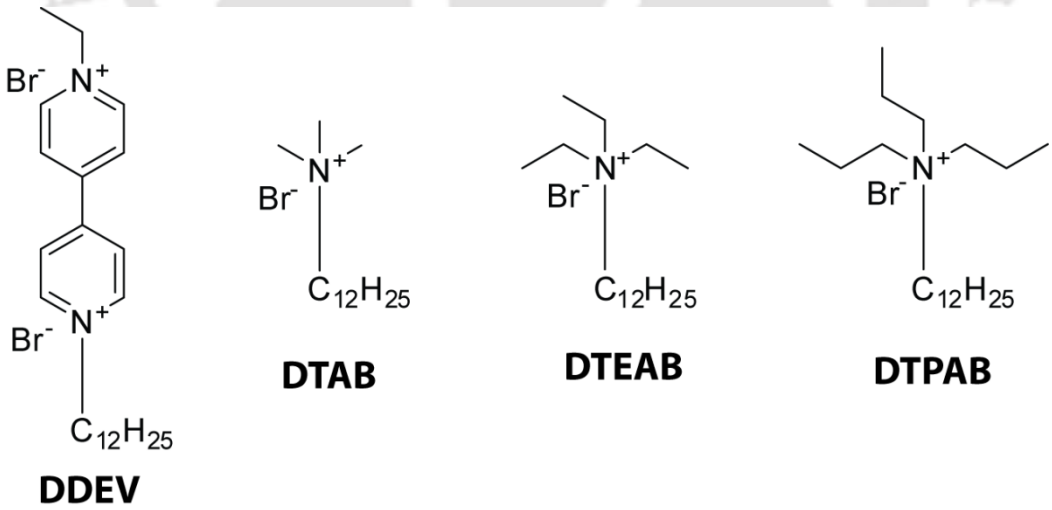

Scheme 2.1 Chemical structures of the synthesized surfactants.

2.2.1 Critical Micelle Concentration (CMC):

The critical micelle concentration and other micellization parameters are determined using surface tension, and conductance. Distinct inflection points in the course of the physical properties with respect to concentration (or log(concentration)) are recognized as the CMC's of the surfactants. The molar ratio of the surfactants is varied from 0 to 100%. The dependences of the surface tension (γ) on the total surfactant concentration (*C*) at 298 K are shown in Figure 2.1. The plots of γ versus log (*C*) show breaks at concentrations corresponding to CMCs of the surfactant mixtures. Similarly the changes in the specific conductivity (κ) with *C* at 298 K are presented in Figure 2.2. The concentration at which a sudden change in the specific conductivity appeared is considered as CMC of the system. The CMC values evaluated from both techniques are in good agreement and for further calculations, the average of the two measurements are taken into consideration (Table 2.1). The observed CMCs of the binary mixtures fall in between the two extreme ends of pure surfactants. The CMC of DTAB observed to be 14.9 mM and is in good agreement with the reported values.[109,110] As the proportion of DDEV increased, the CMC of the system shifted from 14.9 mM to 7.07 mM in case of pure DDEV which is a common trend in case of mixed micellar systems.

The mixing of surfactants to form mixed micelles may involve mutual interaction of the surfactants and deviate from ideal situation. The mixed micelle formation may be represented as,[111]

$$\frac{1}{CMC_{mix}} = \sum_i \frac{x_i}{f_i CMC_i} \qquad (1)$$

Where CMC_i, and CMC_{mix} stand for the CMC of the *i*th species and the mixture respectively; x_i and f_i are the stoichiometric mole fraction and activity coefficient of the *i*th component respectively. For ideal conditions, f_i = 1, and eq. 1 become Clint's equation[112]

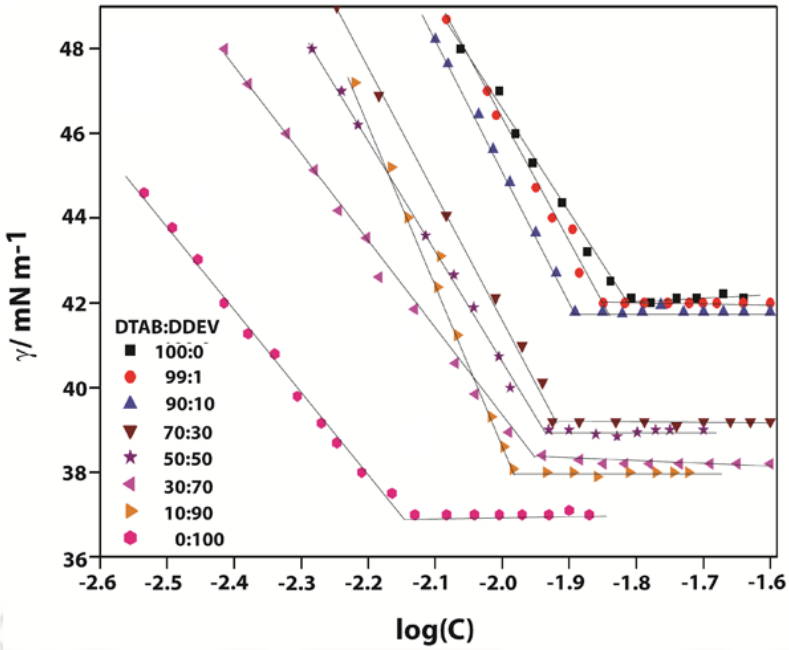

Figure 2.1 Tensiometric determination of the CMC of binary combinations of DTAB, and DDEV at different mole ratio at 298 K.

$$\frac{1}{CMC_{mix}} = \sum_i \frac{x_i}{CMC_i} \qquad (2)$$

A comparison of the observed CMC values of the binaries and those obtained from Clint's equation has been illustrated in figure 2.3A. Although the experimental CMCs match closely with the calculated values at a lower mole fraction of DDEV, a positive deviation from the equation is apparent at higher DDEV content indicating presence of nonideality due to mutual interaction of surfactants in the micelle. These results signify the fact that at 1% doping of DDEV, no significant interaction between DDEV and DTAB is involved and the mixing of these two surfactants at this ratio follow the ideal situation. There are successful theories by Rubingh,[113] Motomura,[114] Sarmoria,[115] puvvada, and Blankschtein[116] to evaluate molecular interaction in the mixed micelles of binary combination as well as predicting CMC and f_i. These theories have taken account of the repulsive or attractive forces acting between the surfactant molecules in the micellar state and consequently determining the activity coefficient. These theories have also been evaluated experimentally for various surfactant mixtures by taking care of the molecular interactions in micellar state.[117-119] Evaluation of the

theoretical models to explain the nonideality in the present binary systems could be of interest and deserves future exploration but beyond the scope of this investigation.

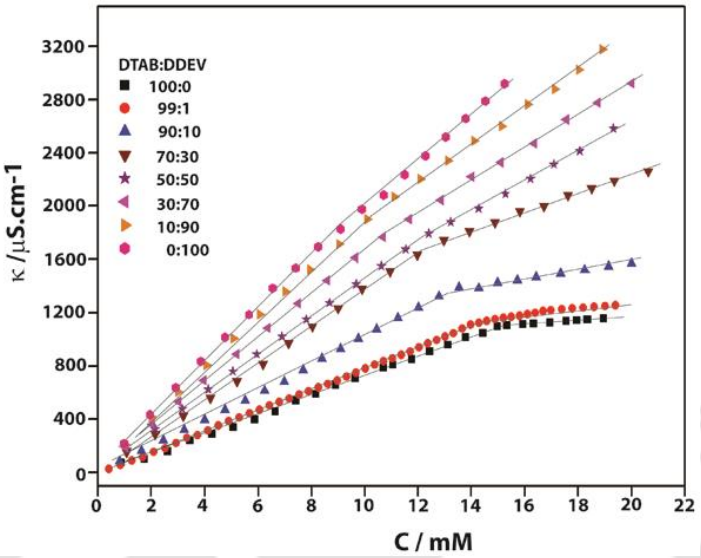

Figure 2.2 Conductometric determination of the CMC of binary combinations of DTAB, and DDEV at different mole ratio at 298 K.

2.2.2 Interfacial Behaviour:

The surface excess $\Gamma_{\max}^{\text{tot}}$, the minimum surface area (A_{min}) are two important parameters which describes the adsorption behaviour and packing density of the micelles at the air/water interface.[119,120] $\Gamma_{\max}^{\text{tot}}$ is the concentration difference between the interface and at a virtual interface in the interior of the volume phase while A_{min} denotes the minimum area of the amphiphile molecules at the surfactant-saturated monolayer at the air/solution interface.[119,120] $\Gamma_{\max}^{\text{tot}}$ and A_{min} can be calculated using the Gibbs adsorption equation.[120] For a multi-component system, the equation has the form,[119]

$$-d\gamma = RT \sum_i \Gamma_i \, d\mu_i \qquad (3)$$

where R, T, γ, Γ_i, and μ_i denote the universal gas constant, temperature, surface tension, surface excess of the *i*th component, and chemical potential of the *i*th component in solution, respectively. Utilizing the differential form of the equation of chemical potential ($\mu_i = \mu_i^0 + RT \ln a_i$, where μ_i^0 is the standard chemical potential and a_i is the activity coefficient of the *i*th component) eq. 3 can be reformed as,

$$-d\gamma = RT \sum_i \Gamma_i \, d \ln a_i \qquad (4)$$

For dilute solutions, the activity term (a_i) is replaced by the concentration term (c_i) and eq. 4 becomes,

$$-d\gamma = RT \sum_i \Gamma_i \, d \ln c_i \qquad (5)$$

In a mixed system with constant composition of constituents,

$$C_1 = K_2 C_2 = K_3 C_3 = \ldots\ldots\ldots \qquad (6)$$

Taking the log and differentiating, we get

$$d \ln C_1 = d \ln C_2 = d \ln C_3 = \ldots\ldots\ldots \qquad (7)$$

Using this identity in eq. 5, the Gibbs adsorption equation for a mixed system is converted to

$$-d\gamma = RT \, (\Gamma_1 + \Gamma_2 + \Gamma_3 + \ldots\ldots) \, d \ln C_1 \qquad (8)$$

Thus, for a surfactant system having *n* species and the total concentration *C*, equation 2 can be generalised as,[119,120]

$$-d\gamma = nRT\Gamma_{\max}^{\text{tot}} \mathrm{d} \ln C \qquad (9)$$

In the present context, for the binary mixtures (DTAB-DDEV), the value of *n* is 3. For the multi-component combination of surfactants, eq. 9 may be written as,

$$\Gamma_{\max}^{\text{tot}} = -\frac{1}{2.303\, nRT} Lt_{C \to C_{CMC}} \frac{d\gamma}{d \log C} \qquad (10)$$

The values of $\Gamma_{\max}^{\text{tot}}$ at the CMC has been calculated using eq. 10 from the least-squares slope of the γ versus log *C* plot and the A_{min} values for the systems have been estimated from the equation,[112,119]

$$A_{min} = 10^{18} \, [N_A(\Gamma_{\max}^{\text{tot}})]^{-1} \qquad (11)$$

where N_A is Avogadro's number and the factor 10^{18} arises as a conversion factor of area from m^2 to nm^2.The values of $\Gamma_{\max}^{\text{tot}}$ and A_{min} for the present binary mixtures are

presented in Table 2.1. Surprisingly the Γ_{max}^{tot} value dropped sharply from 2.76 x 10^{-6} (x_{DDEV} = 1) to 1.44 x 10^{-6} mol m^{-2} (x_{DDEV} = 0.9) by adding 10 % DTAB in DDEV. A reverse effect is observed in case of A_{min}. The significantly low A_{min} and high Γ_{max}^{tot} values for pure DDEV suggest its poor self-assembly behaviour presumably owing to the planer head group which could not provide appropriate packing at the interface.[113] The sudden change in the interfacial parameters by adding DTAB may presumably be connected to the efficient self-assembly behaviour of DTAB which favoring the self-assembly process even at this low (10%) doping. With further increase in the mole fraction of DTAB in the mixture, the total surface excess increased indicating an antagonistic effect by the doping of DDEV in the DTAB system in this mole fraction range.[119] A reverse effect is observed for A_{min} value (in this mole fraction range) which reduced with the increase in the mole fraction of DTAB. The increase in Γ_{max}^{tot} and decrease in A_{min} with increase in DTAB content indicate that the packing density of surfactant molecules at the interface decreases with an increase in the DDEV content.[119] Nevertheless, both the parameters were found to be very much similar in case of x_{DDEV} = 0.01 when compared with pure DTAB.

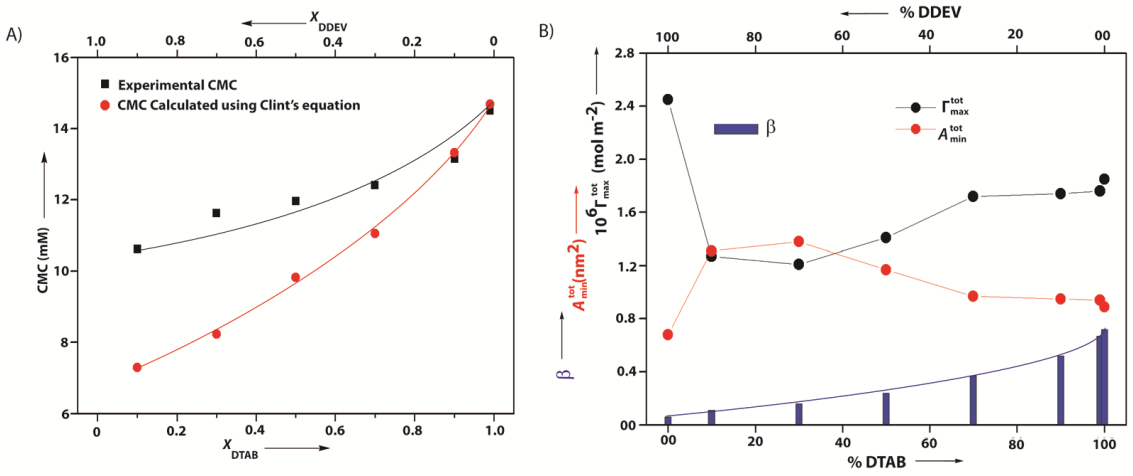

Figure 2.3 (A) Deviation of the dependence of CMCs on mole fractions of the components from ideal behaviour (Clint's equation). (B) Variation of Γ_{max}^{tot}, A_{min}^{tot}, and β values with mole ratios of the surfactants at 298 K.

Table 2.1 Interfacial, and thermodynamic parameters of micellization of pure and binary combinations of DTAB and DDEV at 298K.

Molar Ratio		CMC (mM)			π_{CMC}	$10^6\,\Gamma_{max}^{tot}$ (mol m^{-2})	A_{min} (nm^2)	β	ΔG_m^0 (kJ mol^{-1})	ΔG_{ad}^0 (kJ mol-1)	p^a	MG^b
x_{DTAB}	x_{DDEV}	ST	Con	Av.								
0	1.00	6.91	7.23	7.07	35.0	2.76	0.60	0.06	-23.56	-36.24	0.35	NS
0.10	0.90	10.47	10.77	10.62	33.9	1.44	1.16	0.13	-23.97	-47.51	0.18	S
0.30	0.70	11.48	11.76	11.62	33.8	1.48	1.13	0.16	-24.35	-47.19	0.19	S
0.50	0.50	11.83	12.09	11.96	33.2	1.55	1.07	0.24	-25.94	-47.36	0.20	S
0.70	0.30	11.95	12.88	12.41	32.8	1.72	0.97	0.37	-28.53	-47.60	0.22	S
0.90	0.10	12.88	13.42	13.15	30.2	1.74	0.96	0.52	-31.44	-48.79	0.22	S
0.99	0.01	14.38	14.62	14.50	30.0	1.80	0.92	0.68	-34.34	-51.10	0.23	S
1.00	0	14.86	14.95	14.90	29.9	1.84	0.91	0.72	-35.05	-51.30	0.23	S

[a] p = packing parameter; [b] MG = Micellar Geometry, NS = non spherical, S = spherical.

Table 2.2 Thermodynamic parameters of micellization of pure and binary combinations of DTAB and DDEV at different temperatures.

System		T	CMC	β	ΔG_m^0	ΔH_m^0	ΔS_m^0
x_{DDEV}	x_{DTAB}	(K)	(mM)		(kJ mol^{-1})	(kJ mol^{-1})	(JK^{-1} mol^{-1})
0.90	0.10	298	10.77	0.13	-23.93	-1.68	75
		303	10.88	0.12	-24.09	-1.73	74
		308	10.99	0.13	-24.67	-1.80	74
0.70	0.30	298	11.76	0.16	-24.31	-1.34	77
		303	11.90	0.15	-24.47	-1.38	76
		308	12.05	0.13	-24.41	-1.40	75
0.50	0.50	298	12.09	0.24	-25.90	-2.46	79
		303	12.31	0.21	-25.65	-2.48	76
		308	12.42	0.19	-25.61	-2.52	75
0.30	0.70	298	12.88	0.37	-28.40	-1.86	89
		303	12.99	0.36	-28.64	-1.91	88
		308	13.12	0.34	-28.65	-1.94	87
0.10	0.90	298	13.42	0.52	-31.36	-2.15	98
		303	13.58	0.50	-31.42	-2.20	96
		308	13.68	0.47	-31.28	-2.23	94
0.01	0.99	298	14.62	0.68	-34.34	-3.60	103
		303	14.72	0.66	-34.44	-3.67	102
		308	14.97	0.65	-34.72	-3.77	100
0	1.00	298	14.95	0.72	-35.05	-3.43	106
		303	15.14	0.70	-35.15	-3.50	104
		308	15.33	0.68	-35.25	-3.58	103

Table2.3 Physicochemical parameters of the pure and 1% DDEV doped DTAB, DTEAB, and DTPAB.

System	Temp (K)	CMC (mM)			$10^6\,\Gamma_{max}^{tot}$ (mol m^{-2})	A_{min} (nm^2)	ΔG_{ad}^0 (kJ mol^{-1})	β	ΔG_m^0 (kJ mol^{-1})	ΔH_m^0 (kJ mol^{-1})	ΔS_m^0 (KJ mol^{-1})
		ST	Cond.	Av.							
DTAB											
	298	14.86	14.95	14.90	1.84	0.91	-51.30	0.72	-35.05	-3.43	0.106
	303		15.14		-	-		0.70	-35.15	-3.50	0.104
	308		15.33		-	-		0.68	-35.25	-3.58	0.103
99:1 DTAB-DDEV											--
	298	14.38	14.62	14.50	1.80	0.92	-51.10	0.68	-34.34	-3.60	0.103
	303		14.72		-	-		0.66	-34.44	-3.67	0.102
	308		14.97		-	-		0.65	-34.72	-3.77	0.100
DTEAB											
	298	12.40	12.60	12.50	1.68	0.99	-52.34	0.66	-34.54	-8.70	0.087
	303		13.01		-	-		0.64	-34.53	-8.89	0.085
	308		13.42		-	-		0.62	-34.55	-9.07	0.083
99:1 DTEAB-DDEV											
	298	12.36	12.55	12.46	1.61	1.03	-53.29	0.65	-34.35	-7.32	0.091
	303		12.96		-	-		0.63	-34.34	-7.48	0.089
	308		13.23		-	-		0.60	-34.17	-7.70	0.086
DTPAB											
	298	9.06	9.24	9.15	1.52	1.09	-54.51	0.59	-34.31	-2.79	0.106
	303		9.32		-	-		0.57	-34.38	-2.85	0.104
	308		9.41		-	-		0.55	-34.46	-2.91	0.102
99:1 DTPAB-DDEV											
	298	9.03	9.11	9.07	1.45	1.15	-55.82	0.55	-33.48	-2.57	0.104
	303		9.15		-	-		0.53	-33.57	-2.61	0.102
	308		9.26		-	-		0.51	-33.63	-2.67	0.101

Table 2.4 Comparison of various physicochemical parameters of pure and 1% DDEV doped systems of different tetraalkylammonium surfactants.

Parameters	Systems					
	DTAB-DDEV		DTEAB-DDEV		DTPAB-DDEV	
	$x_{DDEV} = 0$	$x_{DDEV} = 0.01$	$x_{DDEV} = 0$	$x_{DDEV} = 0.01$	$x_{DDEV} = 0$	$x_{DDEV} = 0.01$
CMC (mM)	14.90	14.50	12.50	12.46	9.15	9.07
$10^6\,\Gamma^{tot}_{max}$(mol m^{-2})	1.84	1.80	1.68	1.61	1.52	1.45
A^{tot}_{min}(nm^2)	0.91	0.92	0.99	1.03	1.09	1.15
β	0.72	0.68	0.66	0.65	0.59	0.55
ΔG^0_m(kJ mol^{-1})	-35.05	-34.34	-34.54	-34.35	-34.13	-33.48
ΔG^0_{ad} (kJ mol^{-1})	-51.30	-51.10	-52.34	-53.29	-54.51	-55.82
ΔH^0_m(kJ mol^{-1})	-3.43	-3.60	-8.70	-7.32	-2.79	-2.57
ΔS^0_m (KJ mol^{-1})	0.106	0.103	0.087	0.091	0.106	0.104
P	0.23	0.23	0.21	0.20	0.19	0.18

2.2.3 Degree of Counterion Association (β):

It is well known that adsorption of counterions at the micellar surface reduces electrostatic repulsion between headgroups of micelles and thus permits the aggregation of ionic amphiphiles. The degree of counterion association (β) can be determined by conductivity measurements using equation 12,[121]

$$\beta = 1 - \frac{S_1}{S_2} \qquad (12)$$

where S_1 and S_2 are the slopes of the straight lines after and before the CMC in the conductivity plots, respectively.

The degree of counterion association values are tabulated in Table 2.1 and are in good agreement with the reported value in case of DTAB.[110] The relation of β with the mole fraction of DDEV/DTAB is shown in Figure 2.3B. With increase in the DDEV content, the β-values decreased sharply which suggests the low counterion binding ability of the DDEV surfactants.[122] At high x_{DDEV}, the effect is more prominent which also supports our assumption of intermolecular interactions which leads to non-ideal mixing of the surfactants and abrupt changes in the $\Gamma_{\max}^{tot}$ and A_{min} values. At x_{DDEV} = 0.01, a minor difference is observed in the degree of counterion association when compared with pure DTAB which suggests negligible effect of (low) counterion binding ability of DDEV at this mole fraction.

2.2.4 Thermodynamics of Micellization and Interfacial Adsorption:

The standard free energy of micellization per mole of monomer unit (ΔG_m^0) for the pure and binary combinations were evaluated from the relation,[119,121,122]

$$\Delta G_m^0 = (1+\beta)RT \ln x_{CMC} \qquad (13)$$

x_{CMC} is the CMC expressed in mole fraction unit. The standard free energy of interfacial adsorption (ΔG_{ad}^0) at the air/saturated monolayer interface of micelle has been evaluated from the relation,[119,121,122]

$$\Delta G_{ad}^0 = \Delta G_m^0 - \frac{\pi_{CMC}}{\Gamma_{\max}^{tot}} \qquad (14)$$

Where π_{CMC} stands for the surface pressure ($\gamma_{H_2O} - \gamma_{CMC}$).The ΔG_m^0 and ΔG_{ad}^0 values for all the systems are listed in Table 2.1. ΔG_{ad}^0 for all systems are more negative than ΔG_m^0 which means that the process of adsorption at the surface is more favorable than micelle formation.[123,124] The decrease in the ΔG_{ad}^0 values with increase in DDEV content signifies that the incorporation of DDEV in DTAB leads to decrease in spontaneity of the formation of micelles.[119] The effect is more profound with higher DDEV content and a similar effect was observed in case of ΔG_{ad}^0 values. Nevertheless our point of interest in this work is finding a suitable composition which does not impart any change in the micellization parameters of DTAB and in that respect, the x_{DDEV} = 0.01 stands out to be the most appropriate as there is almost no change in the free energies observed when compared to pure DTAB.

The thermodynamic parameters of micellization, such as the standard enthalpy (ΔH_m^0) and standard entropy (ΔS_m^0) can be obtained according to the following equations,[119]

$$\Delta H_m^0 = -RT^2(1+\beta)\, dlnX_{CMC}/dT \qquad (15)$$

$$\Delta S_m^0 = \frac{\Delta H_m^0 - \Delta G_m^0}{T} \qquad (16)$$

To determine the thermodynamic parameters of micellization for these systems, the conductometric measurements of CMC for each system were carried out at various temperatures (298, 303, and 308 K, Figure 2.4, Table 2.2). Using equations 15-16, the thermodynamic parameters were calculated and are presented along with the CMC values in Table 2.2. The micellization process became less exothermic and less spontaneous with increasing mole fraction of DDEV; the entropy change became less positive.[119] As observed for other parameters, no significant change is observed with 1% doping of DDEV with DTAB when compared with pure DTAB in case of the entropy and enthalpy as well.

2.2.5 Packing Parameters and Geometry of the Mixed Micelles:

According to Israelachvili, the geometry or "packing" properties of the aggregates depend on (i) a_0, cross-sectional area occupied by the hydrophilic group at the micelle−solution interface, (ii) the volume (v) of the hydrophobic chain which can be considered to be fluid and incompressible, and (iii) the maximum effective length, called the critical chain length (l_c).[125] For a saturated hydrophobic chain with n_c numbers of carbon atoms can be derived as,[124]

$$l_c \leq l_{max} \approx (0.154 + 0.1265n_c)\ \text{nm} \qquad (17)$$

And

$$v \approx (0.0274 + 0.0269n_c)\text{nm}^3 \qquad (18)$$

The packing parameter (p) determines whether micelles will be spherical (P < 1/3), non-spherical (1/3 <P < 1/2), vesicles or bilayer (1/2 <P < 1), or "inverted" structures (P > 1).[123-125] These structures indicate the minimum-sized aggregates in solutions which minimize the Gibbs free energy of micellization. The packing parameter (p) has been determined by the following relation:

$$p = v/l_c A_{min} \qquad (19)$$

Here, A_{min} was taken instead of a_0 because of the difficulty in exact determination of a_0.[125] The packing parameters for different combinations are given in Table 2.1. Interestingly the non spherical nature of the micelles of DDEV is converted to spherical as it is mixed with DTAB. Although there is no particular trend observed, from the p values it is clearly seen that there is almost no change in the micellar shape when the DTAB micelle is doped with 1% DDEV.

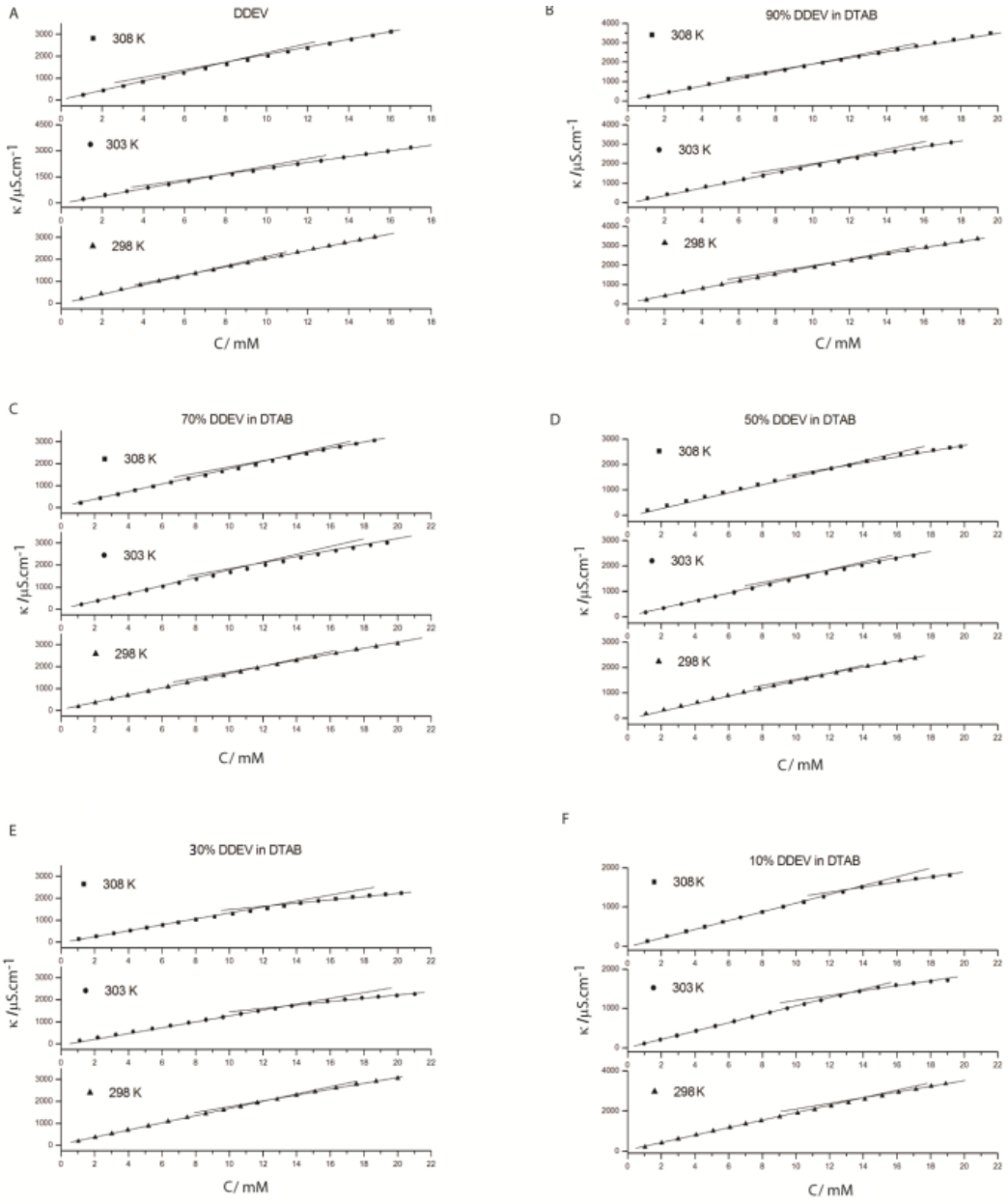

Figure 2.4 Conductomentric measurements of CMCs of various compositions of DTAB and DDEV at different temperatures.

2.2.6 Finding the Most Suitable System: The mixing of DDEV with DTAB clearly imparts molecular interaction which leads to non-ideal mixing. The micellization process is found to be less spontaneous as the mole fraction of DDEV enhances which presumably occurs due to the electrostatic interaction between the head groups of the two surfactants and the planer nature of the DDEV head group. The effects are prominent at a higher mole fraction of DDEV than at the lower doping level. Overall

the effect of the incorporation of a planer head group containing surfactant into DTAB can be summarized as, (a) the micellization process is disturbed due to intermolecular interactions leading to non-ideal mixing; (b) the micellization process is less-spontaneous as seen from the thermodynamic parameters; (c) though all other related parameters are affected, the shape of the micelles remain spherical in nature irrespective of the amount of DDEV doping.

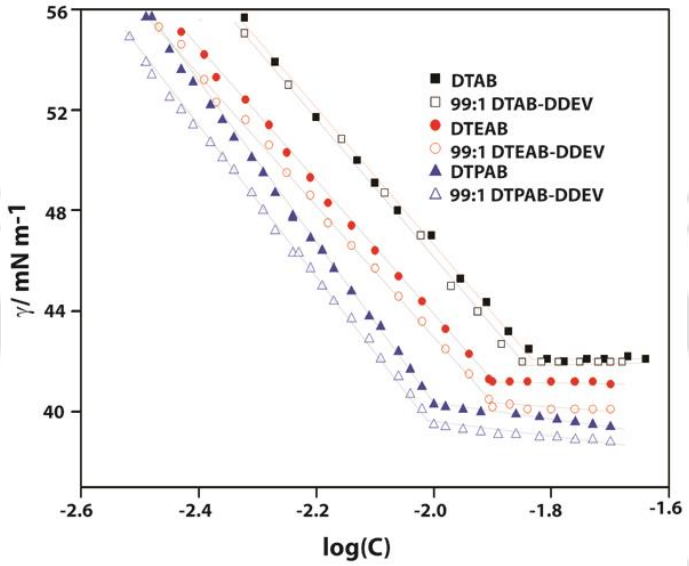

Figure 2.5 Tensiometric determination of the CMCs of different pure and mixed surfactant systems at 298 K.

Irrespective of the non-ideal behaviour at the higher level of DDEV mixing, it is clear that the effect of the presence of DDEV is negligible when only 1% of the surfactant is doped with DTAB. The physicochemical parameters analyzed for the micellization process show no significant change at this doping level. This clearly indicates the possible candidature of this particular system to be explored further.

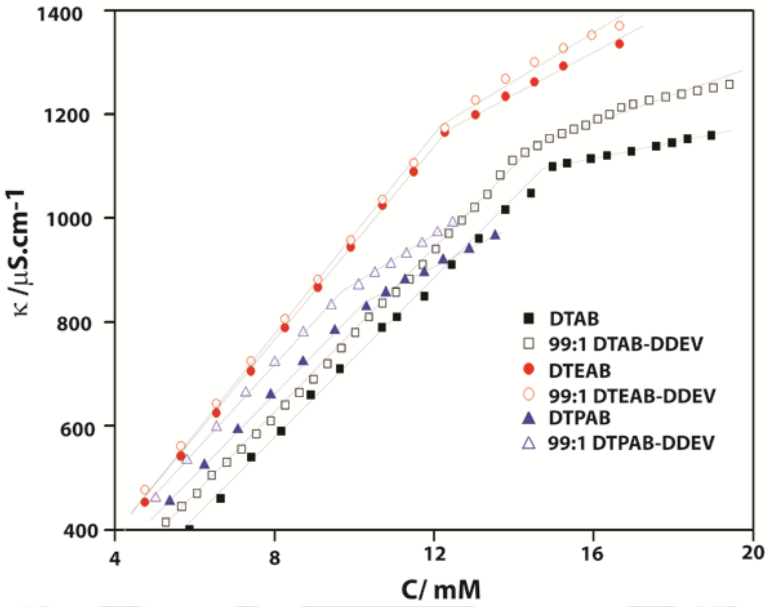

Figure 2.6 Conductometric determination of the CMCs of different pure and mixed surfactant systems at 298 K.

Before moving on to examine the possibility of forming other types of membrane mimetic self-assemblies by this 1% DDEV doped DTAB system, we wanted to generalize the observation with other tetraalkylammonium surfactants. Toward this issue, various micellar parameters for both pure and 1% DDEV doped systems in case of DTEAB and DTPAB were determined and compared (Figure 2.5, 2.6, 2.7, Table 2.3). For the ease of comparison, all the parameters are summarized for the pure tetraalkylammonium surfactants and 1% DDEV doped systems in Table 2.4. Similar to the case of DTAB, the micellar systems remain unaffected for both DTEAB and DTPAB when they are doped with 1% DDEV. The CMC, adsorption behaviour at the interface, counterion binding ability as well as the thermodynamic changes during the micellization process remained unaffected. Moreover the overall calculated shapes of the micelles remain spherical as it was in case of the pure tetraalkylammonium surfactants. From the comparative data listed in Table 2.4 it is clear that 1% doping of DDEV does not impart any perceptible change in the micellar properties of the pure tetraalkylammonium surfactants irrespective of the head group.

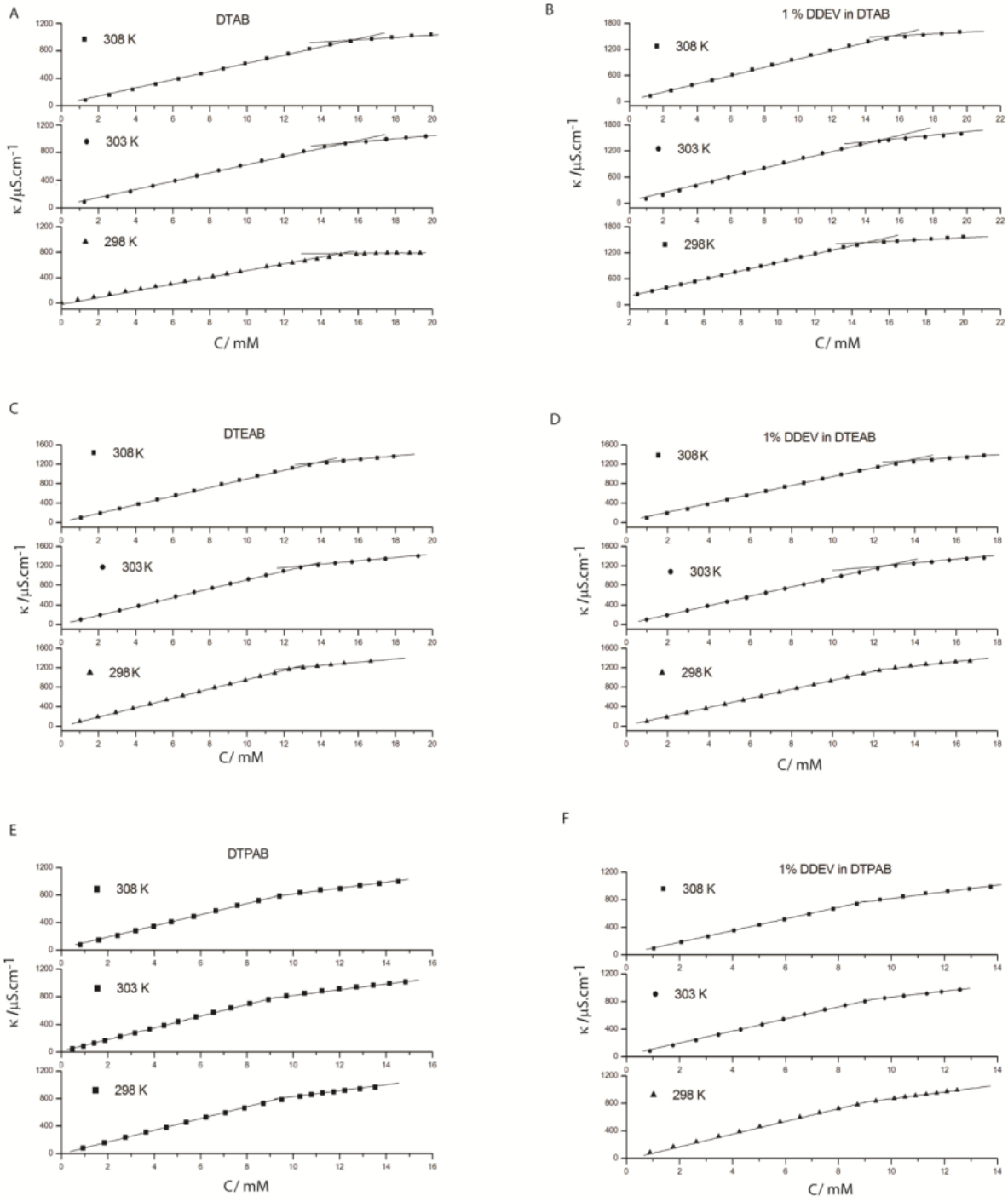

Figure 2.7 Conductomentric measurements of CMCs of pure and 1% DDEV doped DTAB, DTEAB, and DTPAB at different temperatures.

2.3 Conclusion

An attempt has been made through a systematic evaluation of the physicochemical parameters of micellization to find out a suitable combination of DTAB and DDEV where the incorporation of DDEV does not impart any change when compared with pure DTAB. Among the various mole ratios investigated, 1% doping of DDEV with DTAB is found to be an appropriate mixture as all the micelle related parameters remained similar to that of DTAB. Similar results were also obtained for other tetraalkylammonium bromide surfactants with bulkier head groups like DTEAB and DTPAB. The 1% DDEV doped systems can be used for further studies to develop new self-assembled systems where the characteristic features of viologen can be incorporated inside the self-assemblies without affecting the self-assembly parameters of the system.

2.4 Experimental Section

2.4.1 Materials

Dodecyltrimethylammonium bromide, 1-bromododecane, bipyridyl, D_2O, and $CDCl_3$ were obtained from Sigma-Aldrich (USA) and used as received. All other chemicals, reagents and solvents were procured from Merck, India and Spectrochem, India. All surfactants were recrystallized before doing the experiments. For preparing samples, Milli-Q water with conductivity of less than 2 $\mu S.cm^{-1}$ was used. NMR spectra of the synthesized compounds were recorded on a Oxford AS400 (Varian). ESI-MS was performed by using a Q-tof-Micro Quadrupole mass spectrometer (Micromass).

2.4.2 Synthesis

Dodecyltriethylammonium bromide **(**DTEAB) and dodecyltripropylammonium bromide (DTPAB) were synthesized using a literature procedure.[126]

DDEV*:* 1g of 4, 4'-dipyridyl was mixed with 5 mL ethyl bromide in dichloromethane and refluxed for three days when a yellow precipitate formed. The volatiles were removed on a rotory evaporator before washing the residue several times with toluene and finally

with diethylether to get a yellow solid as mono-ethylviologen (yield: 95%). The purity of the product was confirmed by ^{1}H NMR spectroscopy. The obtained solid was then further alkylated on the other pyridyl group by taking it in 7:3 acetonitrile/methanol and refluxing the mixture in presence of 1.5 eq. of 1-bromododecane for 24 h. The precipitate obtained was filtered and washed several times with toluene followed by diethylether. The surfactant was further purified by recrystalizing it three times from methanol/diethylether (Yield: 72%).

2.4.3 Methods

2.4.3.1 Surface tension

The surface tension of the surfactants at the air/water interface was measured using a tensiometer (Jencon, India) by the du Noùy ring detachment method. Previously prepared concentrated aqueous solutions of the surfactants were added progressively with a Hamilton syringes to a measured quantity of water, gently stirred for 2 minutes and kept in a constant temperature bath for 10 minutes without disturbing to reach equilibrium. The surface tensions of these solutions were then measured in triplicate while maintaining the temperature.

2.4.3.2 Conductance

The conductance of the surfactant solutions were taken using a Cyberscan Con-510 (Eutech) conductivity meter with cell constant of 1 cm^{-1}. After adding concentrated stock solutions of surfactants to a measured quantity of water, the solutions were stirred for 2 minutes and kept without disturbing for 10 minutes in a constant temperature bath before each measurement.

2.4.4 Characterization of the synthesized compounds:

DDEV*:* ^{1}H NMR (400 MHz, D_2O) δ/ppm = 9.19 (d, 2H), 9.13 (d, 2H), 8.58 (d, 2H), 8.55 (d, 2H), 4.80-4.73 (m, 5H), 2.26 (t, 2H), 1.67 (m, 2H), 1.38-1.21 (br, 18H), 0.81 (t, 3H); MS (ESI): m/z calcd for $[M-2Br]^{2+}$ $C_{24}H_{38}N_2$: 354.30, found: 354.31.

DTEAB (Yield: 90%): ^{1}H NMR (400 MHz, $CDCl_3$) δ/ppm 3.36 (q, 6H), 3.12-3.09 (t, 2H), 1.56 (m, 2H), 1.25 (t, 9H), 1.17 (br, 20H), 0.73 (t, 3H); MS (ESI): m/z calcd for [M-Br] $^{+}C_{18}H_{40}N$: 270.31, found: 270.33.

DTPAB (Yield: 85%): ^{1}H NMR (400 MHz, $CDCl_3$) δ/ppm 3.33-3.29 (t, 8H), 1.76-1.706 (m, 6H), 1.63(m, 2H), 1.31-1.20 (m, 20H), 1.03-0.99 (t, 9H), 0.843-0.814 (t, 3H). MS (ESI): m/z calcd for $[M\text{-}Br]^{+}$ $C_{21}H_{46}N$: 312.36, found: 312.37.

CHAPTER 3

Mutual Sharing of Properties of Individual Surfactants in the 1% DDEV Doped Systems

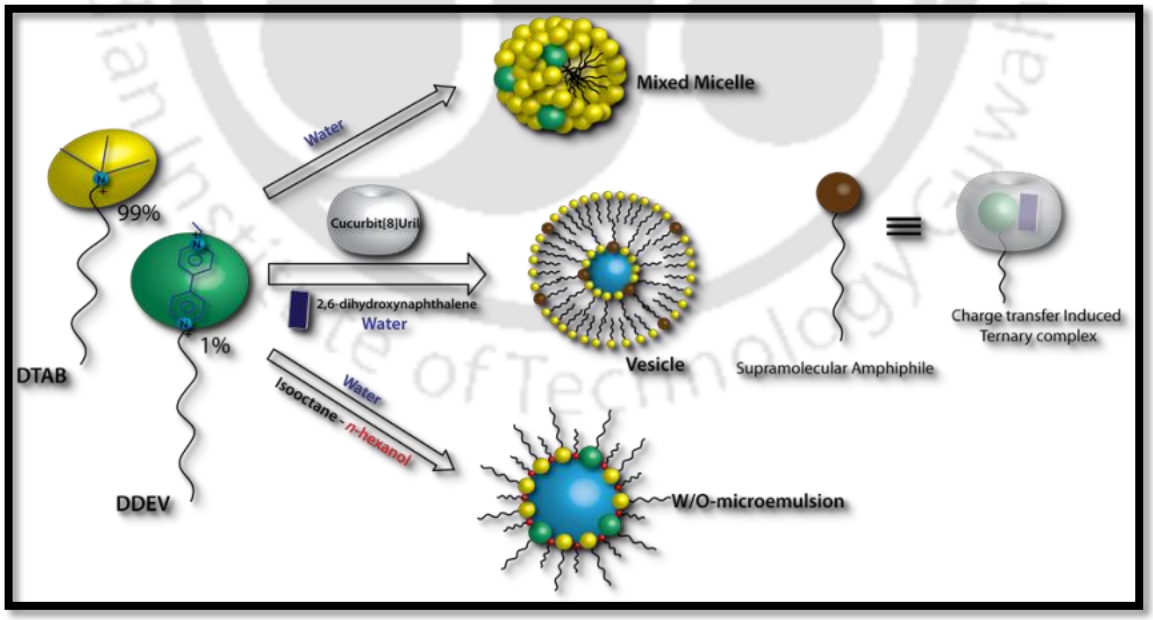

3.1 Introduction:

As discussed in chapter 1 (Section 1.2.4 and 1.5), in recent years, utilization of the viologen mediated charge transfer complexes to prepare novel self-assemblies have gained considerable attention.[49-57,101-104] The observation of Prof. Kim about the formation of vesicles by the asymmetric viologen surfactants through ternary complexation have fetched considerable attention.[101] This particular observation also opens up the possibility of preparing other types of useful self-assemblies using these viologen surfactants.[102-104]

As observed in the previous chapter (Chapter 2), the physicochemical properties of the mixed micelles of 1% DDEV doped tetraalkylammonium bromide surfactants remain very much similar to the micelles formed by the pure tetraalkylammonium bromide surfactants. The 1% doping of the surfactant could not impart any characteristic change in the micellar properties of the pure surfactant. In this process of doping DDEV, it is also possible that the constituent surfactants mutually share their characteristic features in the mixed micellar system. Introduction of a redox-active surfactant like DDEV may allow the system to be electro-active while DTAB alone cannot form a redox-active micellar system. Similarly, the viologen surfactants are not capable of forming w/o microemulsions but the presence of the tetraalkylammonium bromide surfactants may allow this 1% DDEV doped systems to form such membrane mimicking assemblies. In addition to that the ability of DDEV to form vesicles through ternary complexation in presence of cucurbit[8]uril and 2,6-dihydroxynaphthalene as observed by Kim et al., can also be tested in this new mixed system.[101]

In this chapter, we have evaluated the mutual sharing of these properties of individual surfactants in the new mixed surfactant systems. In this process we have successfully prepared w/o-microemulsions, CB[8] assisted vesicles and also redox acive systems using the 1% DDEV doped composition.

3.2 Results and Discussion

3.2.1 Electrochemical Properties of the Mixed Micelles: In order to determine the mutual sharing of properties by the surfactants, we have evaluated the possible redox active micelle formation by this 99:1 DTAB-DDEV mixed micellar system which is otherwise impossible for DTAB alone. A cyclic voltammogram (CV) of pre-micellar solution (below CMC) of DDEV in 0.05 M NaCl was recorded and shown in Figure 3A. The two couples observed are due to the well-known two-step reduction of viologens represented by the following equations and are in good agreement with literature report on its dimethyl analogue (MV^{2+}).[127]

$$DDEV^{2+} + e^{-} \leftrightharpoons DDEV^{+} \qquad (3.1)$$

$$DDEV^{+} + e^{-} \rightleftharpoons DDEV \qquad (3.2)$$

Both the electrochemical half-reactions were clearly observed at a concentration below CMC of DDEV as shown in figure 3.1.[128] The sharp peak in the voltammogram indicates the insolubility of the cation radical and the neutral species (generated by the reduction process) and their consequent precipitation on the electrode surface. Increasing the concentration to a post micellar concentration (above CMC) drastically change the peak shape along with a shift in the peak position. The aqueous solution of DTAB did not show any measurable couple in the CV experiment while doping of 1% DDEV in DTAB showed two redox couples similar to DDEV. In case of 99:1 DTAB – DDEV, both pre and post micellar conditions yielded similar voltammogram where no tendency of precipitation was observed in contrast to the pre-micellar DDEV system. The presence of excess DTAB in case of 99:1 DTAB-DDEV system probably allowed the reduction products to get solubilize in the micellar core which restricted the precipitation. Similar voltammograms were obtained when 1% diethylviologen was added to a DTAB system (Figure 3.2). Although the observed results are very much a preliminary work, it clearly indicates the incorporation of the redox behaviour of viologen in the otherwise inactive DTAB micellar system.

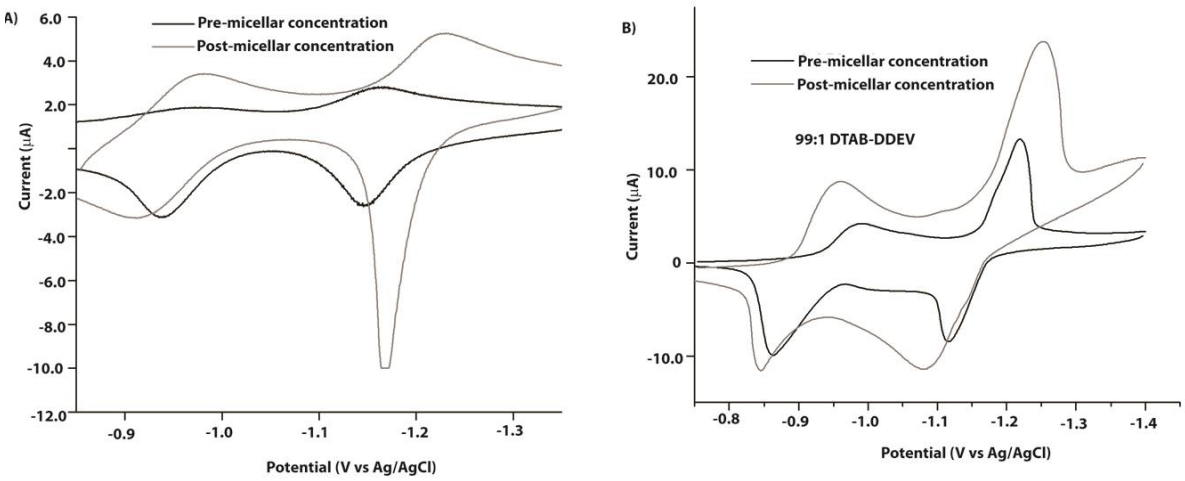

Figure 3.1 CV (0.1 Vs^{-1}) of A) DDEV and B) 99:1 DTAB-DDEV at pre and post micellar concentrations (in 0.05 M NaCl).

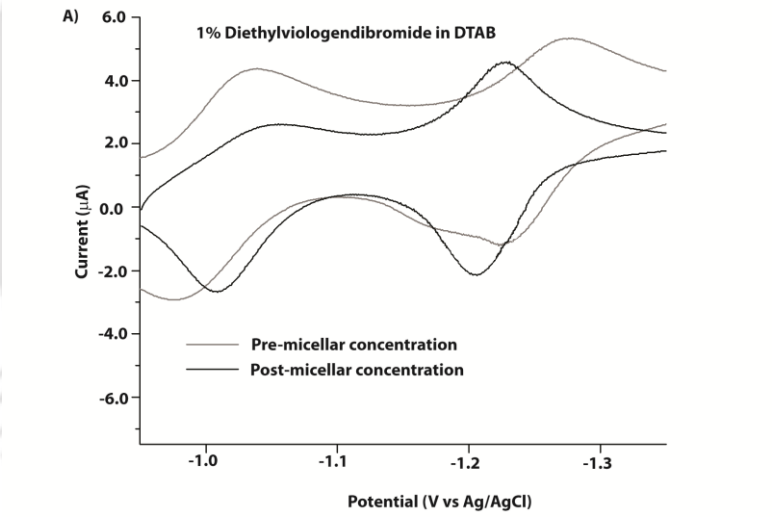

Figure 3.2 CV (0.1 Vs^{-1}) 99:1 DTAB-DDEV at pre and post micellar concentrations (in 0.05 M NaCl).

3.2.2 W/o-microemulsion Formation by the Mixed Surfactants: W/o microemulsions or so called reverse micelles are optically transparent nanometer size aggregates of water and surfactants in an apolar bulk solvent.[63,129] Structurally, a monolayer of surfactant molecules surrounds a microdroplet of water by organizing their polar heads toward the aqueous core, known as the water-pool, and the hydrophobic tails in contact with the bulk apolar solvent. In this process, an anisotropic interface is formed separating the polar aqueous part from the nonpolar oily region.[68] Technological potentials of such thermodynamically stable w/o microemulsions are ample owing to their enhanced interfacial area and superior ability to solubilize otherwise immiscible substrates.[130,131] Although reports have been published on the utilization of the electrochromic properties of viologens in reverse micelles,[131,132] to the best of our knowledge, no work has so far been reported on the reverse micellar systems formed by viologen containing surfactants.

In order to check the possibility of the formation of reverse micelles by DDEV alone, we have examined the w/o-microemulsion formation of DDEV (100 mM) in isoocatne-*n*-hexanol (9:1, v/v) system where *n*-hexanol works as a co-surfactant to facilitate favorable interfacial arrangement of the surfactant head group. In accordance with our expectation, the surfactant failed to form any self-aggregated system within a very wide range of W_0 (mole ratio of water to surfactant, 1-120).

The inability of forming such self-aggregates by DDEV may possibly because of the planar head group of the surfactant which does not allow the required packing to form w/o microemulsion. In order to estimate the minimum mole fraction of DTAB required to form w/o microemulsion using the mixed surfactant system, we have checked the w/o microemulsion formation by all the compositions utilized for this study. Although the formation of w/o microemulsion was observed for X_{DDEV} = 0.3, a narrow W_0 range (4-12) was recorded for the system. Systems containing more DDEV than this composition failed to form such microemulsion. The W_0 range increased with increase in X_{DTAB} (Table 3.1).

The pseudoternary (as four components are used but the phase-diagram consists only three axes as the surfactant and *n*-hexanol are taken together) phase diagrams of DTAB and 99:1 DTAB-DDEV with n-hexanol (1:2, w/w)/water/isooctane systems at 298 K are represented in Figure 3.3A. From the diagram it is evident that even at 1% doping, there is a negligible effect of the presence of DDEV as amount of the isotropic phase decreased by only ~2.6% compared to that of pure DTAB. Similar effect was also observed in case of DTEAB (Fig. 3.3B) where the decrease is ~1.8% while in case of DTPAB (Fig. 3.3C) the effect is <1%. The phase behaviour of the pure surfactants showed a clear dependency on the head group size as the area covered under isotropic phase decreased with increase in the headgroup size. The almost unchanged phase behaviour with 1% doping of DDEV can be correlated with the observation from the micellar systems. The very small addition of the viologen surfactant is unable to impart any thermodynamic changes in the self-assembly process while it introduces the important electrochemical behaviour of the viologen unit to the otherwise electrochemically inert systems. The electrochemistry of these new w/o-microemulsions as well as the dynamics of their formation need to be addressed in future but is beyond the scope of the present study.

Table 3.1 Experimentaly determined W_0 values for different mixed surfactant systems.

Molar Ratio		W_0 Range[a]
x_{DTAB}	x_{DDEV}	
0	1.00	-
0.10	0.90	-
0.30	0.70	-
0.50	0.50	-
0.70	0.30	4-12
0.90	0.10	4-48
0.99	0.01	4-48
1.00	0	2-50

[a] for w/o microemulsions, [Surfactant] = 100 mM.

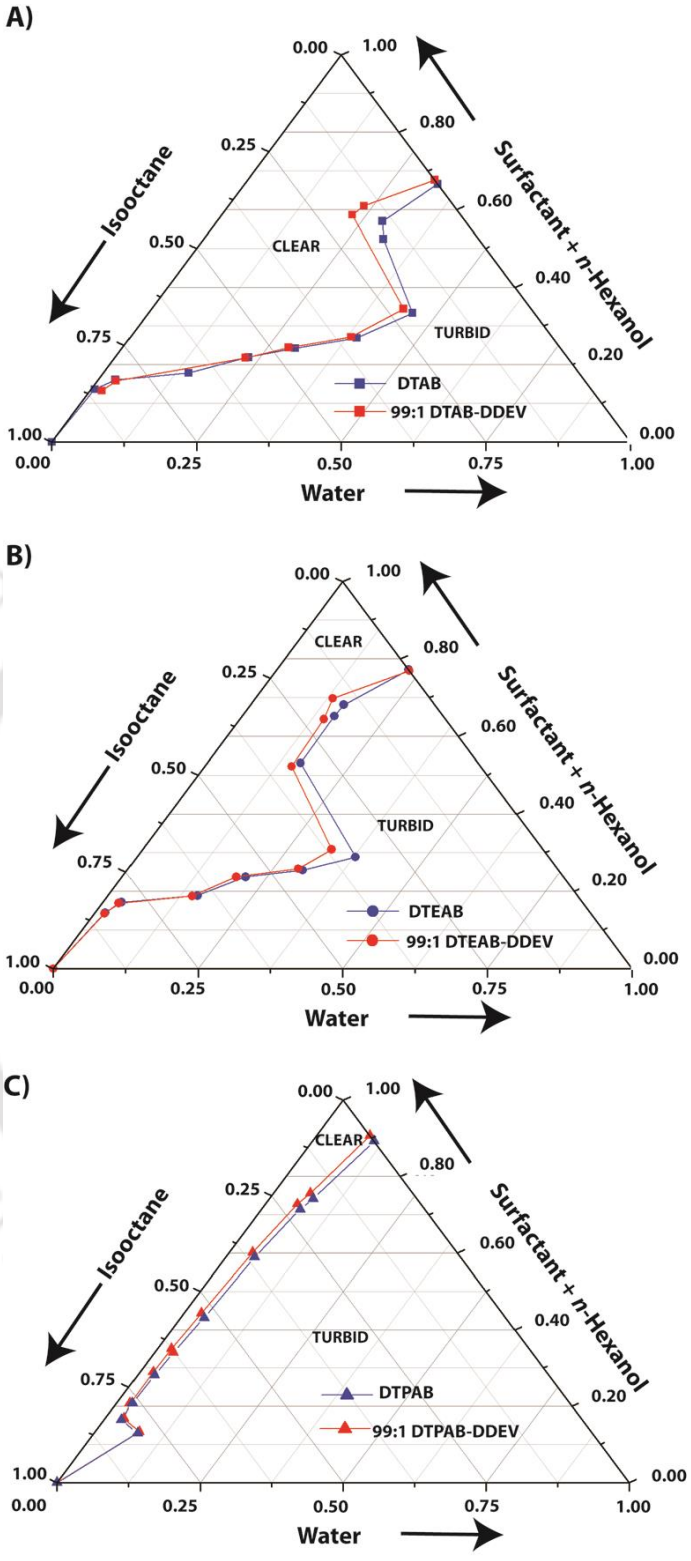

Figure 3.3 Pseudoternary phase diagrams of pure and mixtures of surfactants-*n*-hexanol (1:2, w/w)/water/isooctane at 298 K. The clear areas represent the phase where w/o-microemulsion formation occur and the turbid area indicates the composition where phase separation takes place. The scale magnitudes are reduced by 1/100th of the plot.

3.2.3 Cucurbit[8]uril Assisted Vesicle Formation by the 1% DDEV Doped Systems: As mentioned in the introduction, the formation of vesicles by hexadecyl or dodecyl viologens through ternary complexation[101] in presence of CB[8] and DHN, made us curious to evaluate the prospect of introducing the vesicle formation ability into the tetraalkylammonium surfactants by only 1% doping of viologen surfactants. In order to assess the possibility, we have used the new system of 1% DDEV in DTAB which have shown no significant deviation from the self-assembly characteristics of DTAB both in micellar and reverse micellar systems. Using similar protocol utilized by Kim,[101] we have prepared a solution of DTAB containing 1% DDEV and added equimolar CB[8] and DHN with respect to DDEV. The overall concentration (16 mM) of the surfactant mixture was kept well above the CMC (14.9 mM) of the mixture while the concentration of DDEV (0.16 mM) remains much below the CMC of the pure surfactant (7.07 mM). Sonication followed by incubation of the sample for 4 days at room temperature resulted in a transparent light violet solution. UV-visible absorption spectrum of the sample showed appearance of a charge transfer band at 535 nm formed by the ternary complexation of viologen- DHN@CB[8] (Figure 3.4).[101] A similar experiment with DDEV (0.16 mM) in absence of any DTAB also showed analogous absorption spectrum (data not shown).

In order to appraise the vesicle formation, TEM images of both solutions were taken and to our expectation, while DDEV alone failed to form any vesicle at this concentration (Figure 3.5), DTAB-DDEV mixture formed uniform sized vesicles with average diameters of ~30 nm (Figure 3.6A). The diameters of the vesicles were further confirmed by Dynamic Light Scattering (DLS) experiments (Figure 3.7A). The failure of DDEV alone to form vesicles can be attributed to the concentration range where the experiments were performed which is ~44 fold lower than its CMC. The role of concentration could not be verified owing to low solubility of CB[8] (~1 mM) which is much lower than the CMC of DDEV (7.07 mM, Table 2.1). It is worth mentioning that the formation of vesicles by the methyl analogue reported by Kim was achieved at a post CMC concentration.[101]

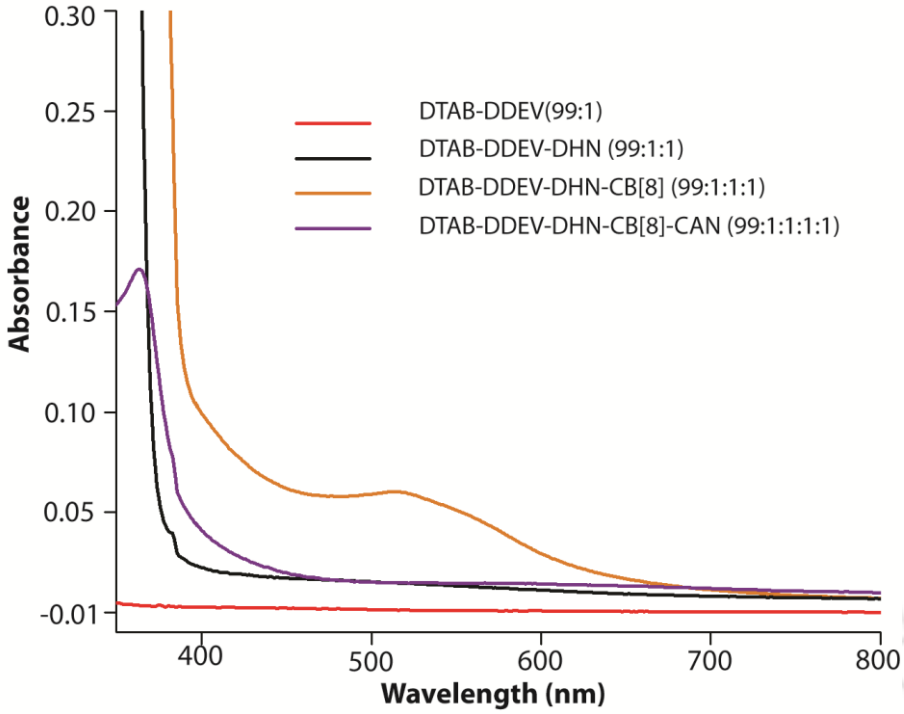

Figure 3.4 UV-Visible spectra of aqueous solutions prepared by the mixture of DTAB, DDEV, DHN, and CB[8] at different combinations at 298 K showing the appearance of the charge transfer band upon binding of viologen unit with DHN, and CB[8] and the disappearance of the same upon treatment with CAN. [DTAB] = 15.84 mM; [DDEV], [CB[8]], [DHN] = 0.16 mM; [CAN] = 0.24 mM.

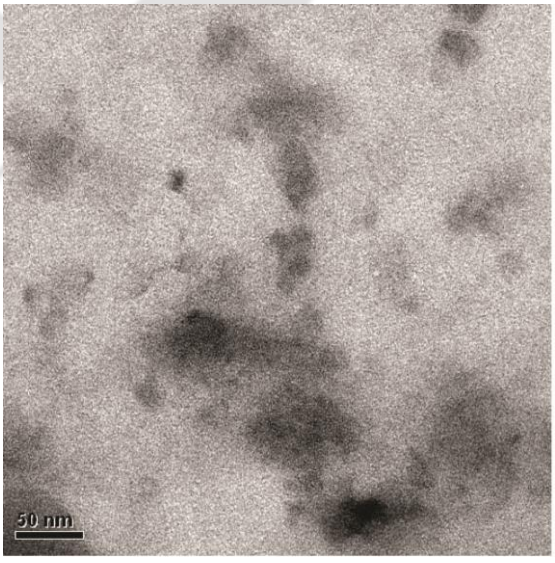

Figure 3.5 TEM image of the solution prepared with 1:1:1 DDEV-DHN-CB[8].

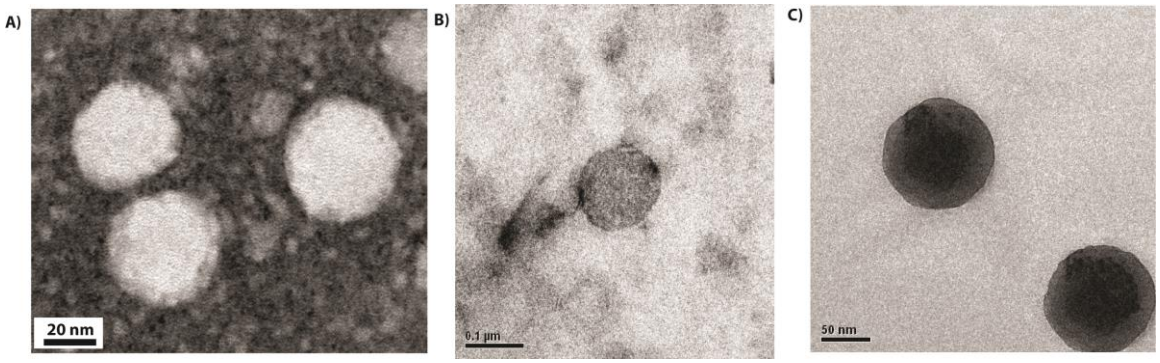

Figure 3.6 TEM images of the vesicles formed by 99:1:1:1 tetraalkylammonium bromide-DDEV-DHN-CB[8] in water at 298 K. A) for DTAB, B) DTEAB and C) DTPAB.

The stability of the vesicles was measured by the dye entrapment and release study. A water soluble anionic reporter, 5(6)-carboxyfluorescein (CF) was entrapped into the vesicles formed by the new system and the release of the dye through the vesicles was measured at 298 K (Figure 3.8). The very slow release of the dye demonstrates the stability of the vesicles at this temperature. A similar permeability pattern of sulphorhodamine G was also observed by Kim for the vesicles formed by N-methyl-N'-hexadecylviologen-DHN@CB[8].[101] Addition of Triton X-100 ruptured the vesicle and all the dye was released spontaneously as observed in Figure 3.8.

The role of the charge transfer complexation was further proved by the addition of cerium (IV) ammonium nitrate (CAN) to the vesicles. The charge transfer band disappeared spontaneously (Figure 3.4) and the TEM image of the sample showed no sign of any vesicle (Fig 3.10). Oxidation of DHN to naphthoquinone by CAN leads to the deconstruction of the ternary complexation which eventually leads to the collapse of the vesicle. This observation points to the definite role of the ternary complex (viologen-DHN@CB[8]) toward the transition from micelle to vesicle. It is quite interesting to find out the fact that even at this low concentration, the supramolecular amphiphile formed by the ternary complexation can induce the vesicle formation to the bulk DTAB solution which otherwise remains in micellar state at the applied concentration. To confirm this particular phenomenon, we have prepared an equimolar solution of DDEV, DHN, and CB[8] by sonication and when the light violet color from the charge transfer complex was generated it was added to a preformed micellar solution of DTAB and maintained the final concentration as 15.84 and 0.16

mM for DTAB and DDEV respectively. Upon standing for four days, analysis of this solution revealed the fact that the micellar solution has transformed into vesicles.

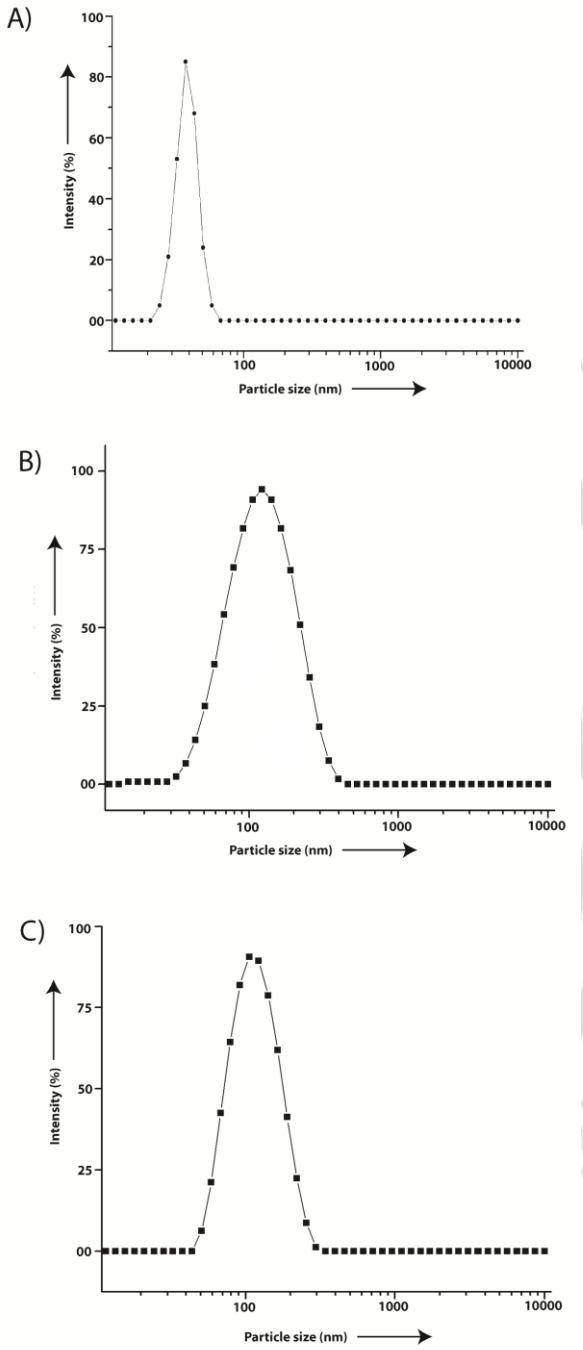

Figure 3.7 Intensity-weighted distributions obtained from DLS measurements of the vesicles formed by 99:1:1:1 tetraalkylammonium bromide-DDEV-DHN-CB[8] in water at 298 K. A) for DTAB, B) DTEAB and C) DTPAB.

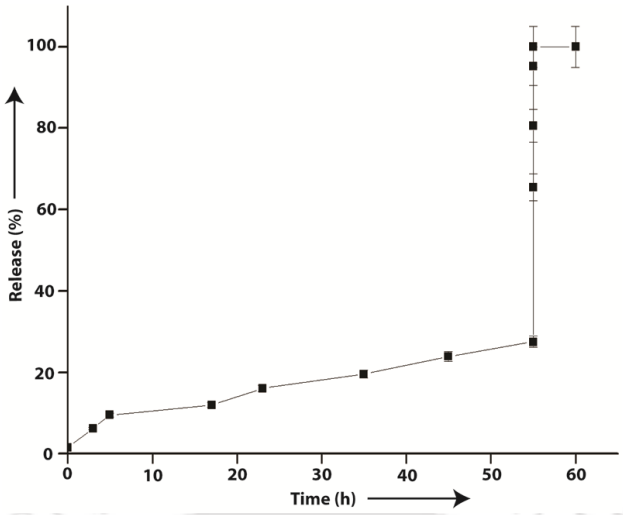

Figure 3.8 Release profile of 5(6)-carboxyfluorescein trapped inside the vesicles formed by 99:1:1:1 DTAB–DDEV–DHN–CB[8] in water at 298 K. [DTAB] = 15.84 mM.

To further generalize the observation, we performed similar experiments using 1% DDEV doped DTEAB and DTPAB. In both cases, the charge transfer bands appeared (data not shown) indicating the formation of the ternary complexes. DLS (Figure 3.7B, C), TEM (Figure 3.6B, C), and dye release studies for both systems (Figure 3.9) show the formation of uniform sized stable vesicles. The diameter of the vesicles increased (30 nm, 106 nm, and 120 nm for DTAB, DTEAB and DTPAB respectively) as the head group size of the surfactant enhanced.

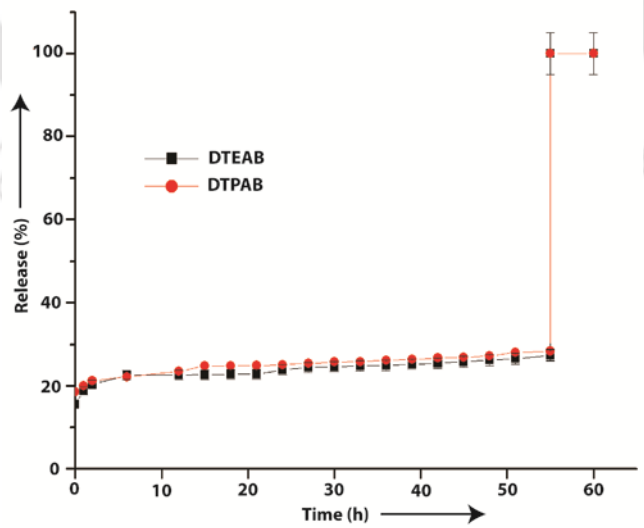

Figure 3.9 Release profile of 5(6)-carboxyfluorescein trapped inside the vesicles formed by 99:1:1:1 DTEAB-DDEV-DHN-CB[8] and 99:1:1:1 DTPAB-DDEV-DHN-CB[8]in water at 298 K. [DTEAB], [DTPAB] = 15.84 mM.

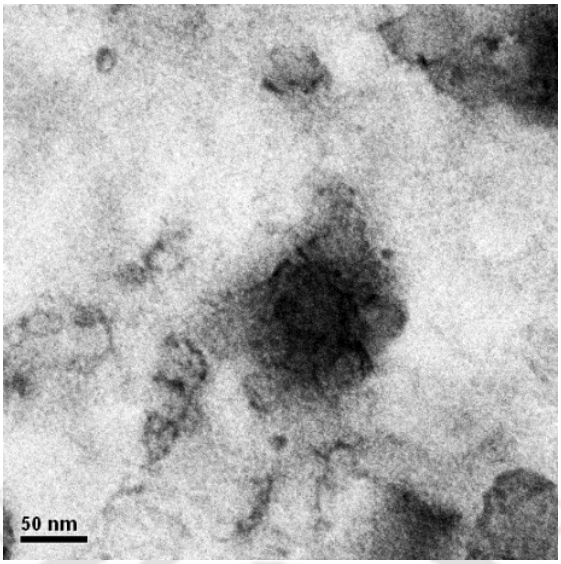

Figure 3.10 TEM image of the solution prepared with 99:1:1:1 DTAB-DDEV-DHN-CB[8] after CAN treatment.

3.3 Conclusions

In summary, in this work, we have shown the mutual sharing of characteristic properties of individual surfactant in the 1% DDEV doped system. The new system allowed us to prepare other types of self-assemblies which are not achievable otherwise. Though DDEV does not have the ability to form w/o-microemulsions, the presence of DTAB in the mixture facilitated the preparation of stable w/o-microemulsions incorporating the redox active viologens in the self-assembled system. Such microemulsions can be further utilized for future applications. When CB[8] and DHN were added to the micellar solution of this 1% DDEV doped DTAB, stable uniform sized vesicles were formed. The vesicles were characterized through TEM, DLS and dye release experiments. The charge transfer mediated ternary complex formation by the viologen surfactant with CB[8] and DHN possibly transforming the micelles to vesicles. Moreover the presence of DTAB allowed the vesicle formation by DDEV even at a submicellar concentration. Though the mechanism behind such micelle to vesicle transformation is not yet understood completely but these findings will certainly be of assistance in future exploration of such systems. Moreover, all these observations associated with 99:1 DTAB-DDEV mixture were found to be true in case of other similar tertraalkylammonium surfactants as well.

3.4 Experimental Section

***3.4.1 Cyclic Voltammetry*:** Cyclic voltammetric experiments were carried out with a CHI680C Amp Booster from CH Instruments Inc. having a glassy carbon as the working electrode, Pt as counter electrode and a Ag/AgCl as reference electrode. Glassy carbon and platinum working electrodes were customarily polished with 0.05-μm alumina prior to use dimethylviologen Before doing each experiment, the solutions were deoxygenated by passing nitrogen gas and inert atmosphere was maintained during the experiments. As a reference, electrochemistry of dimethylviologen was measured under similar working condition and a satisfactory result was obtained (data not shown). For all systems, pre and post micellar concentrations are maintained at 3 and 16 mM respectively.

3.4.2 Preparation of Water-in-oil (w/o)- Microemulsions (W_0 range): Constant amount of surfactants (to reach 0.1 M) and required amount of *n*-hexanol (to get 9:1 isooctane - *n*-hexanol ratio) were mixed in volumetric flasks and isooctane was added to these mixtures to make up the mark, vortexed and put in a constant temperature bath (at 298 K) to attain the temperature. Minimum amount of water was added to these solutions to completely solubilize the systems while maintaining the temperature. Water was then added in small portions till the phase separation or turbidity observed and after every addition, the temperature was maintained at 298 K. The minimum amount of water required to get a clear solution was used to calculate the lowest W_0 value while the amount of water required to destabilize the system provided the highest W_0 value.

3.4.3 Phase Diagram Experiment: Microemulsions were prepared by titrating the mixtures of surfactants, *n*-hexanol, and isooctane with water. A mixture of the surfactant and *n*-hexanol (1:2 mass ratio) was prepared and solubilised with minimum amount of water. Equal amounts of these mixtures were taken in different screw-topped test tubes and different amounts of isooctane were added to them and kept in a constant temperature bath at 298 K. These turbid solutions were then titrated with water to bring clarity. The values of isooctane, water and surfactant-*n*-hexanol were

used to calculate the pseudo-ternary phase boundary between the clear and turbid regions.

3.4.4 Vesicle Preparation: To a volumetric flask (10 mL) containing a measured quantity of DDEV-tetraalkylammonium bromide surfactant, CB[8] and DHN (in 0.3 ml THF) were taken. To these mixtures, water was added to make up the mark. The resulting suspensions after sonication for 1 h at 333 K were kept undisturbed at 298 K for four days to give clear (DTAB, DTEAB) or slightly turbid (DTPAB) light violet colored solutions. The concentrations of each components were maintained as, [DDEV], [CB[8]] and [DHN] = 0.16 mM, [tetraalkylammonium bromide surfactant] = 15.84 mM.

3.4.5 Dye Release Experiment: The vesicles were prepared according to the method mentioned above but in these cases, 10 mg of CF was added to the 10 mL flask prior to the preparation of the samples. The resulting vesicle solutions were passed through Sephadex G-25 to remove the excess dye, diluted and used for fluorescence measurements. The dye release was monitored on a Cary-Eclipse luminescence spectrometer (Agilent) by exciting the solutions at 492 nm and measuring the fluorescence intensity at 512 nm.

3.4.6 Transmission Electron Microscopy (TEM): TEM images were recorded on JEM-2100 microscope. TEM samples were prepared as follows. A drop of the vesicle solution was placed on a copper grid and held in air for 2-3 minutes and then with a tissue paper excess solution was blotted out. With a drop of 2% uranyl acetate solution the sample was negatively stained before removing the excess liquid with a filter paper.

3.4.7 Dynamic Light Scattering (DLS): The particle sizes of the prepared vesicles were measured at 298 K on a zetasizer Nano ZS90 from Malvern using a He-Ne laser 632.8 nm. The samples were prepared as mentioned earlier and used after 10 fold dilution with water.

CHAPTER 4

Dual Self-sorting by Cucurbit[8]uril to Transform a Mixed Micelle to Vesicle

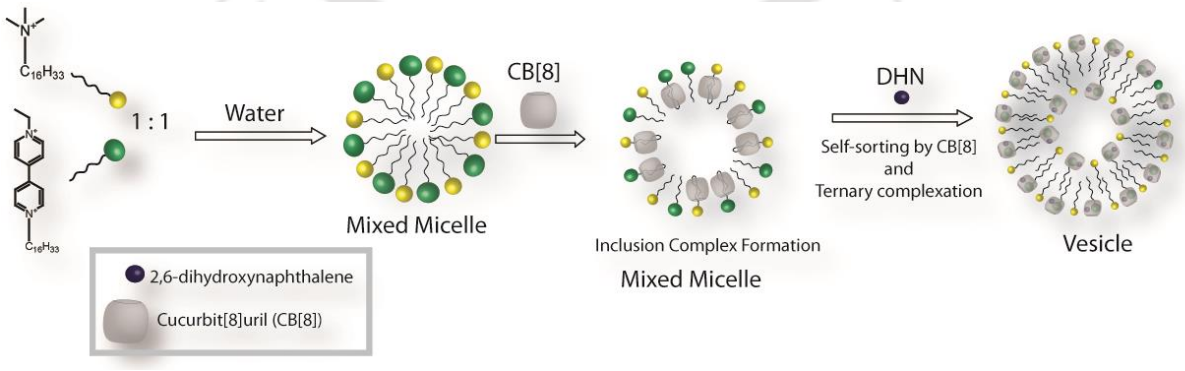

4.1 Introduction

In the previous chapters, we have demonstrated the formation of vesicles by a mixed system of DTAB and *N*-ethyl-*N*'-dodecylviologen dibromide (DDEV) through ternary complexation with CB[8] and DHN. Interestingly, the ternary complex driven vesicle formation was achieved even at a molar ratio of 99:1 (DTAB-DDEV). The high content of DTAB (99%) in this system made it difficult to study the changes based on NMR techniques as the signals from DDEV could not be detected because of its very low population (1%). Based on these observations we envisioned that a mixed micellar system of equimolar ratio might be helpful to investigate the mechanistic detail behind such self-aggregation process. In order to get the insight to the mechanistic detail, ideally we need to work with 1:1:1 mixture of the surfactants and CB[8]. The poor solubility of CB[8] (<0.01 mM in water)[12] makes it difficult to work at the ratio of 1:1:1 using surfactants with higher CMCs. We have also observed that the solubility of CB[8] enhances up to 1 mM in different surfactant solutions. Thus to overcome the difficulty arising from the low solubility of CB[8], we selected the hexadecyl analogues (CTAB and HDEV, Scheme 4.1) of the surfactants having much lower CMCs than their dodecyl analogues.[128,133]

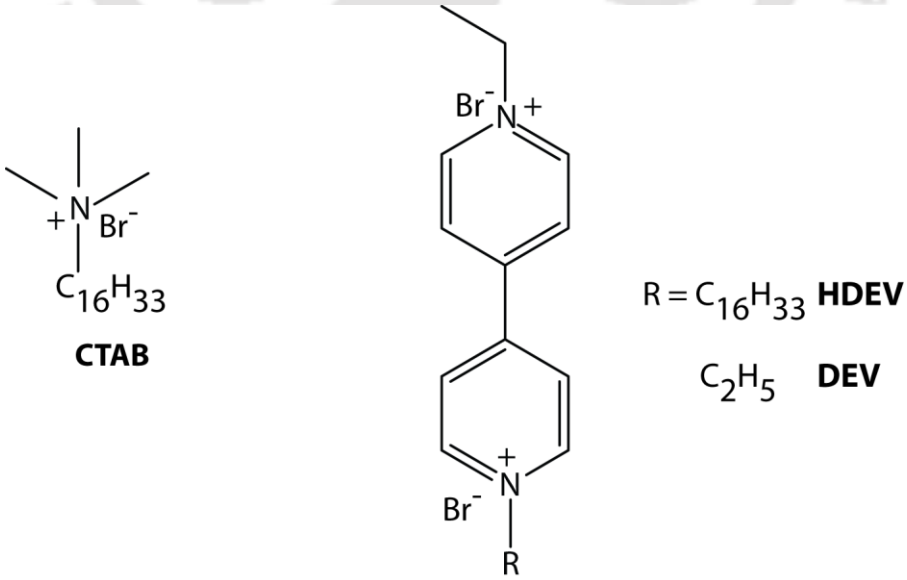

Scheme 4.1 Chemical structures of the surfactants used.

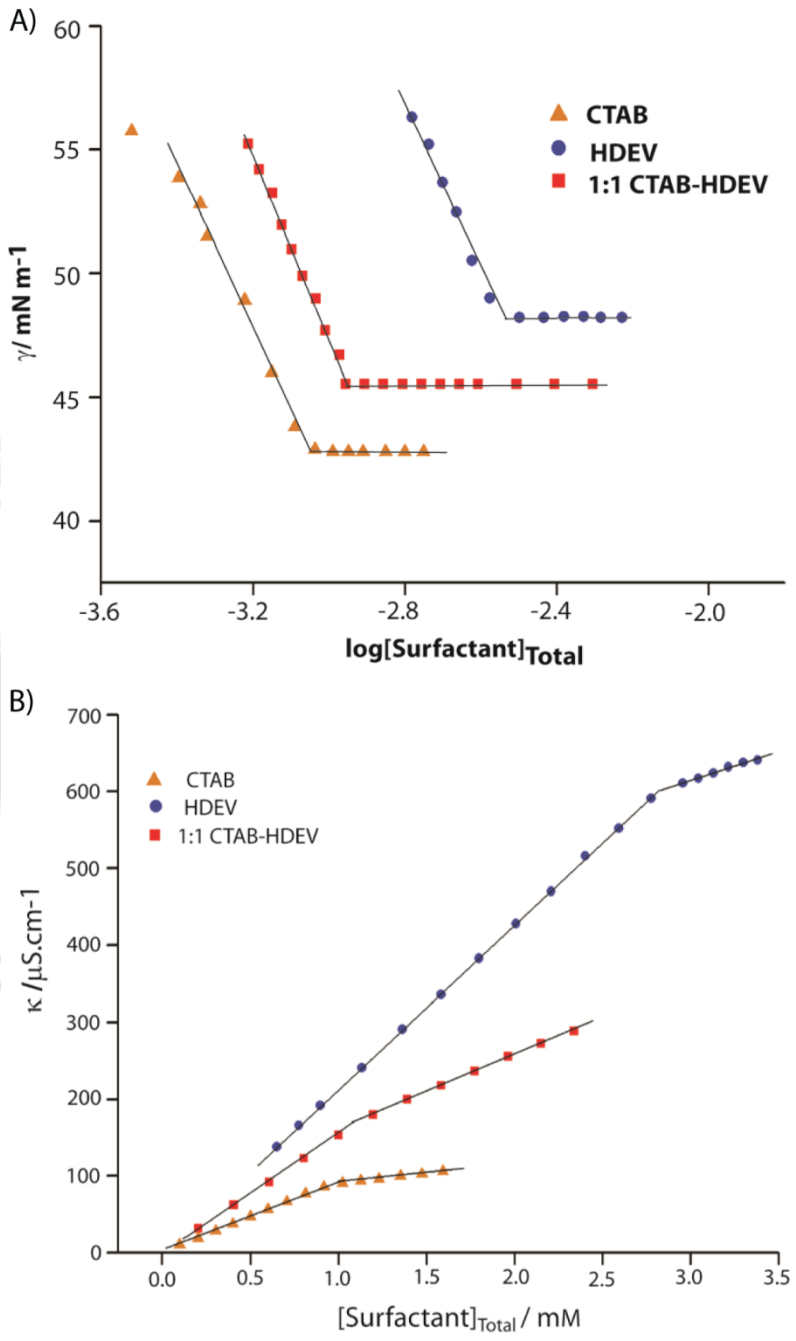

Figure 4.1 Tensiometric (A) and Conductometric (B) determination of the CMCs of CTAB, HDEV and 1:1 CTAB-HDEV at 298 K.

4.2 Results and Discussions

The CMC of the pure and 1:1 mixture of CTAB and HDEV were determined using both surface tension and conductometric methods (Figure 4.1). The average (CMC_{av}) of the values obtained from these two techniques are taken in consideration for all other studies. All the values are listed in Table 4.1.

Table 4.1 CMC values of surfactants and their mixtures determined using surface tension and conductometry at 298 K.

System	CMC (mM) Surface Tension	CMC (mM) Conductometry	CMC_{av} (mM)
CTAB	0.99	1.10	1.05
HDEV	2.77	2.85	2.81
CTAB-HDEV (1:1)	1.17	1.23	1.20
CTAB-HDEV-CB[8] (1:1:1)	1.26	1.34	1.30

4.2.1 Formation of Vesicle Through Ternary Complexation: The vesicles were prepared following the protocol described by Kim where all the components were taken in water and sonicated for one hour prior to incubation at room temperature for one day.[1]

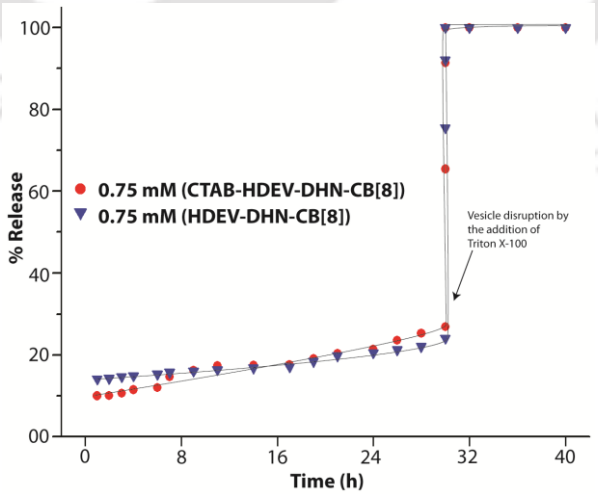

Figure 4.2 Release profile of 5(6)-carboxyfluorescein trapped inside the vesicles formed by different combinations of CTAB, HDEV, DHN and CB[8] in water at 298 K.

The vesicle formation by the 1:1 CTAB-HDEV system in presence of CB[8] (1 equiv.) and DHN (1 equiv.) was evidenced by the entrapment and slow release of a water soluble anionic reporter 5(6)-carboxyfluorescein (CF) over two days (Figure 4.2). The sudden change in the fluorescence intensity was triggered by the addition of Triton X-100 which is known to disrupt vesicles and thus releases the entrapped dye. The slow release of the dye also signifies the stability of the formed vesicles.[13] Another confirmation of the formation of vesicle was obtained by the FESEM image (Figure 4.3) of the solution which shows nearly spherical vesicles. The vesicles formed by mixed surfactant system were observed to be of various sizes (diameter: 500 – 2500 nm) and are much bigger than the vesicles formed by HDEV alone under similar experimental condition (Figure 4.4). The formation of CT complex in the system was evidenced by the appearance of a CT band at 535 nm in the UV spectra of the system which disappeared upon addition of cerium (IV) ammonium nitrate (CAN), an oxidizing agent converting DHN to naphthoquinone and subsequently breaking the CT complex (Figure 4.5). The ESI-MS (Figure 4.6) of the vesicle also confirmed the formation of the ternary complex between HDEV-DHN and CB[8] as a signal appeared at 949.45 (M^{2+}).

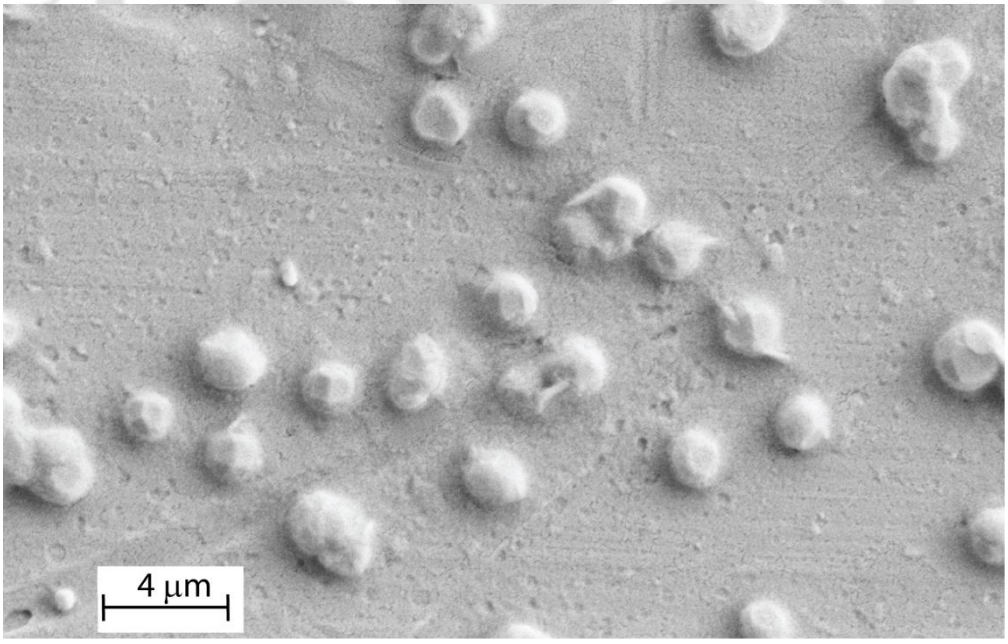

Figure 4.3 FESEM images of 0.75 mM (CTAB-HDEV-DHN-CB[8]) showing larger vesicles.

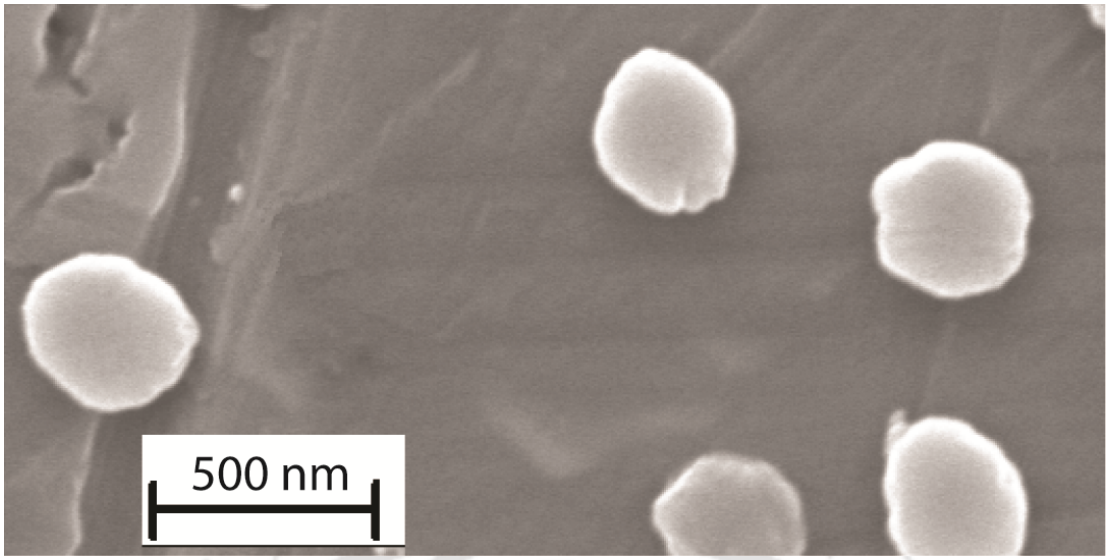

Figure 4.4 FESEM images of 0.75 mM (HDEV-DHN-CB[8]) showing smaller vesicles.

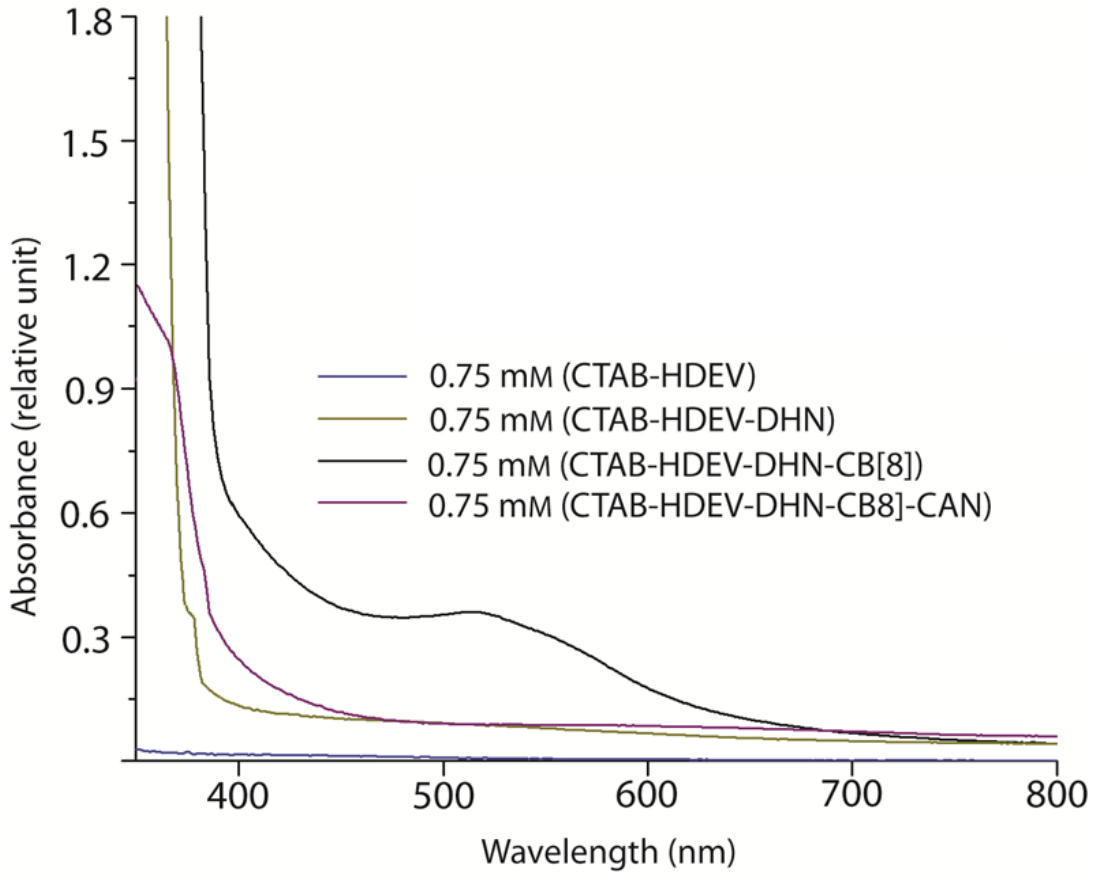

Figure 4.5 UV-Visible spectra of aqueous solutions prepared by the mixture of CTAB, HDEV, DHN, and CB[8] at different combinations at 298 K showing the appearance of the charge transfer band upon formation of HDEV-DHN@CB[8] ternary complex and the disappearance of the same upon treatment with CAN.

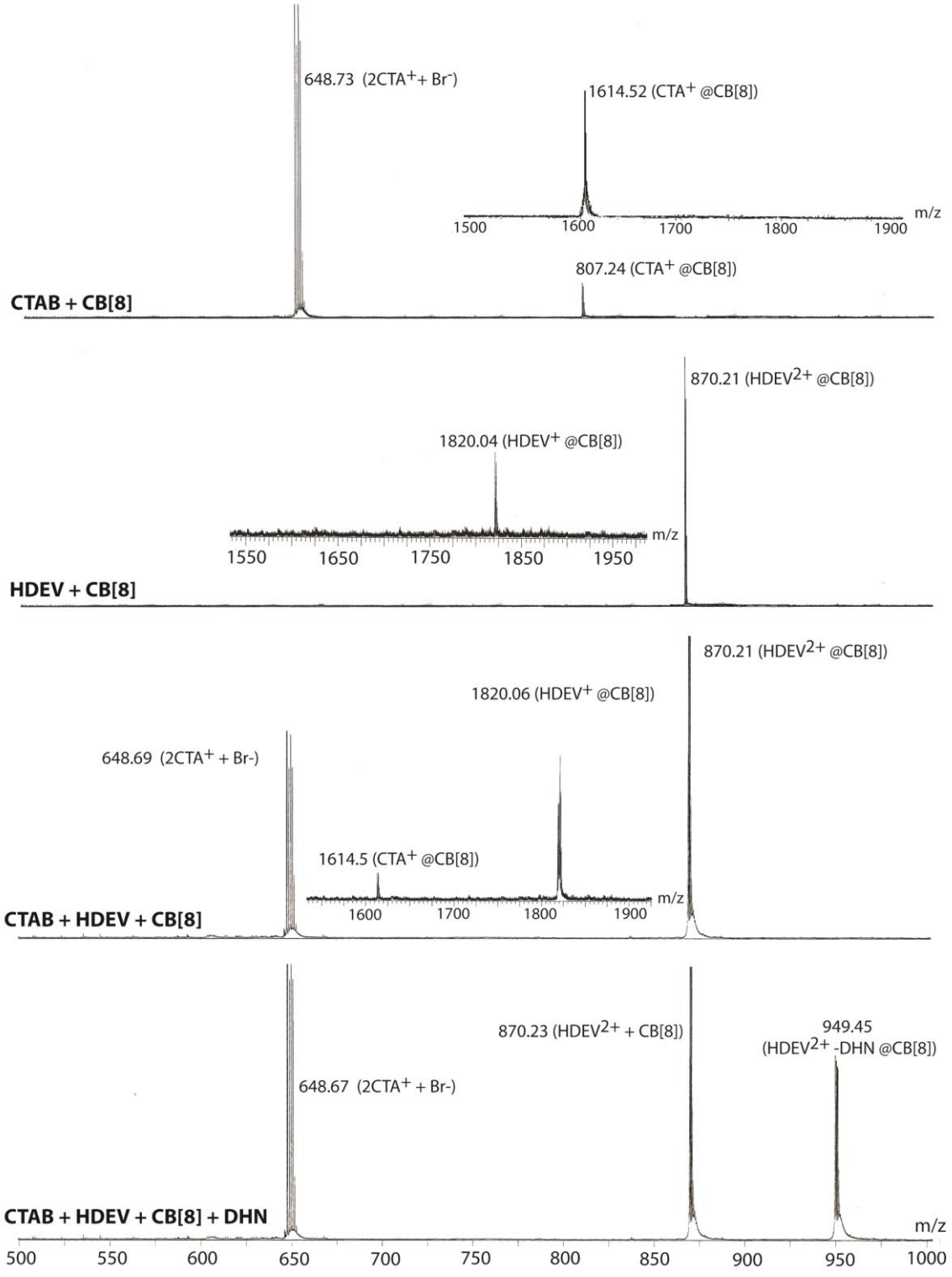

Figure 4.6 ESI-MS spectra of various compositions showing the observed masses of pure surfactants and their binary or ternary complexes. The concentrations of individual components were kept constant at 0.75 mM for all experiments. Insets: expanded mass spectra of the M^+ regions.

4.2.2 Micelle to Vesicle Transformation Irrespective of Method of Preparation: The experimental procedure for the preparation of vesicle through ternary complexation adopted by Kim involves the mixing of all the components (surfactant, CB[8], and DNH) together in water followed by sonication and incubation.[101] A fundamental question arises at this point whether the CB[8] assisted vesicle formation depends on the experimental procedure or it is a micelle to vesicle transformation that happens independent of the order of addition of the second guest (DHN). To verify, we have premixed the surfactants in water to get an overall surfactant concentration of 1.5 mM. To this mixed micellar system, CB[8] was added and sonicated for six hours to achieve the inclusion complex as well as reach a 1:1:1 molar ratio of CTAB, HDEV, and CB[8]. CF was mixed in this solution followed by dividing the solution in two parts (Solutions A and B). In solution A, was added one equivalent of DHN and both the solutions (A and B) were sonicated for one hour and allowed to stand for two days. Simultaneously, another solution (C) was prepared where all the ingredients were mixed together in water to get exactly the same concentration ranges as in case of solution A and sonicated for one hour followed by standing for two days. The emission spectra recorded for all three solutions showed that the intensity of the emission peaks (λ_{em}= 512 nm) were significantly lower in case of A and C than that of the solution (B) (Figure 4.7). The intensity enhanced significantly in case of solution A and C upon addition of Triton X-100 and showed similar value as in case of solution B. These results indicate the entrapment of the dye and hence the formation of vesicles in case of solution A and C but not in case of B where it remain in micellar form. When the dye release profiles of solution A and C were recorded, both showed similar results. The entrapment of the dye in case of solution A and C suggests formation of vesicle and the process is independent of the order of addition of DHN. This is a clear indication of the micelle to vesicle transition aided by the ternary complexation by CB[8], viologen unit and DHN. Similar experiments with HDEV alone also provided alike results.

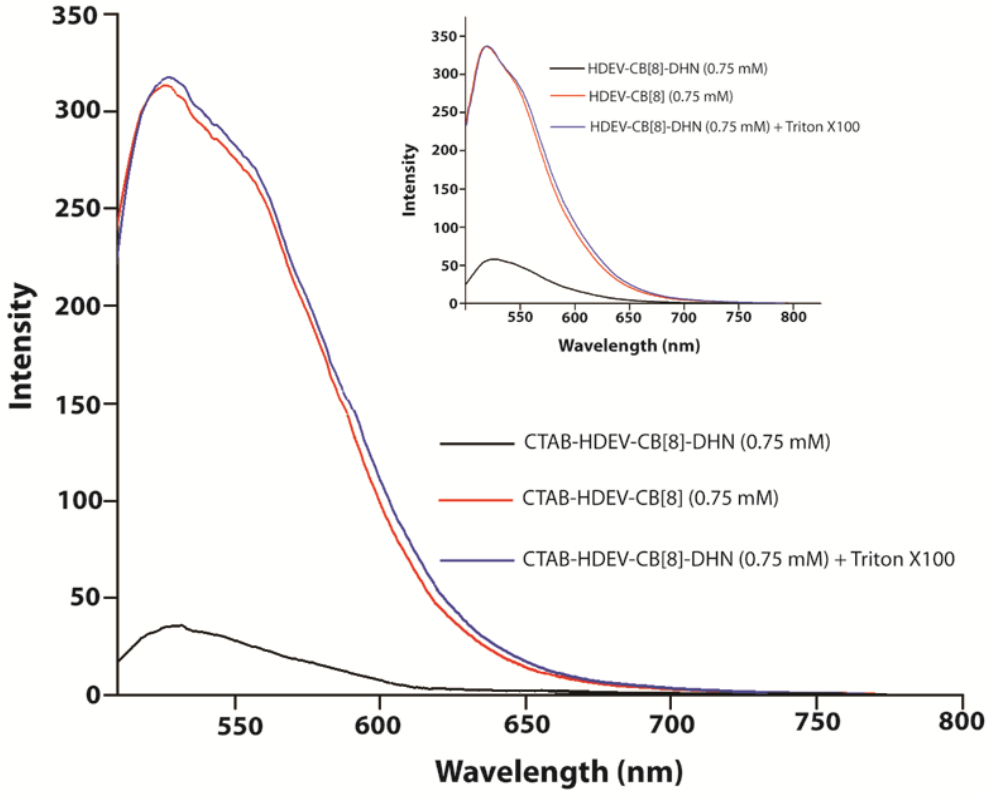

Figure 4.7 Flurescence spectra of CF in the micelles and vesicles formed by CTAB-HDEV-CB[8] and CTAB-HDEV-DHN-CB[8] and after the addition of Triton-X100 into the vesicle. Inset: the same with HDEV alone (in absence of CTAB).

4.2.3 Binary Complexes: U-shaped Binding of Surfactants with CB[8]: The binding of CB[8] with amphiphiles like DTAB, as reported by Kim shows a 1:1 complex with U-shaped conformation of the alkyl chain inside the macrocyclic host.[96] However, no report on the binding pattern of the viologen amphiphiles with CB[8] has so far been published. Moreover, the report on the DTAB binding is also studied at a concentration (0.0043 mM)[96] much lower than the CMC (14.90 mM)[134] of DTAB which again does not provide any information on the self-assembly of the CB[8] bound DTAB. In order to understand the vesicle formation through ternary complexation, a systematic demonstration of the binding of CB[8] with the amphiphiles in pure and mixed conditions is required. We sought to employ ^{1}H, and diffusion-ordered (DOSY) NMR, and ESI-MS techniques to evaluate the binding of the surfactants with CB[8].

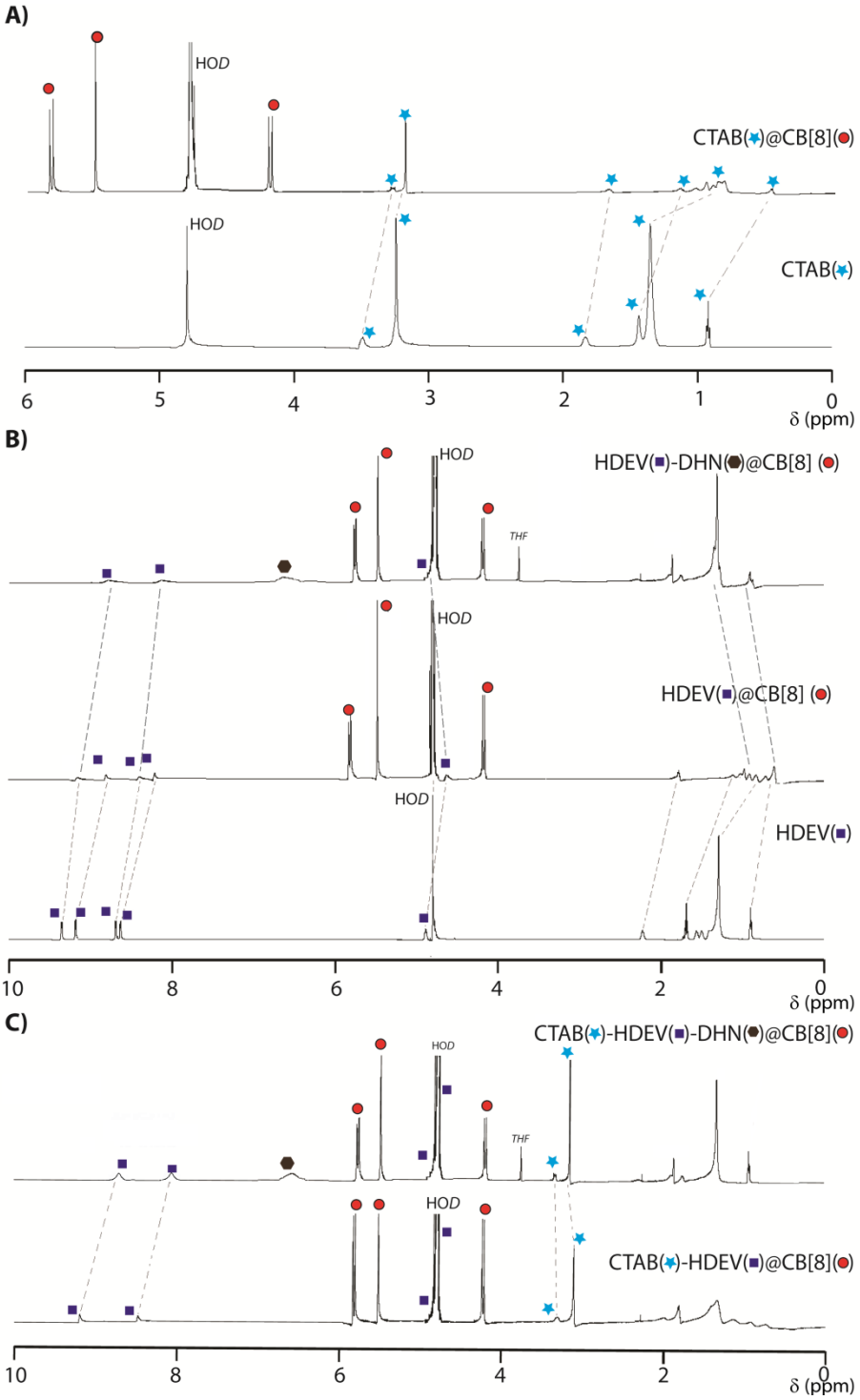

Figure 4.8. ^{1}H NMR spectra of various compositions showing the chemical shifts of protons upon complexation. A) CTAB and CTAB@CB[8]; B) HDEV, HDEV@CB[8], and HDEV-DHN@CB[8]; C) CTAB-HDEV@CB[8] and CTAB-HDEV-DHN@CB[8]. The concentrations of individual components were kept constant at 0.75 mM for all experiments.

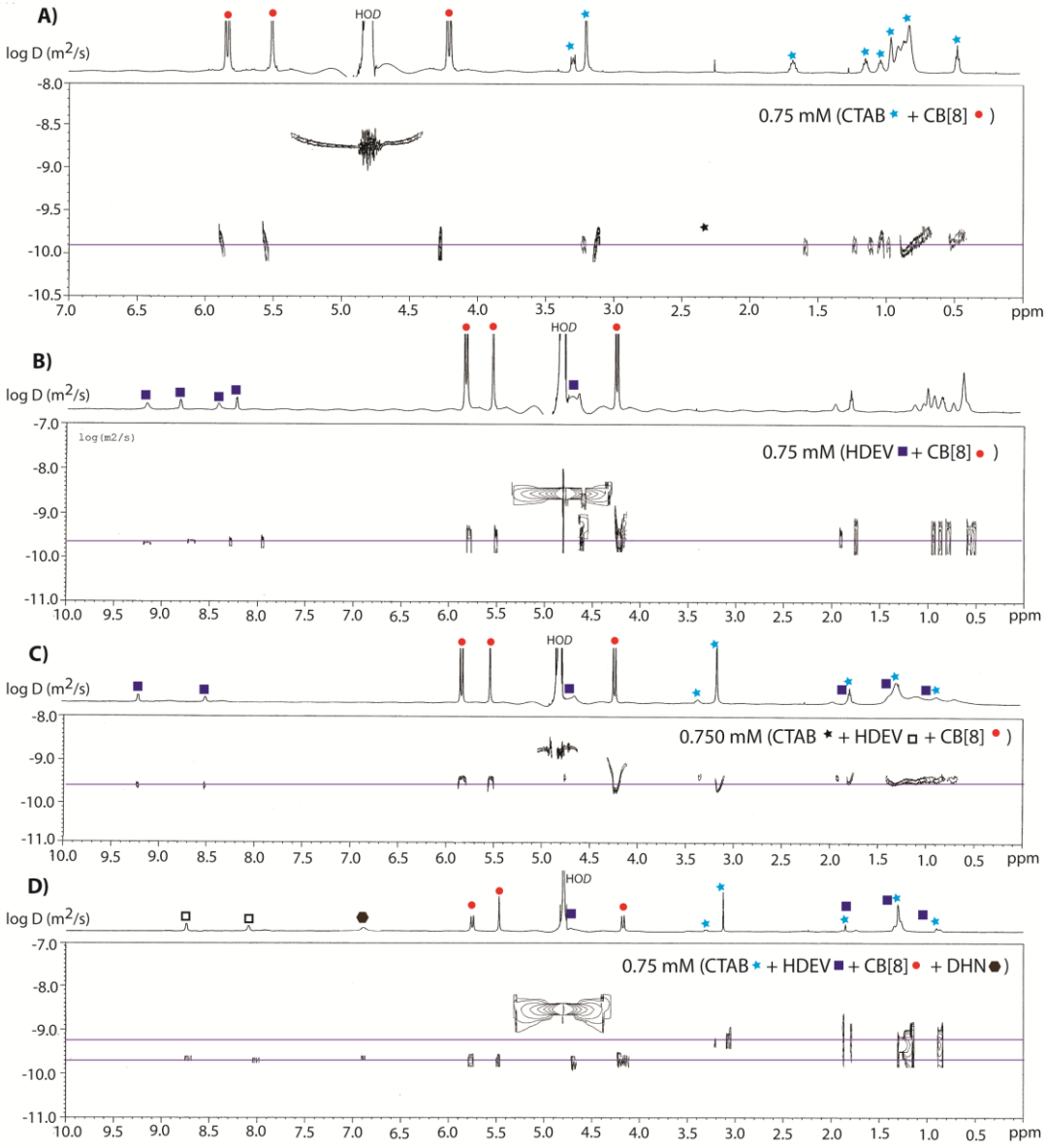

Figure 4.9 DOSY spectra of various compositions showing the diffusion of the components. A) CTAB and CTAB@CB[8]; B) HDEV and HDEV@CB[8]; C) CTAB-HDEV@CB[8] and D) CTAB-HDEV-DHN@CB[8]. The concentrations of individual components were kept constant at 0.75 mM for all experiments.

Similar to Kim's observation, an U-shaped conformation of the hydrophobic tail inside the CB[8] cavity has been observed in case of both CTAB and HDEV separately.[96] A considerable upfield shift (0.1-0.5 ppm) of all the protons from the hydrocarbon chains including the terminal methyl group (0.5 ppm) indicates the deep burial of the aliphatic tail inside the cavity of CB[8] (Figure 4.8A, B).[96] The ESI-MS of these complexes also showed the presence of 1:1 surfactant@CB[8] complexes (Figure 4.6).

Similarly in the mixed micellar system, both the peaks (CTA^+@CB[8], and $HDEV^{2+}$@CB[8]) were observed (Figure 4.6C) indicating a distribution of CB[8] within the surfactants present in the system. The distribution of CB[8] within the surfactants to form surfactant@CB[8] binary complexes is also confirmed from the ^1H NMR spectrum of this composition. The upfield shift of characteristic peaks in each case indicates the formation of inclusion complexes with CB[8] (Figure 4.8C). In the DOSY spectra, the diffusion coefficients of the surfactants and CB[8] were observed to be same in these cases pointing toward the formation of the binary complexes (Figure 4.9A, B, and C).[135] Interestingly, in case of the mixed system (Figure 4.9C), all three components showed same log D value (-9.61 m^2S^{-1}) signifying the distribution of CB[8] among the surfactant molecules present in the system. The distribution of CB[8] among the surfactants could be explained in terms of their similar binding constants K_a (2.0 (± 0.1) × 10^5 M^{-1} for CTAB and 2.3 (± 0.1) × 10^5 M^{-1} for HDEV, Figure 4.10, Table 4.2) as determined from isothermal titration calorimetry. Both surfactants showed 1:1 binding and similar affinity toward CB[8] which is also reflected in their 1:1 mixture where CB[8] was found to be distributed among the surfactants.

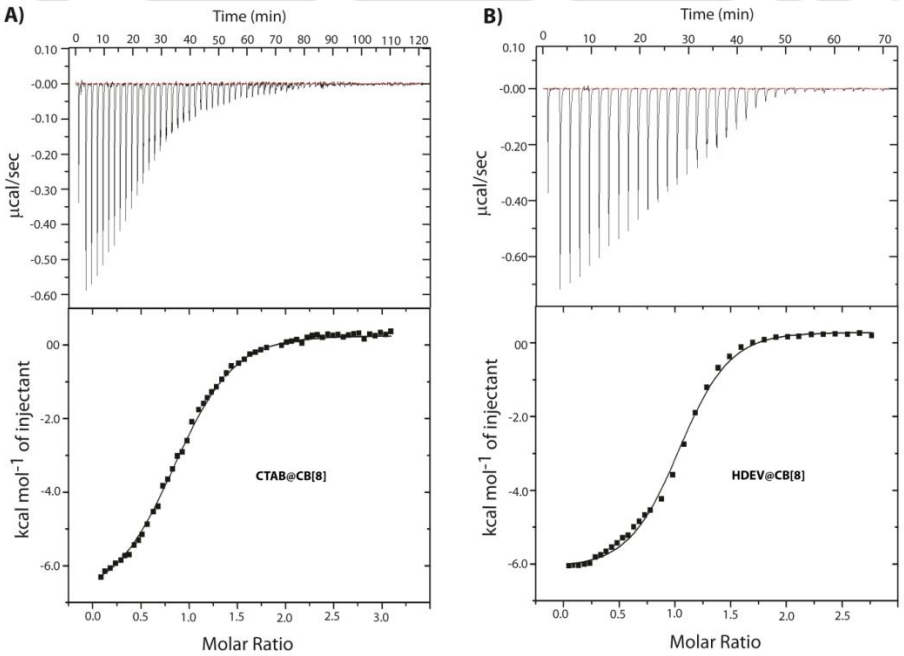

Figure 4.10 Thermograms (top) and binding isotherms (bottom) of CB[8] with (A) CTAB and (B) HDEV at 298 K.

Table 4.2 Binding constants (K_a) and related thermodynamic parameters for the complexation of CTAB and HDEV with CB[8] at 298 K in 100 mM phosphate buffer pH 7.

Guest	K_a [M^{-1}]	$\Delta H°$ [kj mol^{-1}]	$T\Delta S°$ [kj mol^{-1}]
CTAB	$(2.0 \pm 0.1) \times 10^5$	-27.1± 0.1	2.97± 0.1
HDEV	$(3.8 \pm 0.1) \times 10^5$	-25.3± 0.1	6.5 ± 0.1

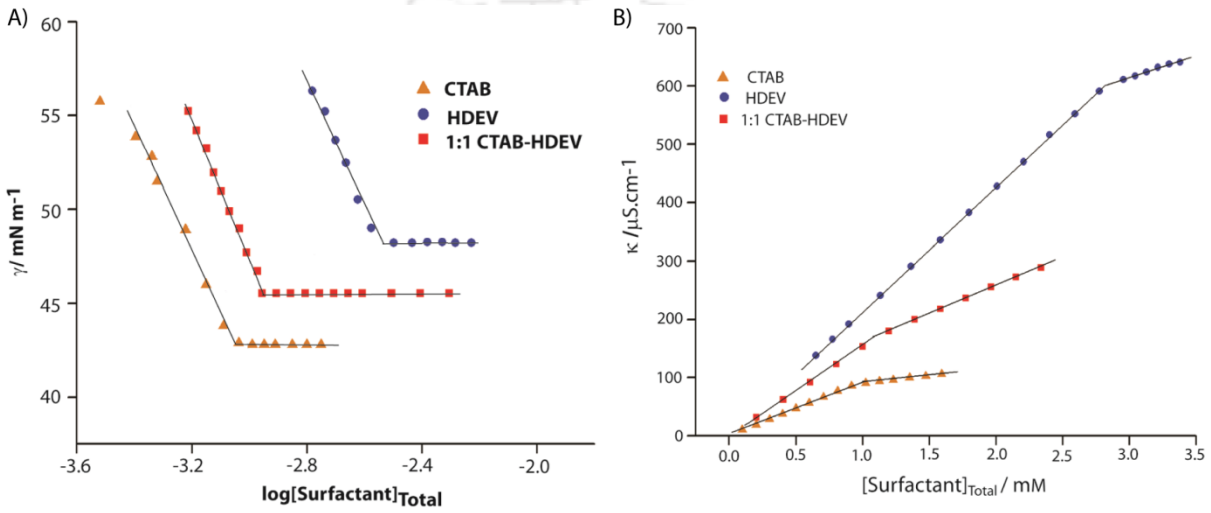

Figure 4.11 Tensiometric (A) and conductometric (B) determination of the CMC of 1:1:1 CTAB-HDEV-CB[8] mixture at 298 K.

A fundamental question arises at this point about the status of the self-assembly of this composition (1:1:1 CTAB-HDEV-CB[8]), whether the presence of the host disrupt the micellar assembly due to the binary complexation or does it still remain in the micellar form. To understand the situation, we have measured CMC of the ternary mixture of CTAB-HDEV-CB[8] (1:1:1) using surface tension and conductometric methods (Figure 4.11). In both cases a small change in the CMC value is observed as the CMC_{av} is shifted from 1.20 mM to 1.30 mM. Similar enhancement in the CMC values of surfactants in presence of CBs have also been reported recently.[98] The same article has also proposed the incorporation of CB bound surfactant complexes inside the micellar structure. Unfortunately, the particle size measurements of the systems by DLS technique produced irreproducible, erroneous results probably due to the absorption property of the viologen unit. In this regard, the particle sizes were

measured for CTAB micellar systems containing various amounts of CB[8] (Figure 4.12). Interestingly, the size of the micelles increased with increase in the CB[8] content and at a higher concentration (0.75 mM CB[8] in 4 mM CTAB) giant micelles[136,137] with more than 100 nm sizes were observed. Such large micelles formed by CTAB can only be achieved at high concentration or in presence of additives where the additives act as a co-solute or co-surfactant. As the concentration of the surfactant is not high enough to create such arrangement, the CTAB@CB[8] binary complexes presumably get incorporated inside the micelles and consequently increased the size. Under such circumstances, it is likely to attain a non-spherical geometry which is otherwise not possible.[136] Though it is not possible to detect the sizes and shapes of the systems containing HDEV owing to non-availability of Cryo-TEM facility, we may assume similar self-organization in those systems as well. These results, though indirect, indicates the probable location of the binary complexes inside these giant micelles.

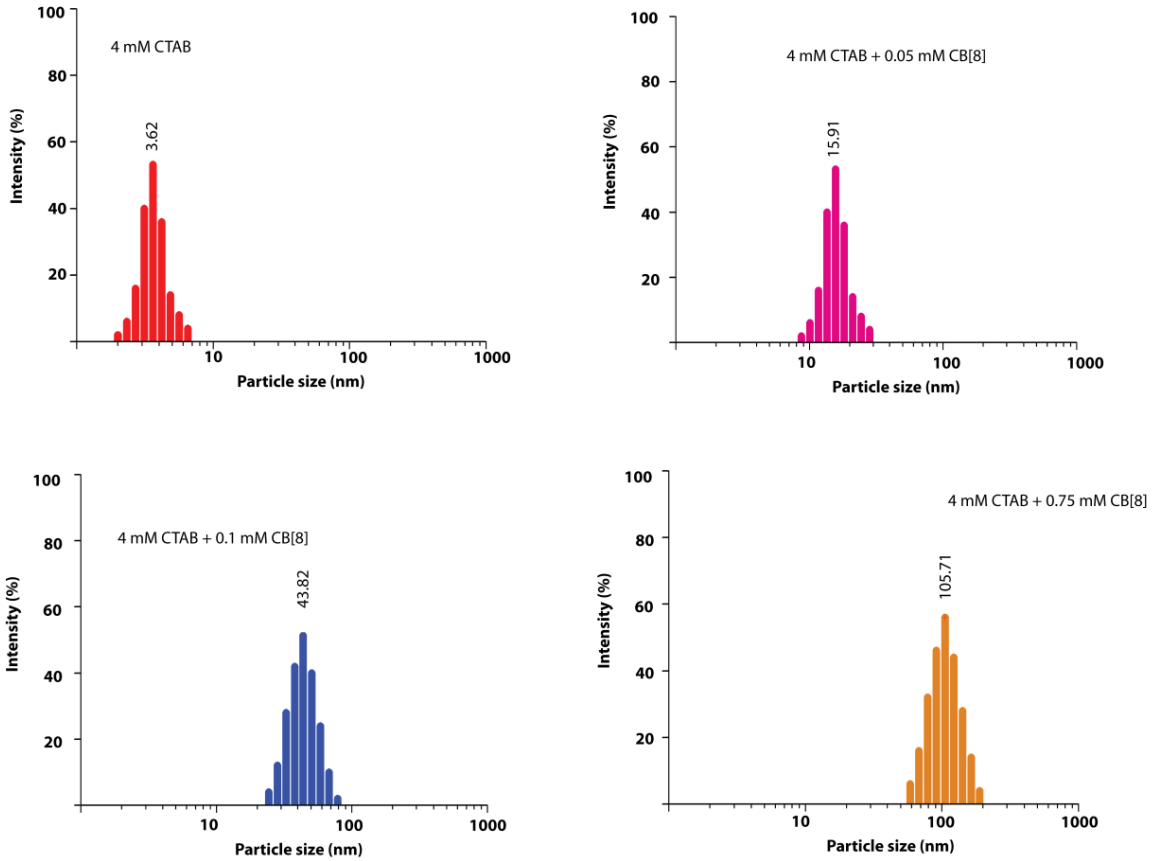

Figure 4.12 Intensity-weighted distributions obtained from DLS measurements of CTAB and CTAB-CB[8] systems.

4.2.4 Ternary Complexation: Self-sorting by CB[8] Within HDEV Molecule: Introduction of DHN in the HDEV@CB[8] solution leads to the formation of a charge transfer mediated ternary complex (HDEV-DHN@CB[8] as evident from the appearance of the CT band at 535 nm in the UV spectra (Figure 4.5). Investigating the processes involved in the transformation of the micelles to vesicle revealed some interesting features. We have employed individual surfactants as well as the 1:1 mixed micellar systems for the investigation and kept the individual concentrations of each component fixed at 0.75 mM for all the experiments. The ^{1}H NMR spectrum showed no further shift of any characteristic peak of CTAB suggesting no ternary complexation in this case. The FESEM images of the same also showed no trace of any vesicle. Similar experiments with pure HDEV showed the formation of vesicles (~400 nm diameter, Figure 4.4) even though the concentration of HDEV (0.75 mM) is much lower than its CMC (2.81 mM). The comparative analysis of the ^{1}H NMRs of the 0.75 mM HDEV@CB[8] and HDEV-DHN@CB[8] (Figure 4.8) shows a further up-field shift ($\Delta\delta$ = 0.1-0.3 ppm) of the viologen protons in presence of DHN. Moreover, the peaks corresponding to the protons from aliphatic chain shifted back to their original positions as in free HDEV. The ternary complex formation is further confirmed by the DOSY NMR where all three components showed similar diffusion coefficients (log D = -9.65 m^2S^{-1}, Figure 4.9). These observation indicates a movement of CB[8] from the hydrocarbon tail to the viologen unit. The ITC experiment for the ternary complexation could not be performed as the process was found to be very slow for the experimental time scale. Considering similar binding constants for MV-DHN@CB[8] ($5.9 \pm 0.5 \times 10^5$ M^{-1}) [43] and HDEV-DHN@CB[8], the binding constant for the ternary complex is considerably higher than the binary complex of HDEV@CB[8]. The higher affinity toward the formation of ternary complex certainly favors the self-sorting[138,139] mechanism of CB[8] to move toward the viologen head group.

4.2.5 Ternary Complexation: Self-sorting by CB[8] Between HDEV and CTAB: In case of the 1:1 CTAB-HDEV mixture, upon addition of DHN similar CT band was observed in the UV-visible spectra indicating the ternary complexation. Interestingly, the ^{1}H NMR showed de-complexation of the CTAB@CB[8] binary complex as all the characteristic

CTAB peaks moved back to their respective chemical shift positions as in free CTAB (Figure 4.8C). The de-complexation is further evidenced from the DOSY spectra (Figure 4.9D) of the CTAB-HDEV-CB[8]-DHN mixture which clearly shows two separate diffusion coefficients, one for CTAB (log D = -9.2 m^2S^{-1}) and the other for HDEV-DHN@CB[8] ternary complex (log D = -9.65 m^2S^{-1}). Further evidences were obtained from the ESI-MS analysis of the mixture. The ESI-MS spectrum (Figure 4.6D) showed signals corresponding to the HDEV-DHN@CB[8] (949.45, M^{2+}) and HDEV@CB[8] (870.21, M^{2+}). Though a signal for CTAB (648.67, $2CTA^+ + Br^-$) was obtained, no signal corresponding to the CTAB@CB[8] could be seen even after thorough analysis of the spectrum. Importantly, under similar experimental conditions, signals corresponding to CTAB@CB[8] were observed for both CTAB-CB[8] as well as CTAB-HDEV-CB[8] mixture (Figure 4.6C). All these results certainly indicate the involvement of self-sorting mechanism and selectivity of CB[8] as it prefers to form the ternary complex over the CTAB@CB[8] binary complex. It is important mentioning that similar results were obtained irrespective of the method of solution preparation.

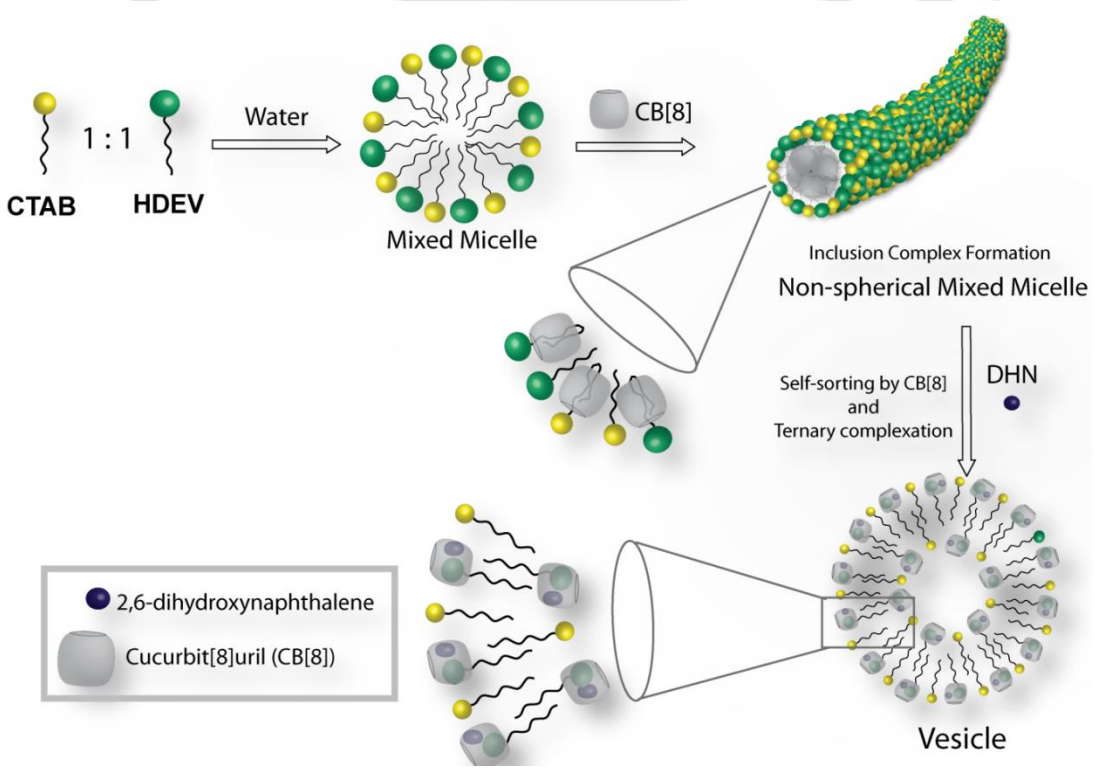

Figure 4.13 Pictorial presentation of the stepwise formation of the vesicles from the mixed micellar system involving self-sorting by CB[8].

4.2.6 The Stepwise Processes: The process of the micelle to vesicle transformation for CTAB-HDEV-CB[8]-DHN system thus can be delineated along the following way, (a) Formation of binary complex between CB[8] and the surfactants leading to U-shaped encapsulation of the hydrophophic tail inside the host cavity; (b) no quantifiable selectivity is shown by CB[8] for any particular surfactant; (c) in spite of the formation of such binary complexes, the system remains in micellar form and most likely obtained non-spherical larger geometry; (d) addition of DHN into this system leads to the formation of a CT complex inside the cavity of CB[8] with the viologen head group of HDEV. This process involves two types of self-sorting by CB[8], (i) in HDEV@CB[8], the host moves to the polar head group leaving the tail free from its cavity, (ii) the CTAB@CB[8] complex breaks down and the host forms complex with the viologen head groups of the remaining HDEV molecules; (f) the charge transfer complex mediated ternary complex leads to the transformation of the micelles to vesicles. The overall process can be pictorially visualized as shown in Figure 4.13.

4.3 Conclusions

The systematic study depicted herein discloses many inherent mechanistic features involved in the micelle to vesicle transformation of a mixed micellar system containing HDEV and CTAB in presence of CB[8] and DHN. Both HDEV and CTAB were found to be forming U-shaped inclusion complexes with CB[8] separately as well as in the mixture. In the 1:1 mixture, CB[8] showed no selectivity toward a particular surfactant. The formation of the binary mixture eventually enhanced the CMC of the system and upon addition of DHN to this mixture (CTAB-HDEV-CB[8], 1:1:1), a step wise ternary complex formation occurred involving two types of self-sorting by CB[8]. This ternary complex consequently led to the formation of the vesicles. Though the exact mechanism involved in stabilizing the vesicles by ternary complexation is not clearly understood, nevertheless the findings from this study contribute a stride further towards understanding such processes and designing new systems for future applications.

4.4 Experimental Section

4.4.1 Materials:

Analytical grade CTAB from Spectrochem (India) was recrystallized three times from methanol/ ether, and the recrystallized CTAB was without minima in its surface tension plot. 1-bromohexadecane, 4,4'-bipyridyl, 5(6)-carboxyfluorescein (CF), D_2O, CF_3CO_2D, and D_2SO_4 were obtained from Sigma-aldrich (USA) and used as received. All other chemicals, reagents and solvents were procured from Merck, India and Spectrochem, India. All surfactants were recrystallized before doing the experiments. For preparing samples, Milli-Q water with conductivity of less than 2 $\mu S.cm^{-1}$ was used. UV-visible spectra of the vesicles were recorded on Lambda 35 (Perkin-Elmer) spectrometers. ESI-MS was performed by using a Q-Tof Premier Quadrupole mass spectrometer (Micromass).

4.4.2 Synthesis:

Cucurbit[8]uril (CB[8]): CB[8] was synthesized following a previously published protocol.[25] ^1H NMR (600 MHz, $D_2O/CF_3CO_2D/D_2SO_4$ (1:1:0.15)): δ 4.25 (d, 16H), 5.55 (s, 16H), 5.86 (d, 16H); MS (ESI): m/z 1461.41 (CB[8] + Cs)+.

HDEV:

1g of 4, 4'-dipyridyl was mixed with 5 mL ethyl bromide in dichloromethane and refluxed for three days and excess (0.5 ml) ethylbromide was added after every 6h. A yellow precipitate formed. The volatiles were removed on a rotory evaporator before washing the residue several times with toluene and finally with diethylether to get a yellow solid as mono-ethylviologen (yield: 95%). The purity of the product was confirmed by ^1H NMR spectroscopy. The obtained solid was then further alkylated on the other pyridyl group by taking it in 7:3 acetonitrile/methanol and refluxing the mixture in presence of 1.5 equiv. of 1-bromohexadecane for 24 h. The precipitate obtained was filtered and washed several times with toluene followed by diethylether. The surfactant was further purified by recrystalizing it three times from

methanol/diethylether (Yield: 70%).^{1}H NMR (600 MHz, D_2O) δppm = 9.39 (d, 2H), 9.24 (d, 2H), 8.73 (d, 2H), 8.68 (d, 2H), 4.94 (br, 2H), 4.84 (br, 2H), 2.26 (br, 3H), 1.75 (m, 2H) 1.45 (br, 26H), 0.95 (t, 3H); E.A : calculated for $C_{28}H_{46}Br_2N_2$: C, 58.95; H, 8.13; N, 4.91. Found : C, 58.88; H, 8.17; N, 4.94; MS (ESI): m/z calcd for $[M-Br]^+$ $C_{28}H_{46}N_2Br$: 489.28, found: 489.35.

DEV:

Excess (10 equiv.) ethylbromide was mixed with 4,4'-dipyridyl in a glass tube and the mouth of the tube was sealed. The tube was heated to 80 °C for 24 h. After cooling down to room temperature the seal was broken and the material was concentrated on a rotory evaporator and the residue was crystallized three times from methanol-diethylether to get a yellow solid (Yiled: 35%). ^{1}H NMR (400 MHz, D_2O) δ 9.15 (d, 4H), 8.56 (d, 4H), 4.77(m, 4H), 1.73 (t, 6H); E.A : calculated for $C_{14}H_{18}Br_2N_2$: C, 44.95; H, 4.85; N, 7.49. Found : C, 44.92; H, 4.87; N, 7.52; MS (ESI): m/z calcd for $[M-Br]^+$ $C_{14}H_{18}N_2Br$: 293.06, found: 293.15.

4.4.3 Methods

4.4.3.1 Surface tension

The surface tension of the surfactants at the air/water interface was measured using a tensiometer (Jencon, India) by the du Noùy ring detachment method. Previously prepared concentrated aqueous solutions of the surfactants were added progressively with a Hamilton syringe to a measured quantity of water, gently stirred for 2 minutes and kept in a constant temperature bath at 298 K for 10 minutes without disturbing to reach equilibrium. The surface tensions of these solutions were then measured in triplicate while maintaining the temperature.

For the measurement of the CMC of CTAB-HDEV-CB[8] (1:1:1) mixture, a solution of 1 mM strength (for each component) was prepared by mixing the appropriate amount of each component in water followed by sonication for 6h. The surface tension of the solution was recorded. Measured quantity of water was added progressively to this solution and stirred for 10 mins and allowed to equilibrate for another 10 mins at 298K before measuring the surface tension.

4.4.3.2 Conductance

The conductance of the surfactant solutions were measured using a Cyberscan Con-510 (Eutech) conductivity meter with cell constant of 1 cm^{-1}. After adding concentrated stock solutions of surfactants to a measured quantity of water, the solutions were stirred for 2 minutes and kept without disturbance for 10 minutes in a constant temperature bath before each measurement.

For the measurement of the CMC of CTAB-HDEV-CB[8] (1:1:1) mixture, a solution of 1 mM strength (for each component) was prepared by mixing the appropriate amount of each component in water followed by sonication for 6h. The conductance of the solution was recorded. Measured quantity of water was added progressively to this solution and stirred for 10 mins and allowed to equilibrate for another 10 mins at 298K before measuring the conductance.

4.4.3.3 Vesicle preparation

To a volumetric flask (10 mL) containing a measured quantity of surfactants (for CTAB, 2.73 mg, for HDEV, 4.3 mg), CB[8] (12.8 mg, the overall molecular weight observed for the used CB[8] was 1730 from the elemental analysis data) and DHN (1.2 mg) was added 0.3 mL THF. To these mixtures, water was added to make up the mark. The resulting mixtures after sonication for 1 h at 333 K were kept undisturbed at 298 K for one day to give clear light violet colored solutions before utilizing for further experiments.

4.4.3.4 Dye Release experiment

The vesicles were prepared according to the method mentioned above but in these cases, a measured amount of CF (0.1 mg) was added to the 10 mL flask prior to the preparation of the samples. The resulting vesicle solutions were passed through Sephadex G-25, diluted and used for fluorescence measurements. The dye release was monitored on a Cary-Eclipse luminescence spectrometer (Agilent) by exciting the solutions at 492 nm and measuring the fluorescence intensity at 512 nm.

4.4.3.5 NMR spectroscopy

^{1}H NMR and DOSY spectra were recorded on a NMR-Bruker Ascend^{TM} 600 MHz (Bruker,Coventry, UK). Spectra were recorded in heavy water (D_2O) at 298 K. The concentration of all the components were fixed at 0.75 mM for all the samples. The experiments were processed with standard Bruker 1D and 2D DOSY softwares.

4.4.3.6 Field Emission Scanning Electron Microscopy (FESEM) and Scanning Electron Microscopy (SEM)

FESEM and SEM images were recorded on Zeiss (Sigma) microscope and LEO1430VP microscope respectively. Samples were prepared by casting a drop of the vesicle solution on a glass slide and dried under ambient condition.

4.4.3.7 Isothermal Titration Calorimetry (ITC)

The formation constants and thermodynamic parameters for the inclusion of CTAB and HDEV in CB[8] were determined by isothermal titration calorimetry using a Nano-ITC instrument from MicroCal. CB[8] solutions (0.1 mM) in buffer (100 mM phosphate, pH 7) was placed in the reaction cell (volume = 200 mL). Injections of CTAB and HDEV solutions (each injection, 0.5 µL, 2.0 mM) were added from a 40-µL microsyringe at an interval of 2 min into the CB[8] solutions with stirring at 600 rpm (CTAB) and 750 rpm (HDEV) at 298 K. The data were fitted to a theoretical titration curve using software supplied by Microcal, with K_a (M^{-1}), $\Delta H°$(kJ mol^{-1}) and $T\Delta S°$(kJ mol^{-1}) as adjustable parameters.

4.4.3.8 Dynamic Light Scattering (DLS)

The particle sizes of the samples were measured at 298 K on a Zetasizer Nano ZS90 from Malvern using a 632.8 nm He−Ne laser. The samples were prepared by dissolving appropriate amount of CTAB and CB[8] in water followed by sonication for 6h. Prior to measurements, the samples were filtered through filters having 0.45 µm pore size.

CHAPTER 5

Aromatic Amino Acids as a Second Guest for CB[8] Induced Vesicle Formation : Development of a Multi-Stimuli Sensitive Vesicle

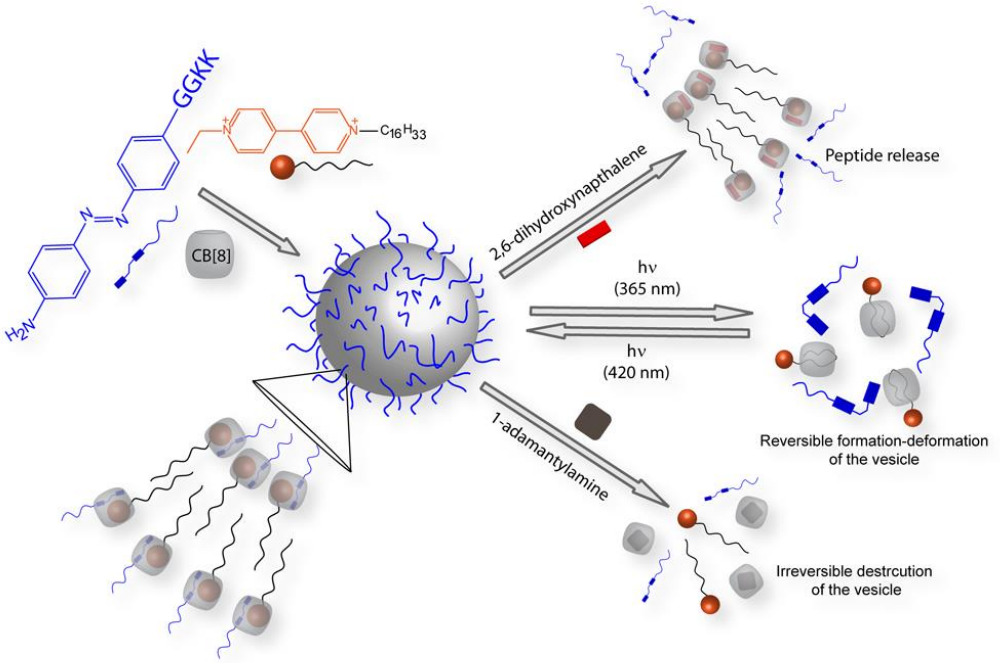

5.1 Introduction

Among the various guests evaluated, the electron rich fused aromatic systems were found to be most efficient as a second guest for MV@CB[8] binary complex.[14] Although the driving force for the ternary complexation is the possibility to form charge transfer complex (CT) with the electron deficient viologen unit, the entrance of the aromatic group into the CB[8] cavity is also governed by the hydrophobicity of the second guest.[42,45] Kim and co-workers reported that MV@CB[8] can bind to other aromatic amino acids, such as tryptophan (Trp), phenylalanine (Phe), and tyrosine (Tyr).[44] In a systematic analysis, Urbach et al. have demonstrated that the affinity of Trp to bind with MV@CB[8] is significantly higher than that of Phe and Tyr respectively.[45] The ability of these amino acids to bind with CB[8] in presence of an auxiliary guest (MV) is more in case when the amino acid occupies the free N-terminal position in a peptide molecule.[45]

Vesicles are integral building blocks of living systems. Use of vesicles in different branches of science including chemistry, biotechnology and material science has become a very prevalent practice.[140-142] Construction of vesicles with defined size, shape and external stimuli responsiveness has become a fascinating challenge for the chemists as they are extremely useful as biomimetic systems, light-harvesting systems, as well as drug delivery vehicles.[143-147] Regulation over the formation/deformation process using external stimuli is most desired for these systems to be utilized as a soft-material.[140-147] Moreover, the reversible formation/deformation by a single trigger could be of immense importance and to the best of our knowledge no such system has been reported so far. In this context, photosensitivity of such self-assemblies is advantageous over the other common forms of stimuli (pH, additives, temperature etc.) as this can be achieved by simple irradiation of light to the systems. Although light sensitive vesicles have been formulated using various polymers and phospholipids, no such effort has been reported with peptide-amphiphiles (PA).[148-150]

In this regard, the observation of Kim and co-workers to form vesicles through ternary complexation could be an extremely convenient tool to construct such stimuli sensitive

systems with desired flexibility by fine tuning the second guests.[101] The ternary complexation by CB[8] provides ample opportunity to create stimuli responsive systems as depicted in Scheme 5.2. Scherman and co-workers have demonstrated the formation of supramolecular peptide amphiphile (SPA) and their stimuli responsive vesicles and used the system as a delivery vehicle.[102] Although never been tested, aromatic amino acids can be of important substitute to the fused aromatic ring containing second guests such as DHN, pyrene etc. for the preparation of vesicles using the ternary complexation. Based on Urbach's report, herein we systematically studied the ability to form the vesicles by HDEV in combination with CB[8] and aromatic amino acids.[45] Interestingly, we have observed that though both Phe and Tyr can form ternary complex with MV@CB[8], they are unable to form vesicles when an asymmetric viologen surfactant (HDEV) replaces MV. Both Trp and Azo-AA (Scheme 5.1) showed the ability to transform solution of HDEV@CB[8] in to vesicles. The findings were further extended to form a supramolecular peptide amphiphile (SPA) by incorporating an Azo-amino acid containing peptide (**1**, Scheme 5.1) as the head group and its corresponding vesicle which showed excellent photo-response in addition to other stimuli-responsiveness.

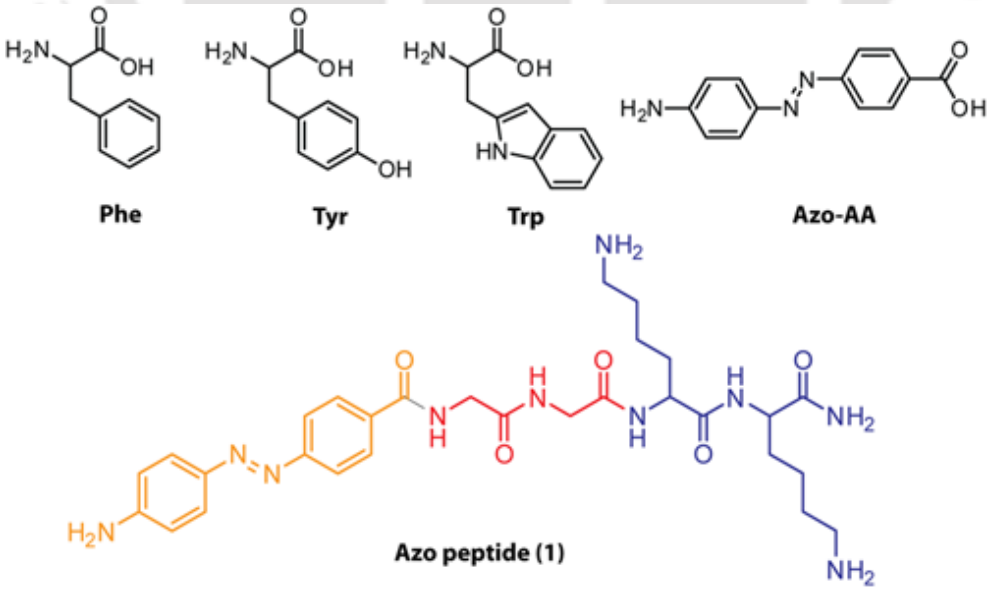

Scheme 5.1 Chemical structures of the aromatic amino acids and the peptide used for the study.

5.2 Results and Discussion

5.2.1 Formation of Ternary Complexes of Aromatic Amino Acids with HDEV@CB[8]:

Urbach et al. have shown that the binding affinity for Trp (K_a = 4.3 × 10^4 M^{-1}) toward MV@CB[8] complex is an order of magnitude higher than the other two aromatic natural amino acids, namely, Phe (K_a = 5.3 × 10^3 M^{-1}) and Tyr (K_a = 2.2 × 10^3 M^{-1}).[45] Based on these reports, we envisioned that the aromatic amino acids can also be a good alternative for DHN or other fused aromatic ring containing molecules (pyrene etc.). A systematic investigation with these natural aromatic amino acids revealed that though Phe and Tyr failed, Trp could successfully transform the micellar solution of HDEV to vesicle through ternary complexation with CB[8].

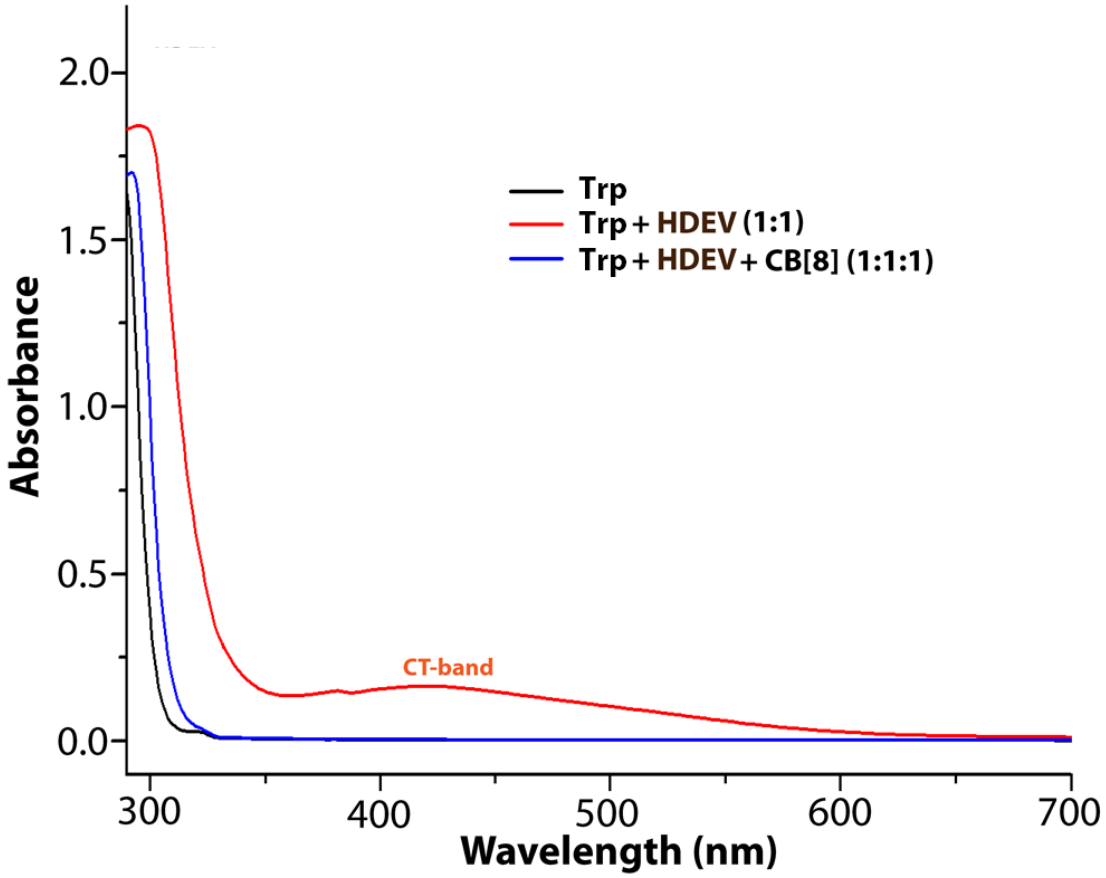

Figure 5.1 UV-Visible spectra of 0.75 mM Trp in absence and presence of HDEV and CB[8] at RT showing the appearance of CT band centred at 435 nm.

Figure 5.1 shows a representative overlay of the three spectra for Trp in absence and presence of HDEV and CB[8]. The appearance of a new transition centred at ~ 416 nm is due to the CT complexation of the indole moiety and viologen unit of HDEV which is stabilized by CB[8]. Similar observation was previously reported by Urbach with Trp and MV@CB[8].[45] Interestingly, no such CT band appeared in case of Phe and Tyr. To further confirm the formation of ternary complex of Trp-HDEV@CB[8], the emission property of Trp was investigated in absence and presence of HDEV and CB[8]. The indole fluorescence was quenched ~10% by the viologen unit of HDEV when mixed together. The quenching signifies the presence of weak CT interaction (Figure 5.2). The emission intensity was further quenched significantly (~90%) in presence of CB[8] indicating strong CT complexation inside the CB[8] cavity. Interestingly, no such CT band appeared in case of Phe and Tyr. The ^{1}H NMR spectra showed significant up-field shift of the aromatic protons of both Trp and HDEV in presence of CB[8] signifying the ternary complexation (Figure 5.3). The ^{1}H NMR spectra of the samples containing Phe/Tyr-HDEV-CB[8] (1:1:1) prominent shift of the aromatic protons indicating no ternary binding (Figure 5.4).

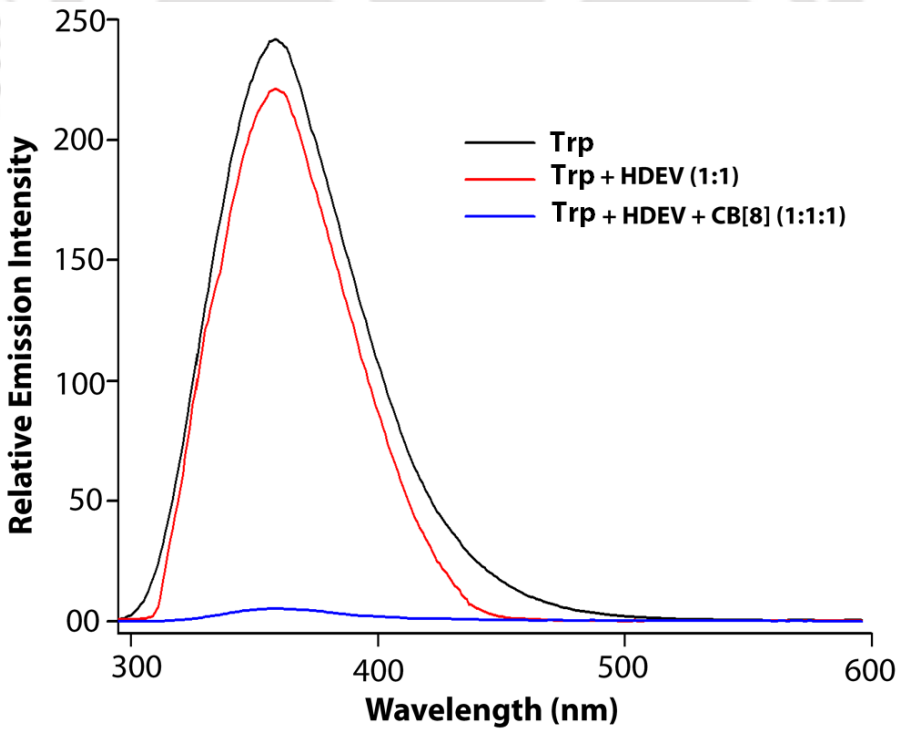

Figure 5.3 Emission spectra of 0.75 mM Trp in absence and presence of HDEV and CB[8] at RT.

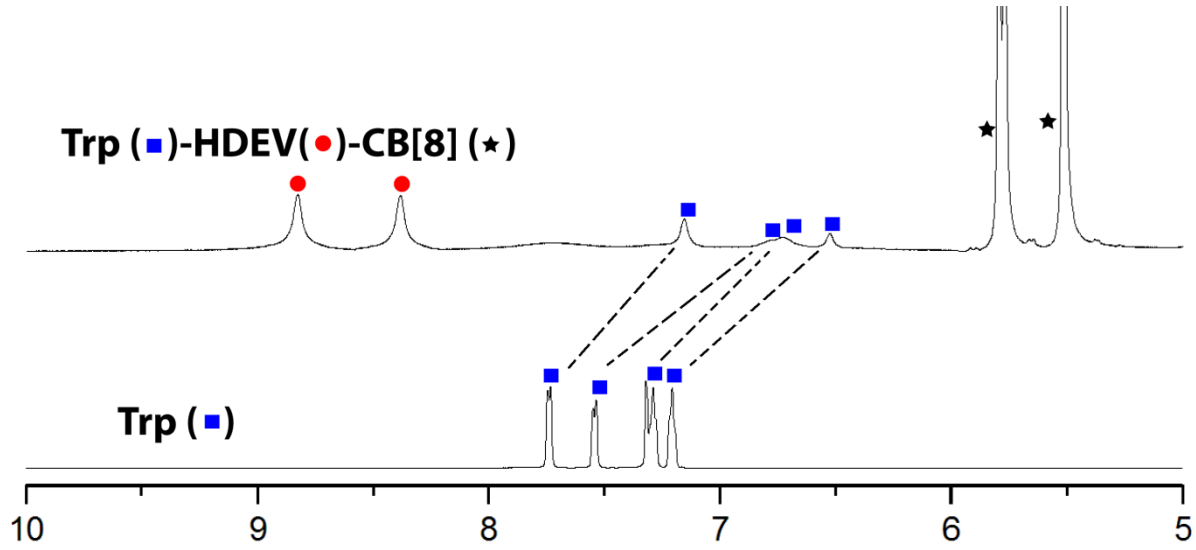

Figure 5.4 ^{1}H NMR of Trp and Trp-HDEV@CB[8] (1:1:1, 0.75 mM) showing the up-field shift of the aromatic protons of Trp upon ternary complexation.

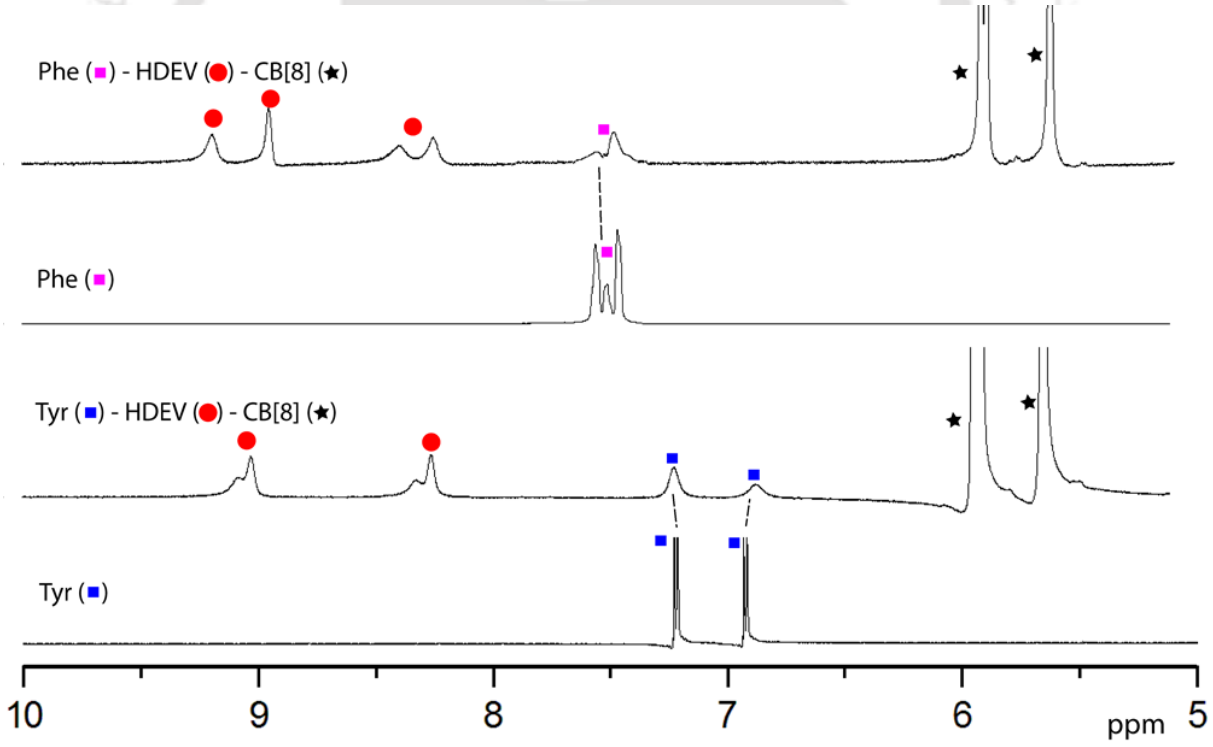

Figure 5.3 ^{1}H NMR of Phe and Tyr in presence and absence of HDEV@CB[8] (1:1:1, 0.75 mM) showing no binding.

From these data it was clear that though Phe and Tyr failed to form any ternary complex with HDEV and CB[8], Trp had shown the ability to do so. The lower binding constants for these two aromatic amino acids for DEV@CB[8] (in the order of 10^3 M^{-1}, Figure 5.5 and 5.6) compared to the affinity of CB[8] ($(2.3 \pm 0.1) \times 10^5$ M^{-1}, Figure 4.10B) toward the hydrophobic tail of HDEV to form U-shaped HDEV@CB[8] pseudo-ternary complex does not allow the self-sorting of CB[8] to move from the tail group to the viologen head to form ternary complex with these amino acids. Moreover, the binding constant for Trp was observed to be $(0.94 \pm 0.1) \times 10^5$ M^{-1} (Figure 5.7) which is very much similar to that of CB[8] toward HDEV. Thus the competitive binding allows Trp to form such ternary complex while the others failed.

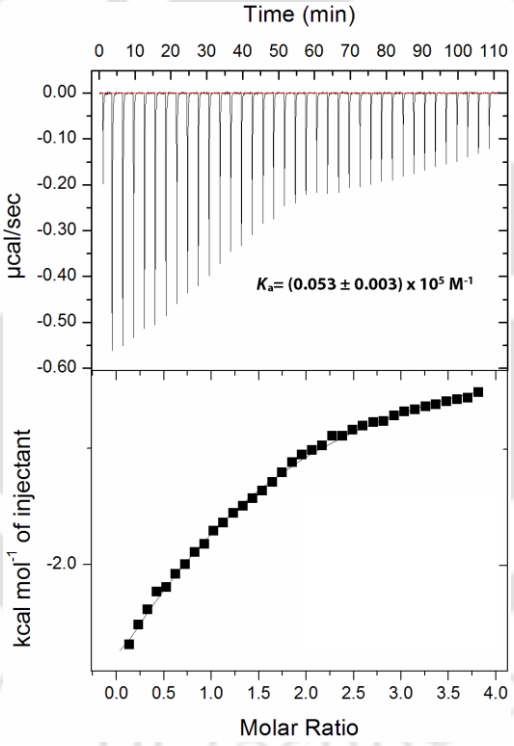

Figure 5.5 ITC Thermogram (top) and binding isotherms (bottom) of DEV@CB[8] with Phe at 298 K.

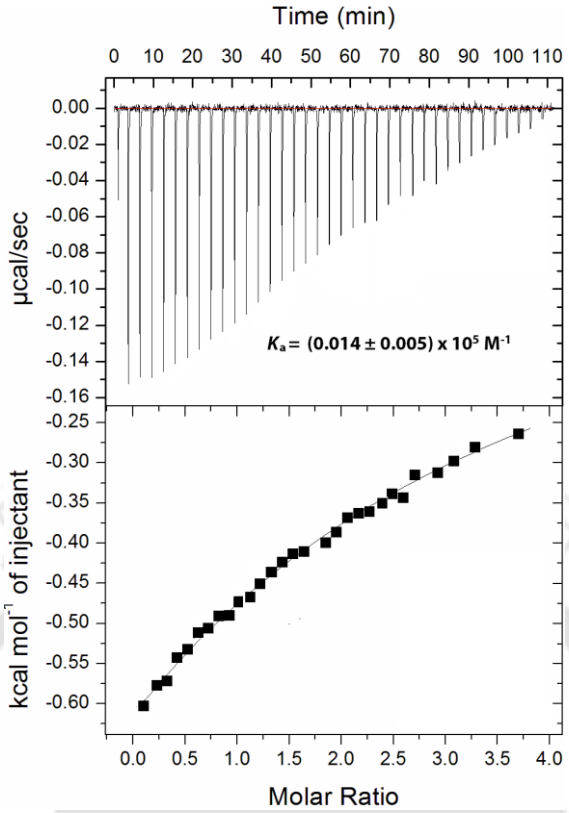

Figure 5.6 ITC Thermogram (top) and binding isotherms (bottom) of DEV@CB[8] with Tyr at 298 K.

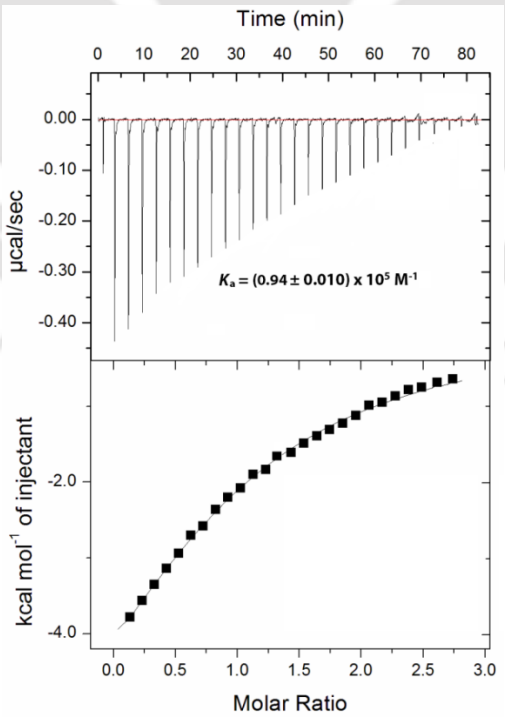

Figure 5.7 ITC Thermogram (top) and binding isotherms (bottom) of DEV@CB[8] with Trp at 298 K.

The ternary complexation between Trp, HDEV, and CB[8] also lead to transformation of the solution to vesicles. FESEM, TEM and DLS experiments showed the formation of giant vesicles of ~ 700 nm size (Figure 5.8 and 5.9). When checked with the other two amino acids, no particular structure could be seen in the FESEM images as well as no particle distribution obtained in the DLS measurement (data not shown). The stability of the vesicles was determined through the dye release experiment. A water soluble reporter dye (CF) was entrapped inside the vesicles and the slow release of the dye was monitored through enhancement of the emission intensity with time. The release profile confirms the formation of a stable vesicle in the solution (Figure 5.10).

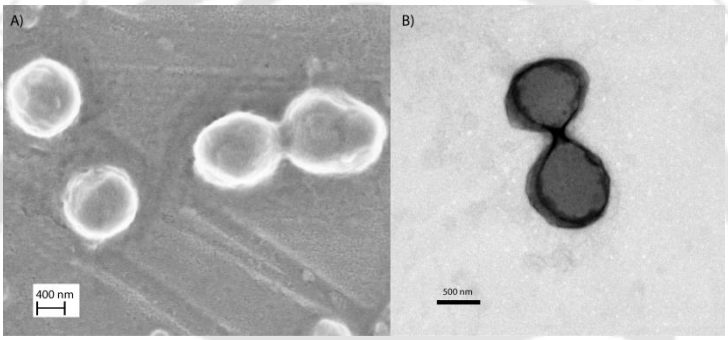

Figure 5.8 A) FESEM and B)TEM images of the vesicles formed by Trp-HDEV@CB[8] (1:1:1) at RT.

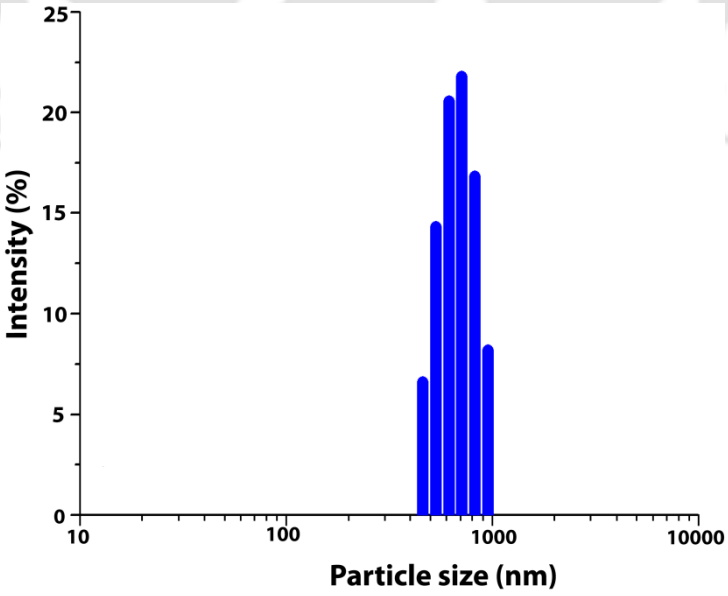

Figure 5.9 Intensity-weighted distributions obtained from DLS measurements of the vesicles formed by 1:1:1 Trp-HDEV@CB[8] at RT.

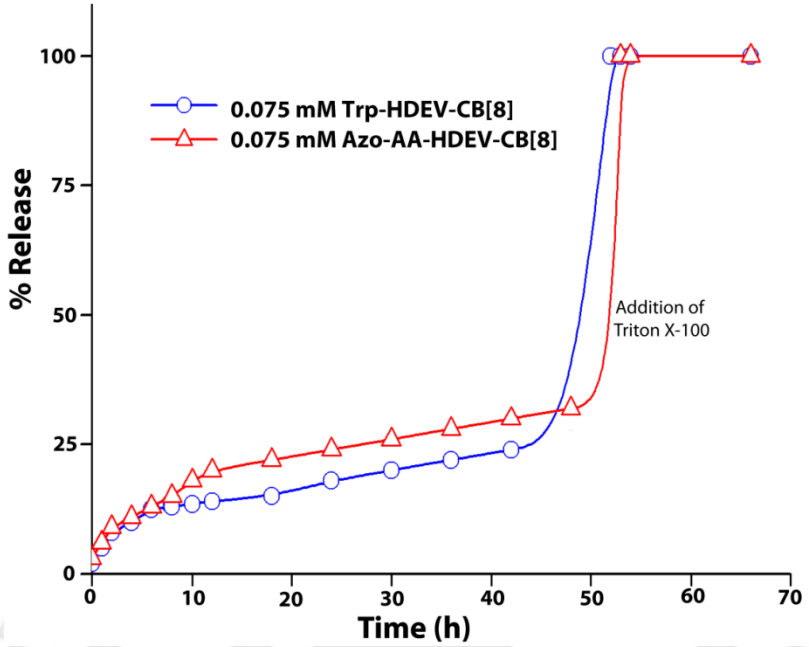

Figure 5.10 Release profile of 5(6)-carboxyfluorescein trapped inside the vesicles formed by Trp/Azo-AA HDEV, and CB[8] in water at 298 K.

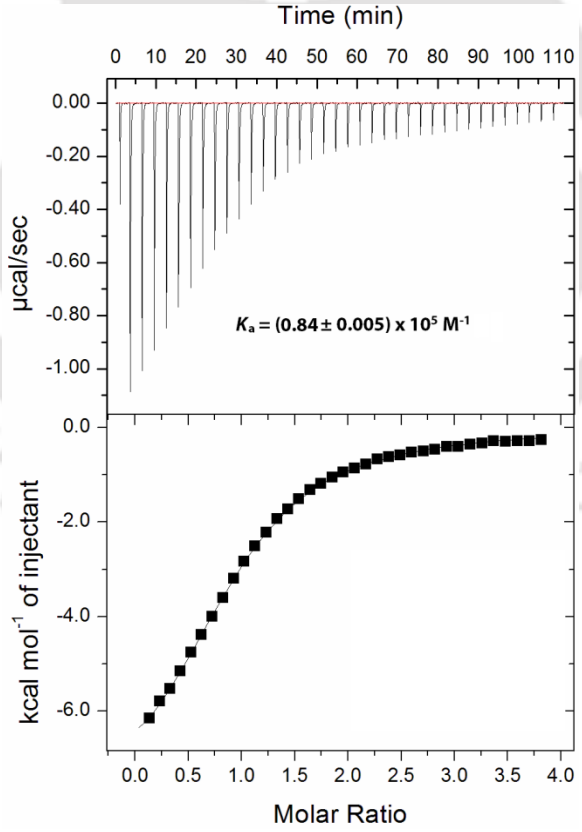

Figure 5.11 ITC Thermogram (top) and binding isotherms (bottom) of DEV@CB[8] with Azo-AA at 298 K.

5.2.2 Ternary Complexation of Azo-AA with HDEV@CB[8]:

As mentioned in the Introduction, we wanted to prepare a stimuli responsive vesicle and for that we have initially chosen Azo-AA and studied its binding properties with both DEV@CB[8] and HDEV@CB[8] binary complexes. The ITC measurement showed a 1:1 binding of Azo-AA with DEV@CB[8] complex with a binding constant of 0.840×10^5 M^{-1} (Figure 5.11) which is very much similar to that of Trp (Figure 5.7). Though no CT band is observed in the UV-visible spectra of Azo-AA-HDEV-CB[8], the proton NMR showed a significant up-field shift of the aromatic protons from both Azo-AA as well as HDEV (Figure 5.12). All these evidences confirmed the formation of the ternary complex between Azo-AA-HDEV-CB[8].

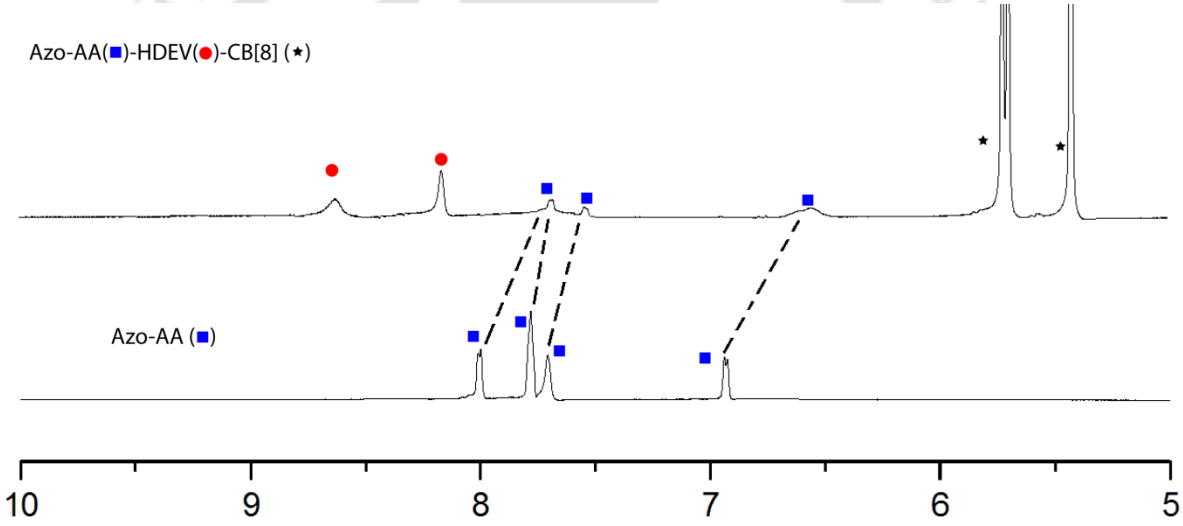

Figure 5.12 ^{1}H NMR of Azo-AA in presence and absence of HDEV@CB[8] (1:1:1, 0.75 mM) showing the no ternary complexation.

Similar to Tryptophan, Azo-AA also could transform the solution of HDEV to vesicles through ternary complexation. The FESEM and TEM images showed uniform vesicles with average diameter of ~ 300 nm (Figure 5.13). The size of the vesicles was further confirmed through DLS measurements which showed similar particle size (Figure 5.14). The vesicles were found to be stable as it showed a slow release profile of entrapped dye (Figure 5.10)

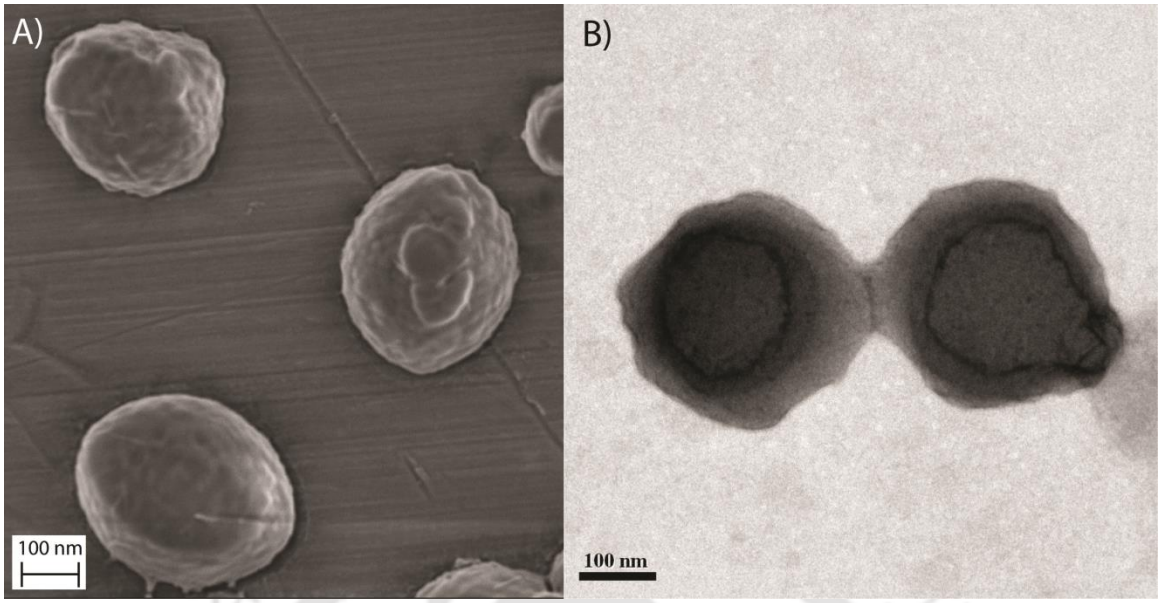

Figure 5.13 A) FESEM and B) TEM images of 0.75 mM Azo-AA-HDEV@CB[8] vesicles.

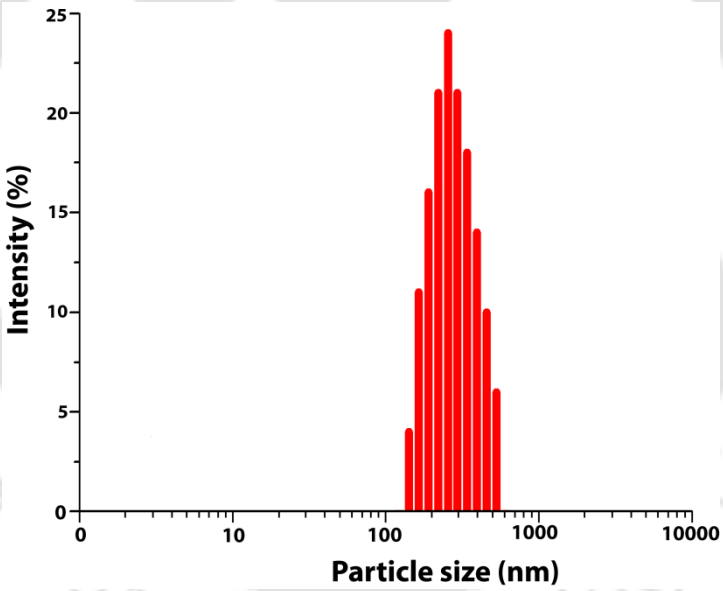

Figure 5.14 Intensity-weighted distribution of particle size distribution of Azo-AA-HDEV@CB[8] at RT.

5.2.3 Formation of Supramolecular Peptide Amphiphile (SPA) and its Vesicle:

As both Trp and Azo-AA were found to be capable of transforming HDEV@CB8] solution into vesicles, we wanted to further extend this phenomenon to construct SPAs and their vesicles. Peptide **1** (Scheme 5.1) was designed where the second guest (Azo-AA) is situated at the N-terminal separated by two Glycines from the hydrophilic Lysine

residues at the C-terminal. The ITC experiment showed a 1:1 binding of the peptide **1** with DEV@CB[8] with an affinity constant of 0.91 × 10^5 M^1 (Figure 5.15). Mixing peptide **1** with HDEV, and CB[8] in equimolar ratio provided a mass corresponding to **1**-HDEV@CB[8] (**2**, Scheme 5.2) ternary complex indicating the formation of the peptide amphiphile (1174.57, $\mathbf{2}^{2+}$). Further confirmation was obtained from the proton NMR where similar upfield shifts of the aromatic protons were obtained as seen in all previous cases of ternary complexes studied (Figure 5.16). DOSY NMR also showed similar diffusion coefficients for all three components (Figure 5.17). Moreover, the aliphatic protons of HDEV which were buried inside the CB[8] cavity as seen from the up-field shift in absence of the peptide now return back to their native position when the peptide is present indicating de-complexation of the U-shaped pseudoternary complex between the hydrophobic tail and CB[8] (Figure 5.18). This in turn also indicates the self-sorting of CB[8] between the hydrophobic tail and the viologen head when the possibility of ternary complexation arises.

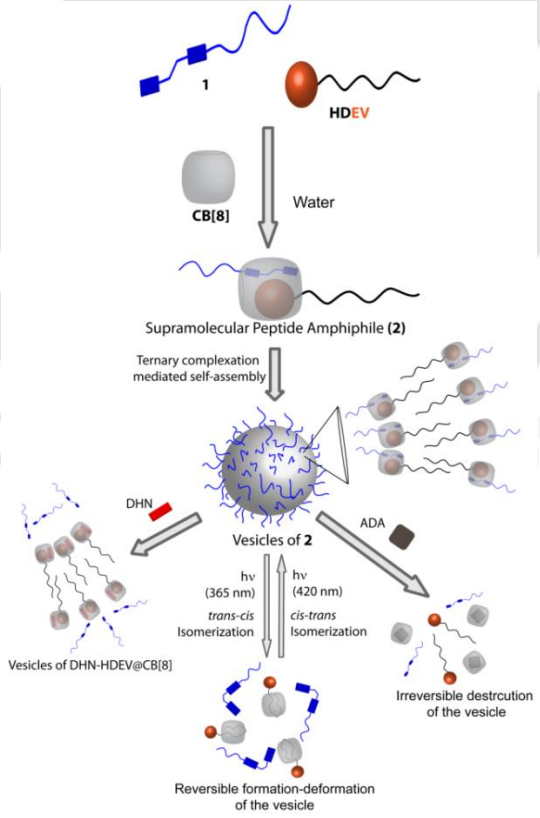

Scheme 5.2 Pictorial presentation of the formation of SPA and its vesicle as well as response to various stimuli.

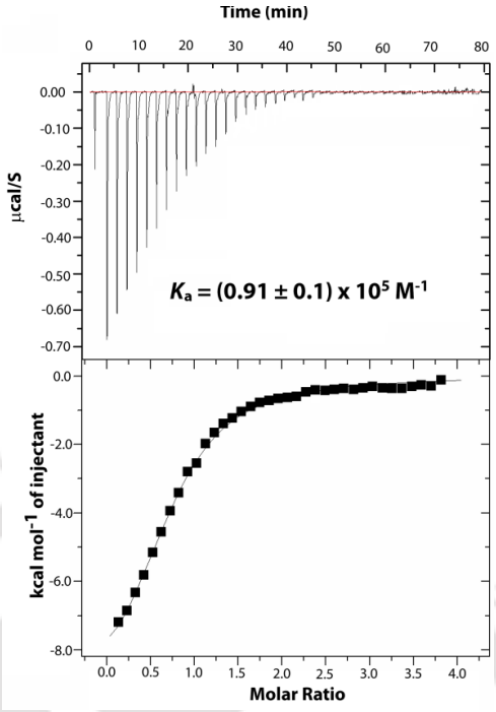

Figure 5.15 ITC Thermogram (top) and binding isotherms (bottom) of DEV@CB[8] with **1** at 298 K.

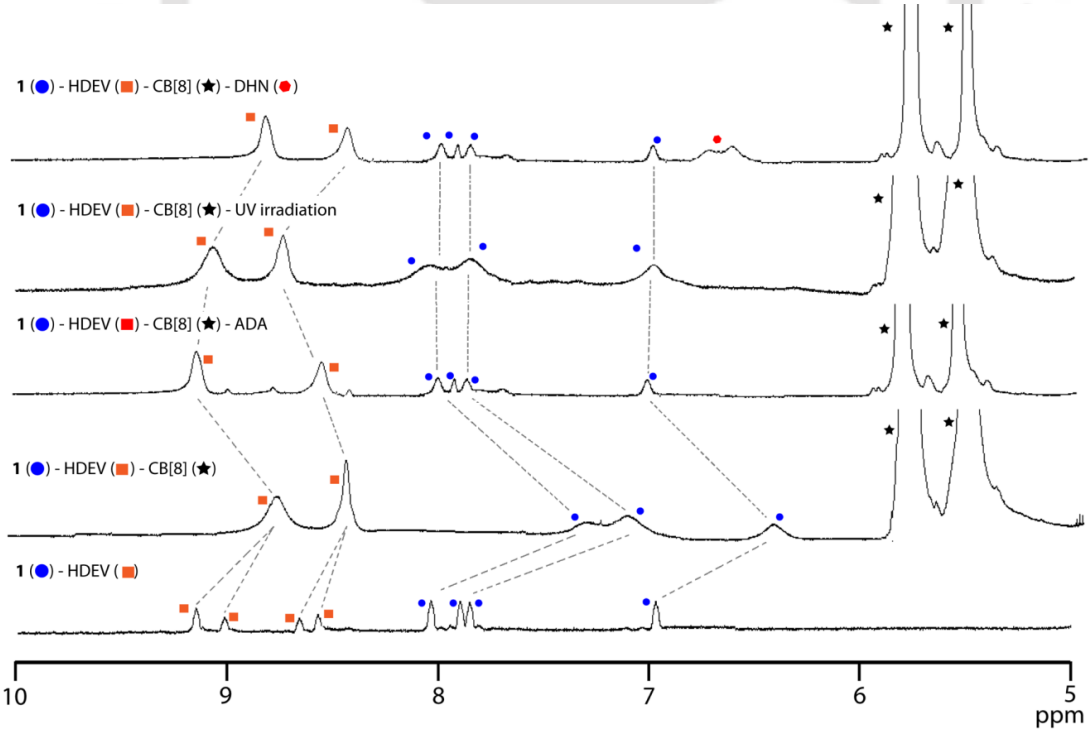

Figure 5.16 ^{1}H NMR (aromatic region only) spectra of various compositions of **1** and under different conditions showing the chemical shifts of protons upon complexation and de-complexation.

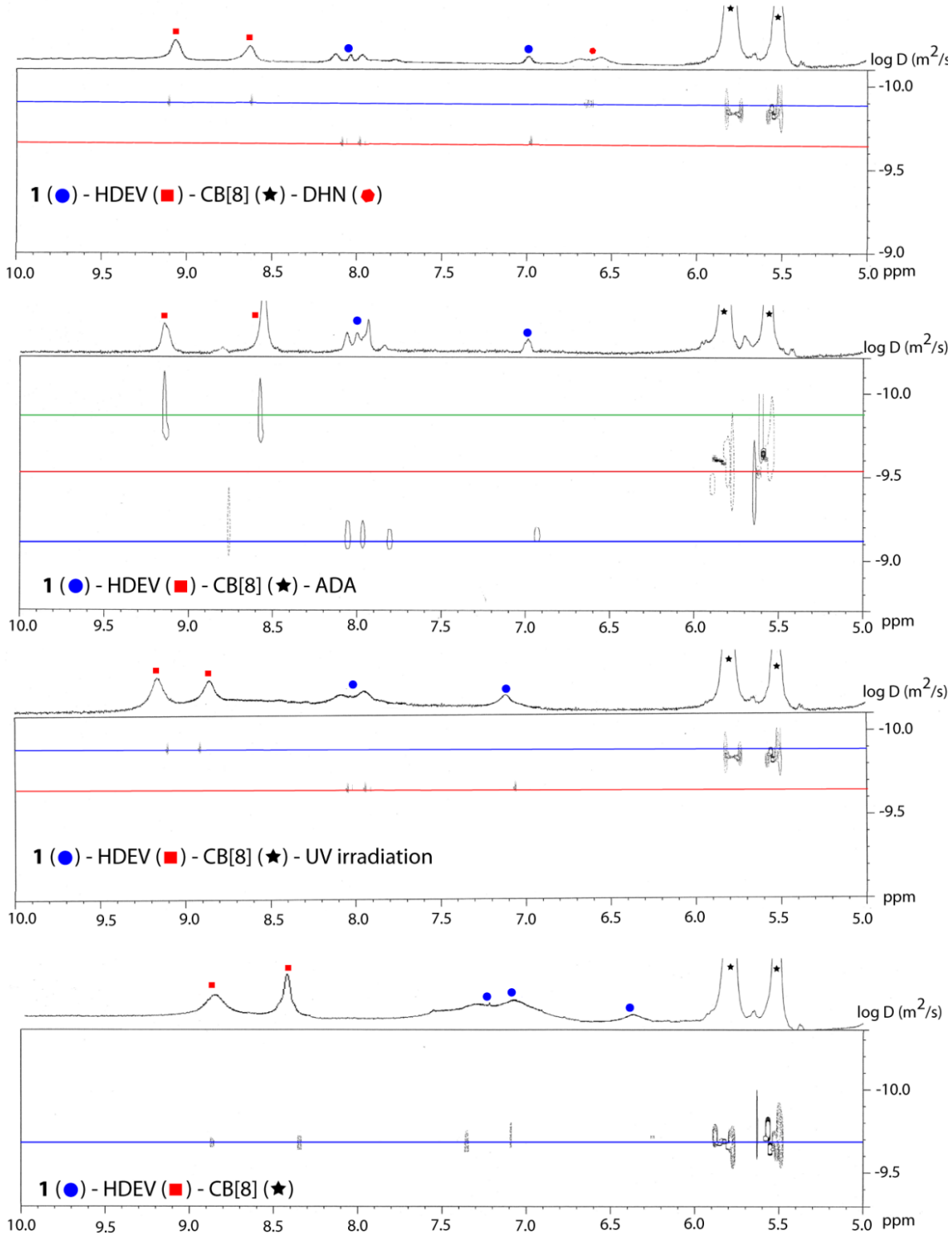

Figure 5.17 DOSY NMR spectra of **1**-HDEV@CB[8] vesicles with and without various stimuli.

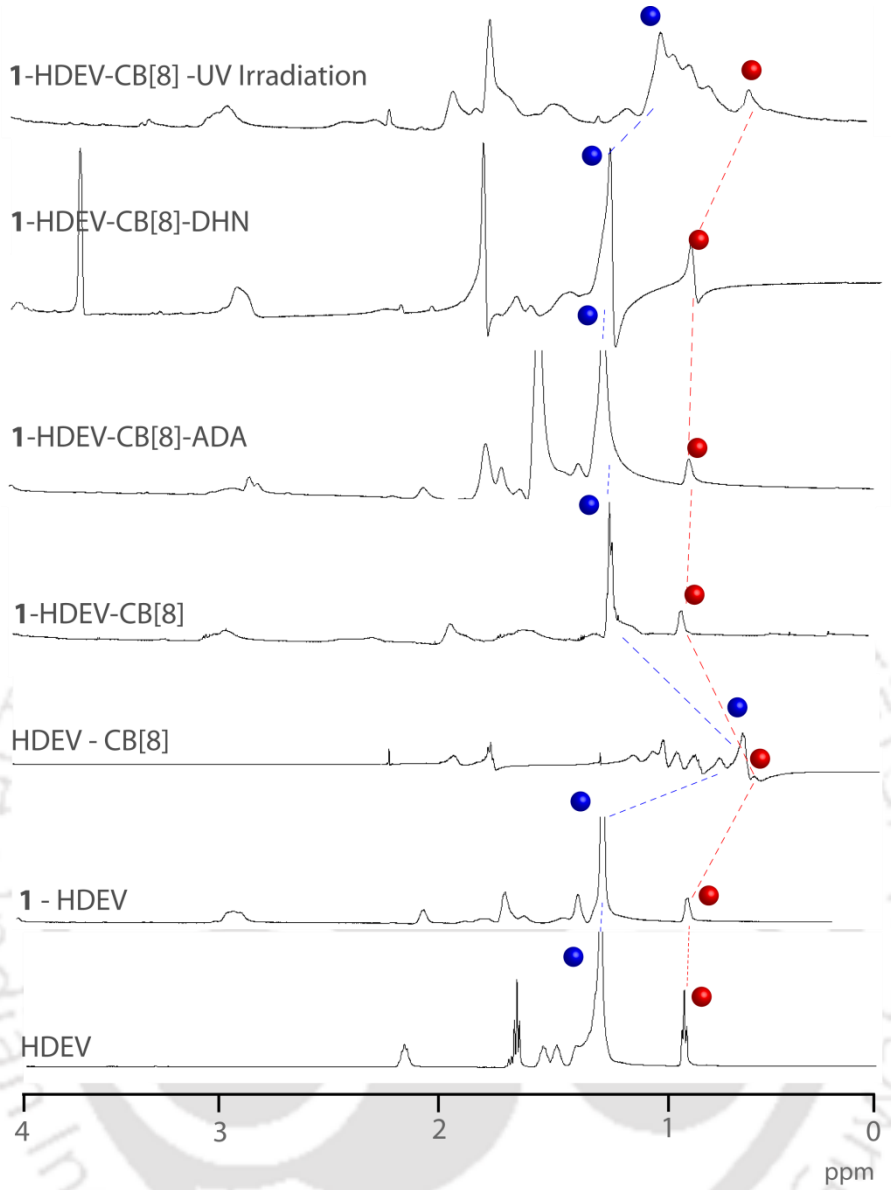

Figure 5.18 The aliphatic region of the ^{1}H NMR spectra of HDEV with different compositions and under different conditions showing the shift in the ^{1}H signals originating from the hydrophobic tail of HDEV. The red-sphere and blue-sphere marked peaks correspond to the terminal methyl group of the tail and the other aliphatic protons of the tail respectively.

The SPA (**2**) formed uniform vesicles as evidenced from the FESEM, TEM and DLS experiments (Figure 5.19 A, B and C). The formation of the vesicles as well as its stability was further confirmed by the slow release (Figure 5.19D) of a water soluble dye 5,6-carboxyfluorescein (CF). A dilution experiment followed by DLS measurements showed that the system maintained the size distribution at about 500 nm when the solution was diluted from 0.75 mM to 0.005 mM (Figure 5.20). After that there is a

sharp decrease in both the diameter (uneven distribution at ~2-3 nm) as well as count rate. The inflection point (0.0025 mM) can be considered as the critical aggregation concentration (CAC) for the SPA.

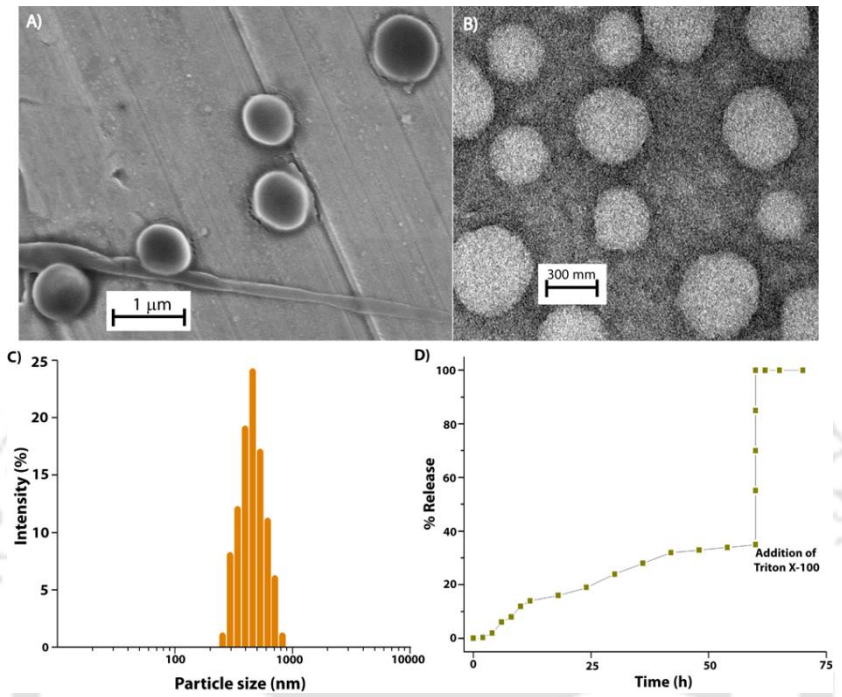

Figure 5.19 A) FESEM, B) TEM images and C). Intensity-weighted distributions obtained from DLS measurements of the vesicles formed by 1-HDEV@CB[8] and D) release profile of the entrapped CF in the same vesicles under ambient condition.

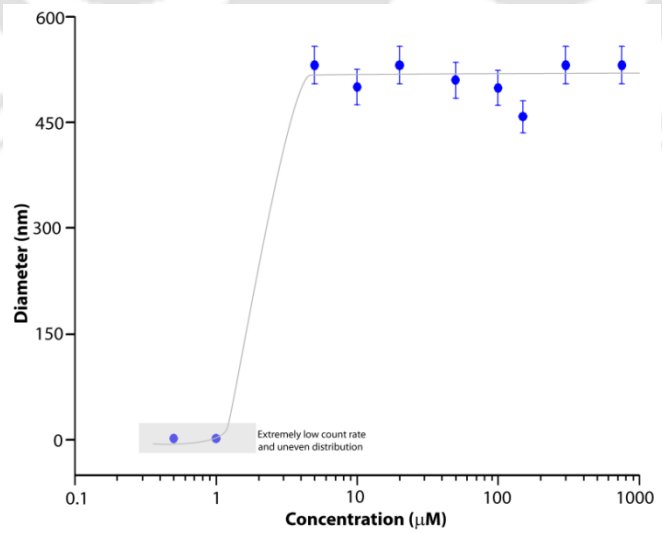

Figure 5.20 The concentration dependent average size of the vesicles formed by **2** to determine the CAC of **2** at 298 K.

5.2.4 Stimuli Sensitivity of the 1-HDEV@CB[8](2) vesicles:

To assess photo-lability of the SPA vesicles, the solution containing entrapped CF was subjected to UV irradiation (365 nm, 8 W lamp) and simultaneously the fluorescence intensity of CF was monitored at 512 nm. A continuous increase in the intensity much faster than the ambient release experiment was observed (Fig. 5.21). The faster release is attributed to the quicker discharge of the dye molecules from the vesicle. The UV irradiation leads to the conversion of *trans*-isomer of the Azo group to *cis*-isomer which eventually comes out of the CB[8] cavity leading to break down of the ternary complex (Scheme 5.2). Consequently the vesicle structure breaks down releasing the entrapped dye. Though the *trans-cis* isomerization could not be monitored using UV-visible spectroscopy owing to overlapping of absorbance regions of the peptide and HDEV, NMR techniques provided conclusive evidences for the dis-assembly of the vesicle (Figure 5.16, 5.17 and 5.18). The dis-assembly of the ternary complex is evident from the DOSY spectrum of the UV-irradiated (for 8h) vesicle solution (without CF) where the free peptide showed a different diffusion coefficient than the other two components (Figure 5.17). Similar diffusion coefficients for HDEV and CB[8] indicates that once the ternary complex breaks down, CB[8] moves back to the tail region to form the pseudoternary complex with the hydrophobic part of HDEV. The formation of the U-shaped pseudoternary complex of HDEV tail inside the CB[8] cavity was further confirmed from the up-field shifts of the aliphatic peaks and especially the terminal methyl group in the UV-irradiated sample (Figure 5.18).

Though the UV-irradiated sample showed no Tyndall effect (Figure 5.22), in DLS analysis, particles with size distribution centred at around 130 nm were observed but with significantly low counts (Figure 5.23). Though the count is extremely small, the appearance of such particles could be attributed to a possible non-spherical micelles formed by the pseudoternary complexes of HDEV@CB[8] as observed previously in similar cases. Interestingly, the vesicle showed reversible deformation-formation based on the wavelength of the light it was exposed to. After complete breakdown (as monitored by DOSY spectra), the solution was irradiated back with a lamp illuminating

light of 420 nm (150 W) for 10 mins, sonicated for 1h and finally incubated at RT in dark for two days. The DLS measurement showed appearance of larger particles of around 500 nm along with a positive Tyndall effect result (Figure 5.22 and 5.23). TEM images of the sample showed similar vesicular structure as obtained from the freshly prepared vesicles. The irradiation of the solution with light of 420 nm facilitated the *cis-trans* conversion and sonication followed by incubation at dark allowed the self-assembly and consequently re-construction of the vesicles. DOSY spectra also showed similar pattern as in the untreated freshly prepared vesicles. Repetition of the cycle for several times leads to similar results showing the reversibility of the vesicle.

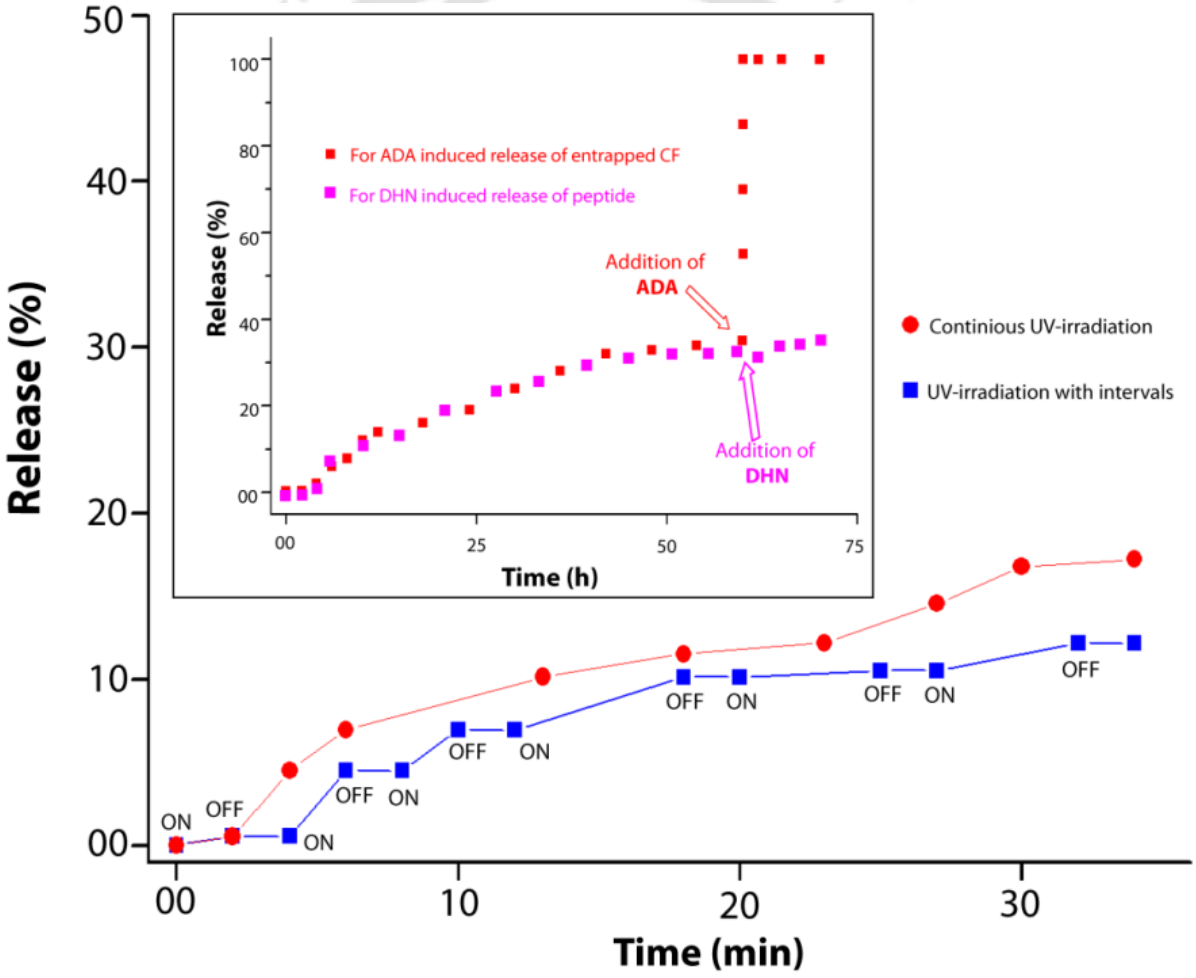

Figure 5.21 UV-irradiation triggered controlled dye release profile of CF trapped inside the vesicles formed by 1-HDEV−CB[8] in water at 298 K. (ON and OFF indicate the time when the irradiation was switched on and off respectively). Inset: The normal CF release profile from vesicles of 2, red: for ADA induced release of entrapped CF and, magenta: for DHN induced release of 1 from the vesicles.

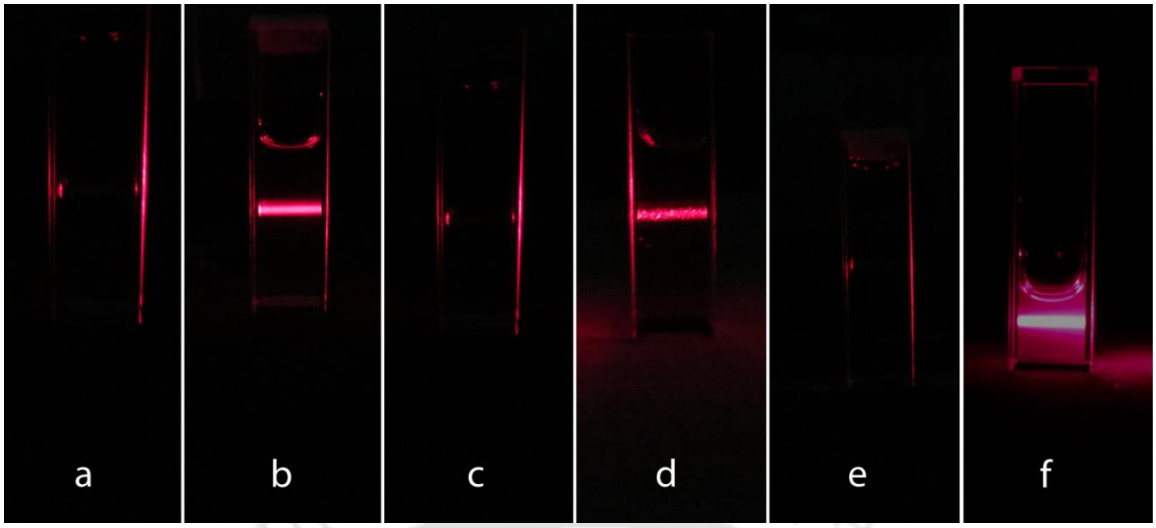

Figure 5.22 Photographs from the Tyndall Effect experiments. a) water used for all the sample preparation; b) vesicle solution of **2**; c) solution of **2** after 8h or irradiation with UV light (365 nm); d) c after 10 mins of irradiation with 420 nm light and incubation for 48 h; e) solution **2** after addition of 2 equivalents of ADA; f) solution **2** after addition of 2 equivalents of DHN. [**2**] = 0.075 mM for all experiments.

Irradiating the vesicle with UV light in a stepwise fashion leads to a controlled release of the dye. The CF release was followed by alternately switching on and off the irradiation. After irradiating the solution for a certain period (on), the fluorescence intensity enhanced but did not change upon keeping the solution in dark for some time (off). The CF release was triggered again by switching on the irradiation when a steady increase in the release was observed. Reiteration of this "on-off" process resulted release of the dye in a controlled manner. This stepwise release evidently established a sequential controlled release mode and facilitating great potential for this SPA based systems to be used as nano-carriers when a time dependent release of cargo is required.

The vesicles formed by SPA **2** was then analysed for its stimuli responsiveness to a number of other stimulus. To start with, we have checked its response to a stronger (than MV) guest of CB[8], 1-adamantylamine (ADA). ADA, having a significantly higher binding constant (K_a = (8.19 ± 1.75) × 10^8 M^{-1}) and larger size, is known to replace other guests from the ternary complex.[11] When added to the vesicles of 2, ADA replaced both the guests and occupied the space inside the CB[8] cavity (Scheme 5.2). Breaking the ternary complex results in the breakdown of the SPA and consequently the

vesicles. When excess ADA was added to the vesicle of **2** containing entrapped CF, the enhancement of the fluorescence intensity was found to be similar to that observed when Triton X-100, a known vesicle destroyer was added to the CF entrapped vesicle of **2** (Figure 5.21). Further confirmation was obtained from the DOSY NMR of the vesicle solution mixed with ADA where three different diffusion coefficients were observed corresponding to that of ADA@CB[8], HDEV and **1** (Figure 5.17). ^{1}H spectrum of the ADA treated solution of **2** showed down-field shifts of the aromatic protons resulting from the de-complexation of the ternary complex (Figure 5.16). Interestingly, the aliphatic region of the spectrum remained unaltered from the sample without ADA except the appearance of the up-field shifted peaks from ADA (compared to free ADA) (Figure 5.18). The ^{1}H NMR of the aliphatic region clearly points to the encapsulation of ADA inside CB[8] as well as no involvement of the hydrophobic tail in any kind of complexation in this solution (Figure 5.18). Negative Tyndall effect as well as absence of any proper distribution in the DLS result also supports complete destruction of the vesicles (Figure 5.22 and 5.23).

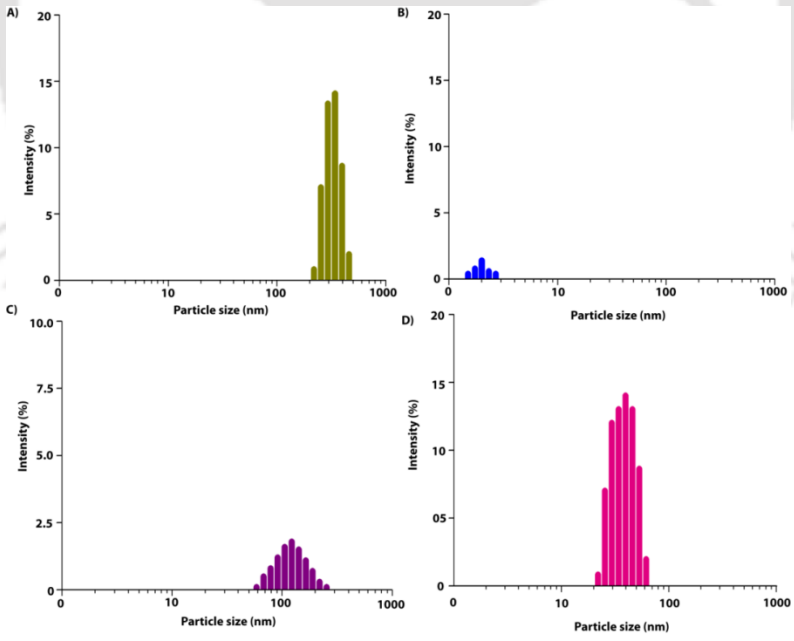

Figure 5.23 Intensity-weighted distributions obtained from DLS measurements 1:1:1 **1**-HDEV-CB[8] (0.075 mM) under various conditions. A) after treatment with 2 equivalent DHN; B) after treatment with 2 equivalent ADA; C) after UV irradiation with UV light (365 nm) for 8h; D) after irradiating the sample from C with a 420 nm lamp for 10 mins and incubation in dark for 48h at RT.

The vesicles of **2** showed interesting response to a competitive guest, 2,6-dihydroxynaphthalene (DHN). Upon addition of 1.2 equivalent DHN to the vesicle of **2**, the DOSY spectra showed two different diffusion coefficients, one for the free peptide **1** and the other corresponding to DHN, HDEV and CB[8] (Figure 5.17). The proton NMR also showed downfield shift of the Azo-protons to its unbound state indicating de-complexation of the azo group (Figure 5.16). An observed up-filed shift of the DHN protons compared to its native spectrum and unchanged peak positions of the viologen protons indicate the inclusion on the DHN molecule in the CB[8] cavity to form DHN-HDEV@CB[8] ternary complex. The aliphatic region of the spectra showed no observable movement of the hydrophobic protons signifying that the CB[8] moiety remains at the head group of HDEV (Figure 5.18). Interestingly, in the dye release, no enhancement in the intensity of the fluorescence was observed upon addition of DHN (Figure 5.21). The DLS distribution of the DHN treated solution showed a slight decrease in the particle size (Figure 5.23). When checked for Tyndall effect, the DHN treated solution also showed positive results (Figure 5.22). All these information lead to the conclusion that the vesicle structure remained intact even after the addition of DHN. DHN is well known for its charge transfer complex (CT) mediated ternary complexation with HDEV and CB[8] and consequently transforming the micelle to vesicle. The solution binding constant for DHN toward MV@CB[8] complex, as reported by Scherman et al. was found to be higher than that of Azo-AA for ternary complex (K_a = (5.9 ± 0.5) × 10^5 M^{-1}).[43] Moreover, the second guest exchange is known to be dynamic and rapid whereas the vesicle formation by these supramolecular amphiphile is a relatively slow process. The observations can presumably be explained as, upon addition of DHN, it replaces the second guest (**1**) from the ternary complex at the head group of HDEV while keeping the vesicle structure intact (Scheme 5.2). This particular response of the vesicle can be utilized for unloading peptide therapeutics in a controlled fashion.

5.3 Conclusions

In summary, an investigation about the aromatic amino acids for their ability to form vesicles through ternary complexation with a viologen amphiphile and CB[8] showed that though Tyr and Phe failed, Trp and Azo-AA showed positive results. Based on these data, a supramolecular peptide amphiphile (SPA) is designed and prepared. In accordance with other such amphiphilic ternary complexes of CB[8], the SPA also transformed the solution into vesicles. The presence of the azobenzene group as the second guest allowed us to utilize this vesicle as a photo-responsive system which is achieved through UV irradiation mediated *trans-cis* isomerization and consequent disassembly of the complex. The release of a dye molecule can be controlled in a time dependent fashion. The system showed reversible light responsivity as the formation-deformation of the vesicle can be controlled by appropriate choice of wavelength. The vesicle also responded by a stronger first guest in the form of ADA where the presence of ADA destroyed the vesicle structure and releases the entrapped dye. In response to a competitive guest like DHN, the vesicle structure remained unaltered while the peptides were released from the vesicle surface. Overall, this new multi-stimuli responsive SPA made vesicle can be utilized in various ways in accordance with the requirement of the delivery of the cargo, as a whole or in a controlled fashion.

5.4 Experimental Section

5.4.1 General: 1-bromohexadecane, 4,4'-bipyridyl, HBTU, DIPEA, HOBT, Rink-amide HMBA resin (0.75 mmol/g loading) Fmoc-Lys(Boc)OH, Fmoc-Gly(OH), 5(6)-carboxyfluorescein (CF), D_2O, CF_3CO_2D, and D_2SO_4 were obtained from Sigma-aldrich (USA) and used as received. All other chemicals, reagents and solvents were procured from Merck, India and Spectrochem, India. For preparing samples, Milli-Q water with conductivity of less than 2 $\mu S.cm^{-1}$ was used. UV-visible spectra of the vesicles were recorded on Lambda 35 (Perkin-Elmer) spectrometers. ESI-MS was performed by using a Q-Tof Premier Quadrupole mass spectrometer. The dynamic light scattering were measured on a Zetasizer Nano ZS90 from Malvern using a 632.8 nm He−Ne laser.

5.4.2 Synthesis:

4-[(4-Aminophenyl)azo]-benzoic acid (Azo-AA)

1.67 g (0.01 mol) 4-Nitrobenzoic acid and 2.0 g (0.018 mol) 1,4-diaminobenzene were suspended in 50 mL 3 % aqueous NaOH and heated up to 95 °C for several hours. After cooling, the red precipitate was collected and washed several times with dichloromethane before drying under reduced pressure (1.6 g, 66 %). ^{1}HNMR (DMSO-d_6, 400 MHz): δ/ppm = 7.98-7.96 (d, 2H), 7.66-7.62 (t, 4H), 6.68-6.66 (d, 2H), 6.09 (s, 2H). m/z calcd for $[M+H]^+$ $C_{13}H_{11}N_3O_2$: 242.45, found: 242.11.

4-[(4-(N-Fmoc)-Aminophenyl)azo]-benzoic acid (Fmoc-Azo-AA-OH)

0.48 g (2 mmol) 4-[(4-Aminophenyl)azo]-benzoic acid was dissolved in 10 mL of 10 % aqueous Na_2CO_3 solution and 5 mL THF. 0.54 g (2.08 mmol) Fmoc-Cl in 5 mL THF was added drop wise at 0 °C to the stirred solution. After 1 h the mixture was allowed to return to room temperature and was then stirred overnight. The solution was poured into 150 mL ice water, washed with ether and acidified with conc. HCl to pH 1. The protected amino acid was extracted with ethyl acetate, the organic phase was dried over Na_2SO_4 and the solvent was removed on a rotory evaporator, purified by column chromatography to yield 0.44 g (48 %) as an orange solid. ^{1}H NMR (DMSO-d_6, 400 MHz): δ/ppm = 10.19 (s, 1H), 8.13-8.11 (d, 2H), 7.94-7.90 (m, 6H), 7.78-7.76 (d, 2H), 7.69 (d, 2H), 7.46-7.42 (t, 2H), 7.39-7.35 (t, 2H), 4.57-4.56 (d, 2H), 4.36-4.33 (t, 1H); m/z calcd for $[M+H]^+$ $C_{28}H_{21}N_3O_4$: 464.15, found: 464.16.

Peptide 1: The peptide was prepared using solid phase peptide synthesis technique employing Rink-amide MBHA resin as the solid support. Sequence elongation at the N-terminus was performed by coupling the appropriate Fmoc protected amino acids under standard conditions employing HBTU, HOBT and DIPEA as coupling reagents. The peptide was cleaved from the resin employing 95% TFA containing 1% triethylsilane in dichloromethane. Precipitation from dry ether followed by lyophilisation provided 90% overall yield. ^{1}H NMR (D_2O, 600 MHz): δ/ppm = 8.03 (d, 2H), 7.89 (d, 2H), 7.85 (d, 2H), 6.96 (d, 2H), 6.90 (d, 1H), 4.85 (m, 4H), 4.37 (brm, 2H),

4.09 (s, 2H), 4.02 (s, 2H), 2.99 (m, 4H), 1.80 (m, 4H), 1.70 (m, 4H), 1.44 (m, 4H); m/z calcd for $[M+H]^+$ $C_{29}H_{42}N_{10}O_5$: 611.33, found: 611.45.

5.4.3 Methods

5.4.3.1 Vesicle preparation

To a volumetric flask (10 mL) containing a measured quantity of HDEV (4.3 mg), CB[8] (12.8 mg, the overall molecular weight observed for the used CB[8] was 1730 from the elemental analysis data) and 1 equivalent of the second guest (Tryptophan or Azo-AA or peptide **1**) were taken. To these mixtures, water was added to make up the mark. The resulting mixtures after sonication for 1 h were kept undisturbed at 298 K for one day to give clear light violet coloured solutions before utilizing for further experiments.

5.4.3.2 Vesicle preparation for Dye Release experiment

The vesicles were prepared according to the method mentioned above but in these cases, a measured amount of CF (0.1 mg) was added to the 10 mL flask prior to the preparation of the samples. The resulting vesicle solutions were passed through a sephadex G-25 column (1 x 30 cm) and the fractions containing the vesicles were collected. The vesicle solution was then diluted and used for fluorescence measurements. The dye release was monitored on a Cary-Eclipse luminescence spectrometer (Agilent) by exciting the solutions at 492 nm and measuring the fluorescence intensity at 512 nm.

5.4.3.3 NMR spectroscopy

^{1}H NMR, ^{13}C and diffusion-ordered spectroscopy (DOSY) spectra were recorded on a NMR-Bruker Ascend^{TM} 600 MHz (Bruker, Coventry, UK). Spectra were recorded in heavy water (D_2O) at 298 K. The concentration of all the components was fixed at 0.75 mM for all the samples. The experiments were processed with standard Bruker 1D and 2D DOSY softwares.

For ADA and DHN related experiments, 1.2 equivalents (with respect to **2**) of the stimuli (ADA or DHN) were added to the vesicle solutions of **2** and incubated for 24h

prior to measurments. For UV irradiation related experiments, the NMR tube containing the vesicle solutions were exposed to the UV-lamp irradiating light of 365 nm wavelength for 8h before measuring the ^{1}H and DOSY NMR.

5.4.3.4 Field Emission Scanning Electron Microscopy (FESEM) and Transmission Electron Microscopy (TEM)

FESEM images were recorded on zeiss (Sigma) microscope while TEM images were taken on a JEM-2100 microscope. FESEM samples were prepared by casting a drop of the vesicle solution (0.075 mM) on a glass slide and dried under ambient condition. For TEM, a drop of the vesicle solution (0.075 mM) was placed on a 300 mesh Cu grid with thick carbon film (Pacific Grid Tech, USA) and held in air for 2 to 3 min. Excess solution was then blotted with tissue paper. With a drop of 2% uranyl acetate solution the sample was negatively stained before removing the excess liquid with filter paper.

5.4.3.5 Isothermal Titration Calorimetry (ITC)

The formation constants and thermodynamic parameters for the inclusion complexes were determined by isothermal titration calorimetry using a Nano-ITC instrument from MicroCal. CB[8] solutions (0.1 mM) in buffer (100 mM phosphate, pH 7) was placed in the reaction cell (volume = 200 mL). Injections of amino acid/peptide solutions (each injection, 0.5 μL, 2.0 mM) were added from a 40-μL micro-syringe at an interval of 2 min into the DEV@CB[8] solutions with stirring at at 298 K. The data were fitted to a theoretical titration curve using software supplied by Microcal, with K_a (M^{-1}), ΔH (cal/mol) and ΔS (cal/mol/deg) as adjustable parameters.

5.4.3.6 Dye release Experiment

The vesicle solution containing entrapped CF was placed in a 3 mL fluorescence cuvette and the emission spectra were recorded at certain time interval by exciting the solution at 492 nm and measuring the emission intensity at 512 nm. The % CF release was calculated following the equation,

CF release (%) = $((I_t-I_0)/(I_\alpha-I_0))\times100$

Where, I_0 and I_t are the fluorescence intensities initially and at time t, and I_α is the fluorescence intensity when all the CF molecules were released from vesicles, which was measured by the addition Triton x-100 and heating for an additional 30 min.

To monitor ADA and DHN induced release, the stimuli was added in portions to reach 2 equivalent concentration of the stimuli compared to **2.**

5.4.3.7 Photoresponsive dye release experiment

A vesicle solution (0.075 mM) loaded with entrapped CF, stored in a screw-capped 3 mL fluorescence cuvette with 10 mm path length, was exposed to UV light of 365 nm (8 W long wavelength lamp from SIAC, India with band path filter of 365 nm) for different times. The fluorescence intensity change at 512 nm was followed on a Cary-Eclipse luminescence spectrometer (Agilent) as a function of UV irradiation time. The time taken to reach intensity maxima was observed to be 6h but to ensure complete destruction of vesicles, for other studies, the samples were irradiated for 8h.

5.4.3.8 Tyndall Effect experiments

The solutions were taken in 3 mL fluorescence cuvettes and in dark, laser was irradiated through these solutions and the images were captured using a hand held camera.

NMR and Mass Spectra of the Synthesized Compounds

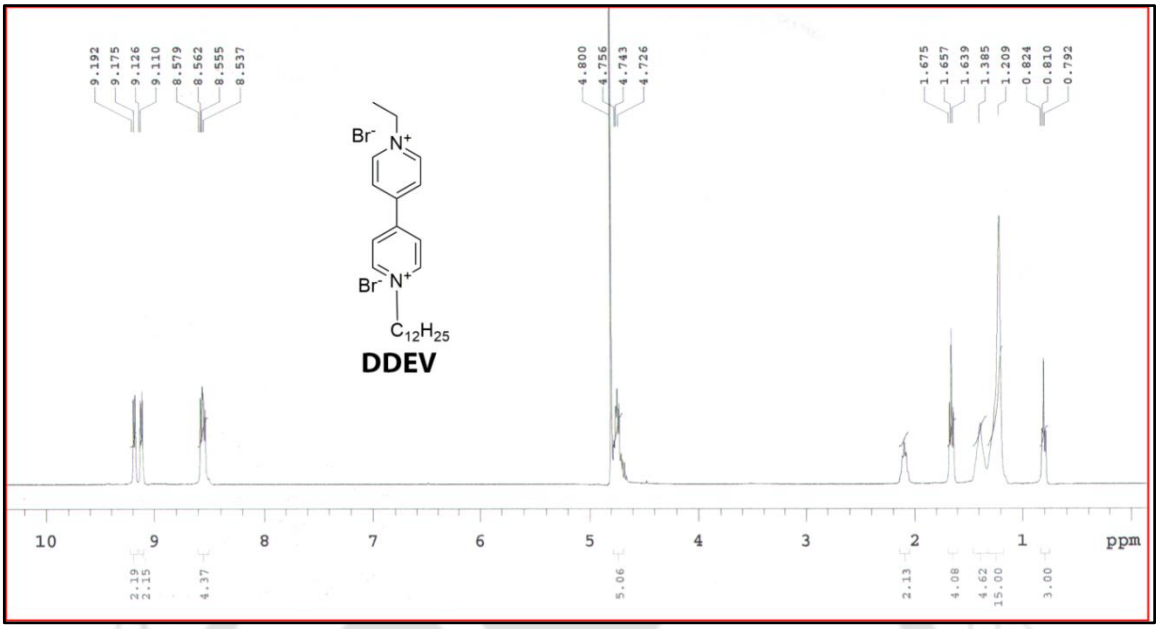

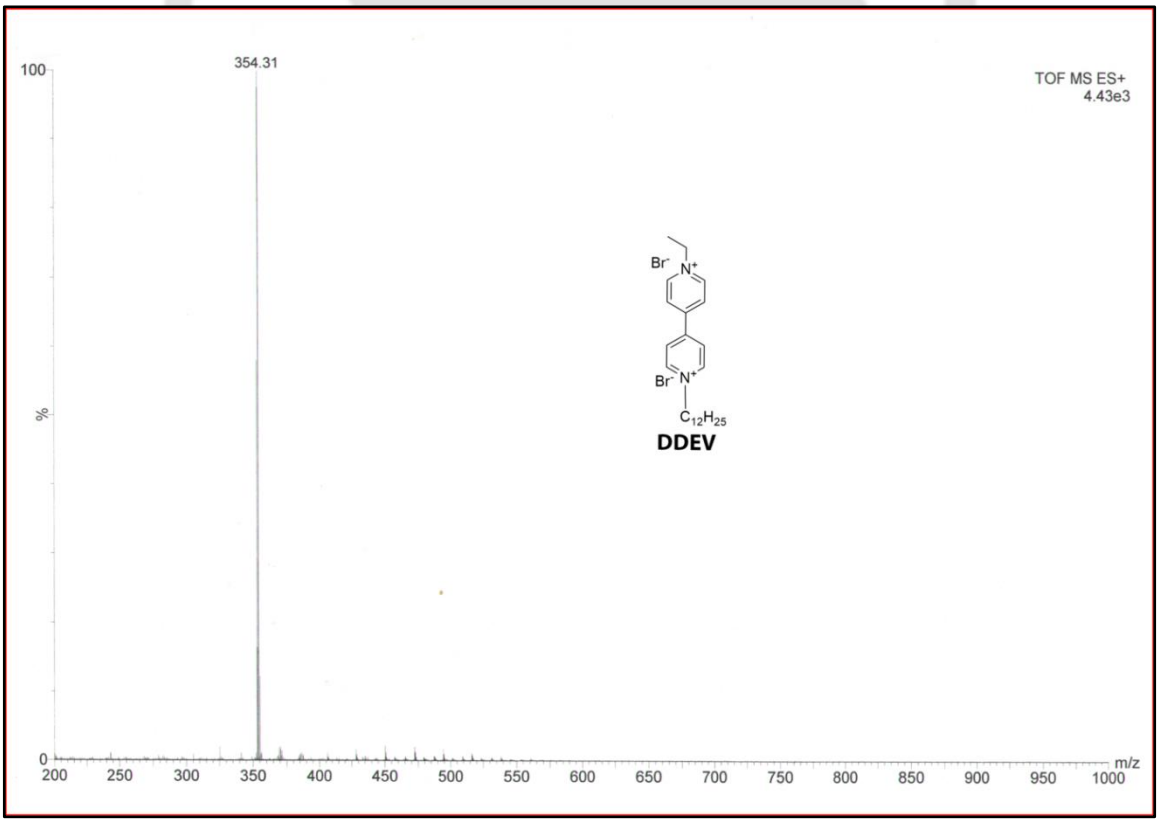

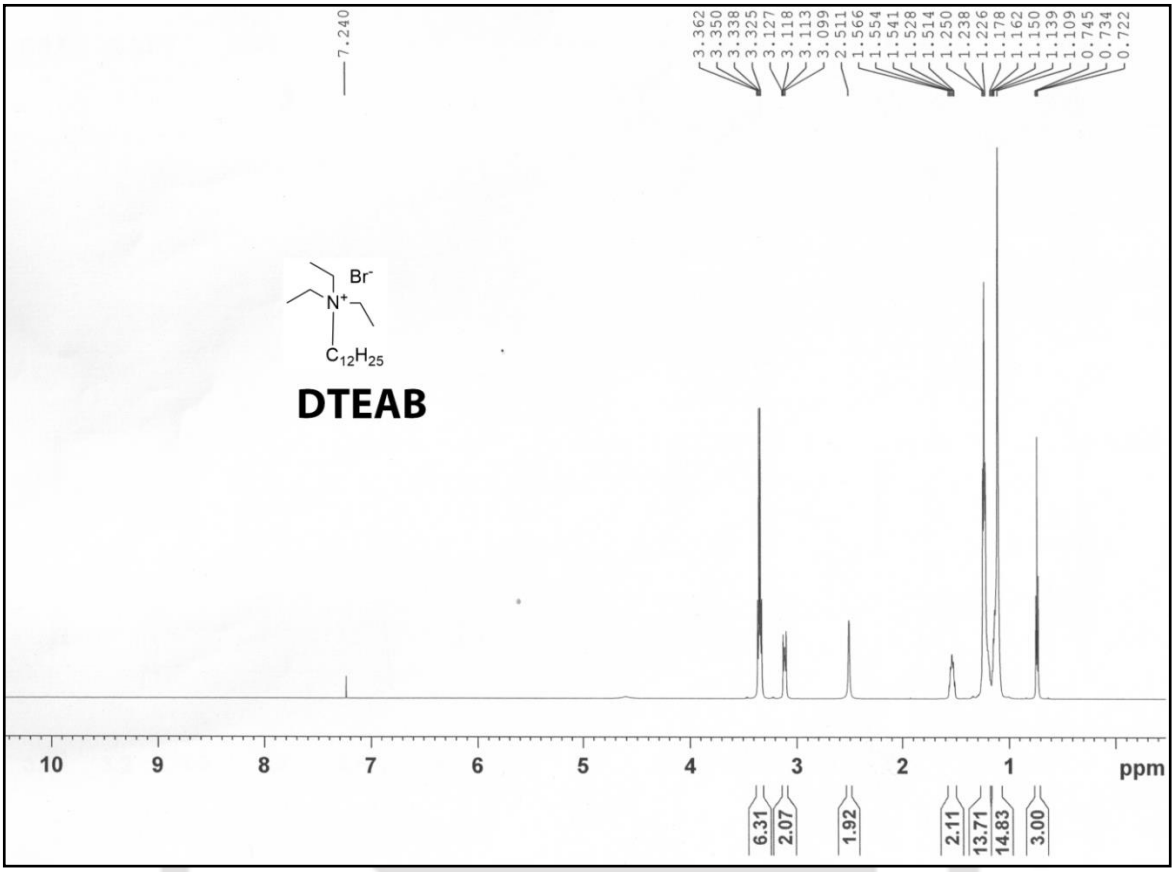

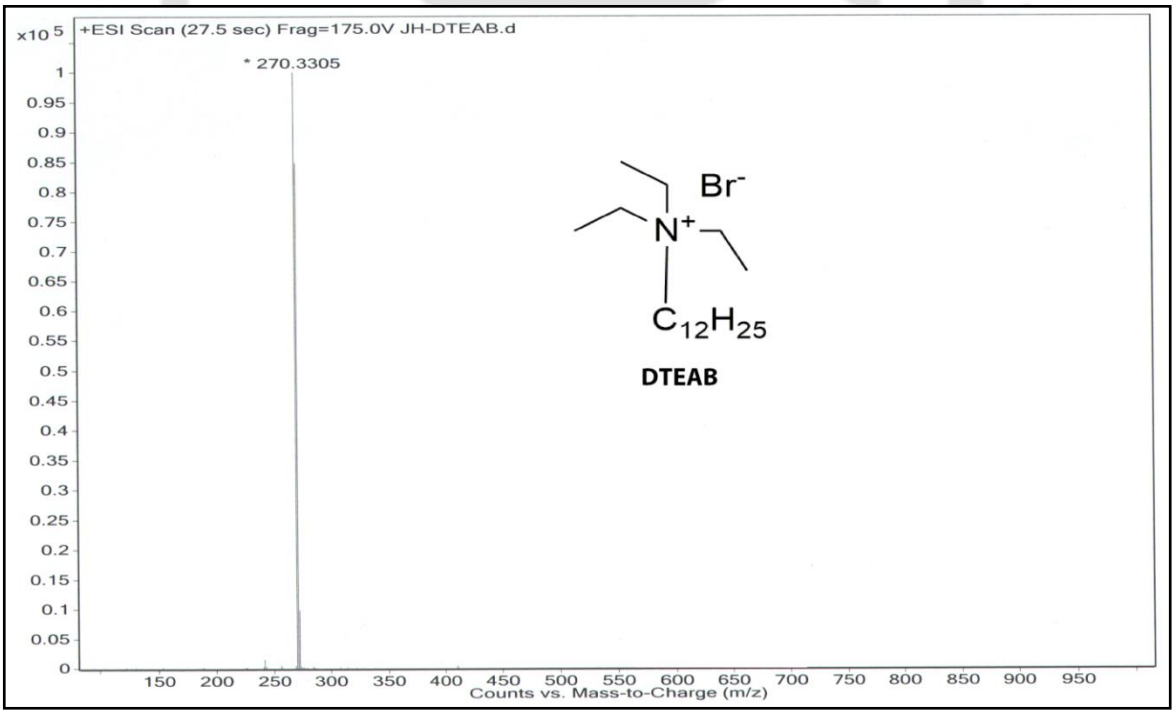

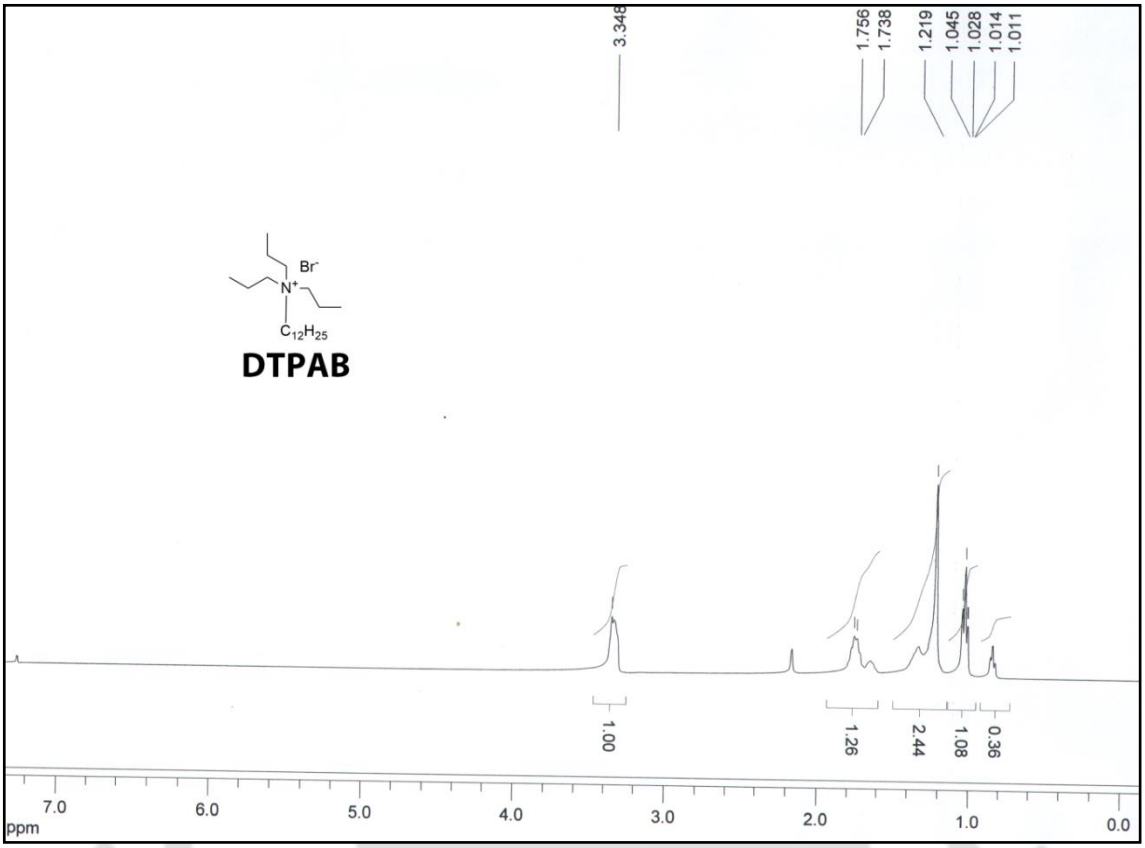

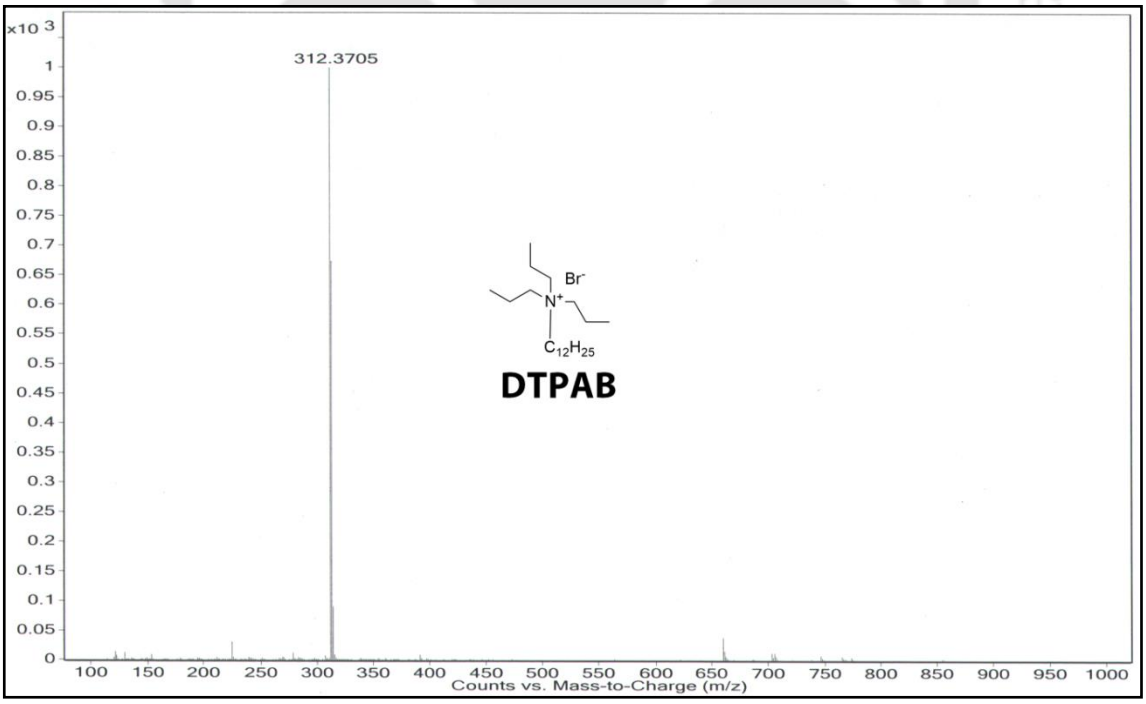

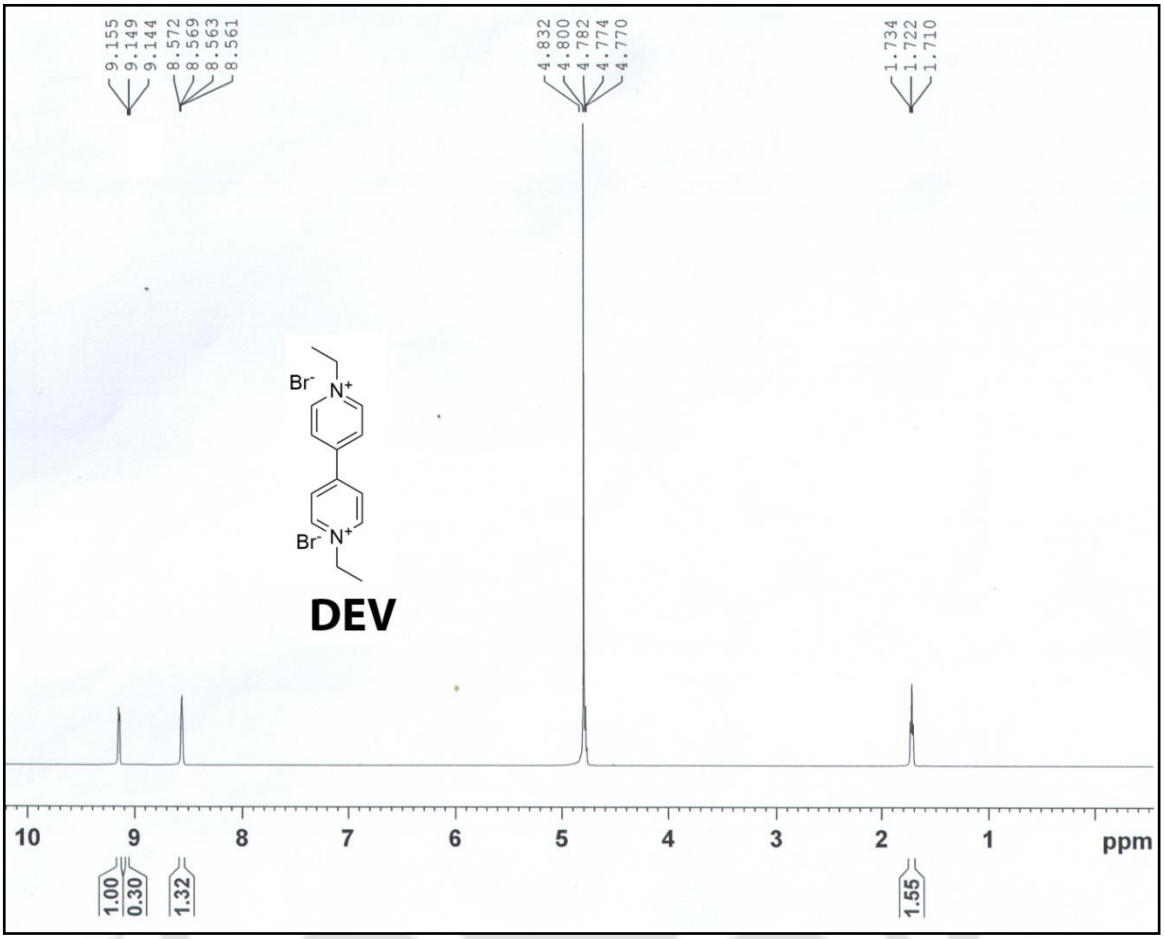
9.155
9.149
9.144
8.572
8.569
8.563
8.561
4.832
4.800
4.782
4.774
4.770
1.734
1.722
1.710
Br⁻
N⁺
Br⁻
N⁺
DEV
10
9
8
7
6
5
4
3
2
1
ppm
1.00
0.30
1.32
1.55

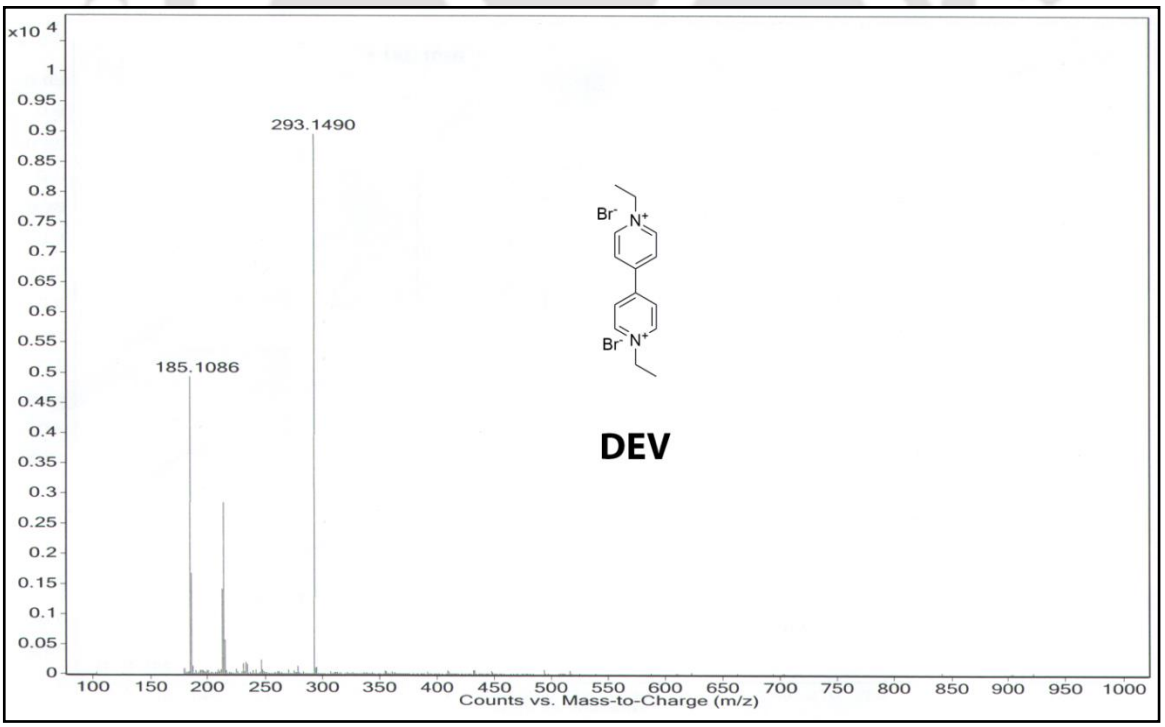
x10 4
293.1490
185.1086
Br⁻
N⁺
Br⁻
N⁺
DEV
Counts vs. Mass-to-Charge (m/z)

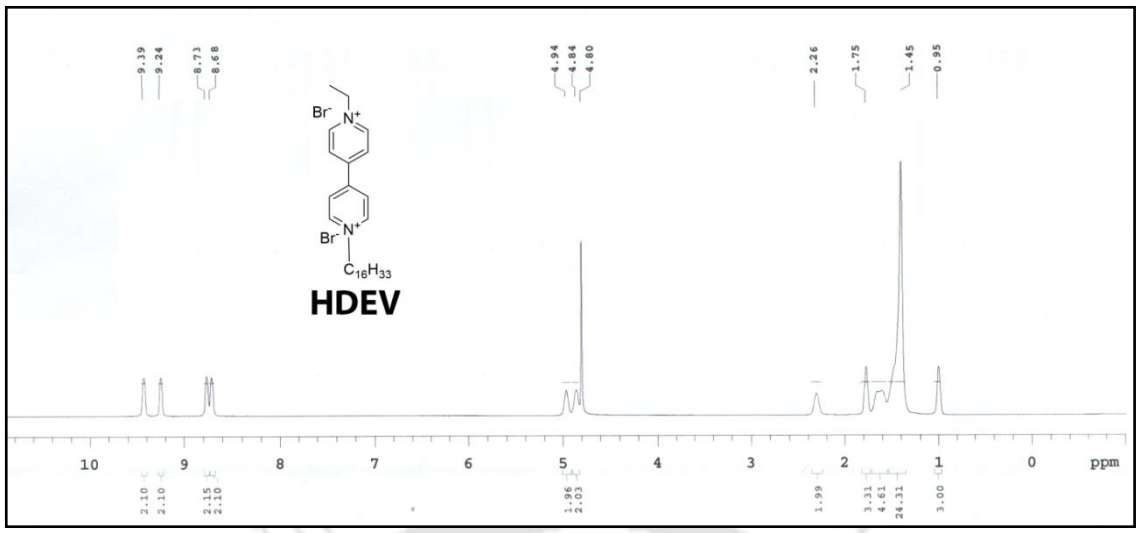

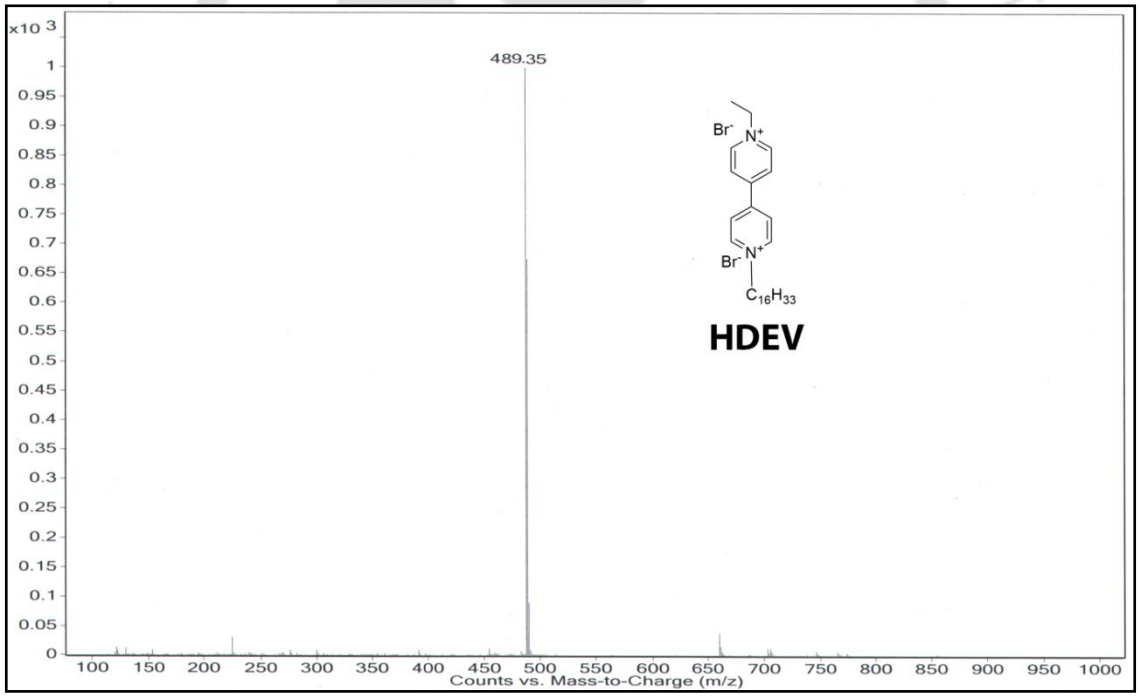

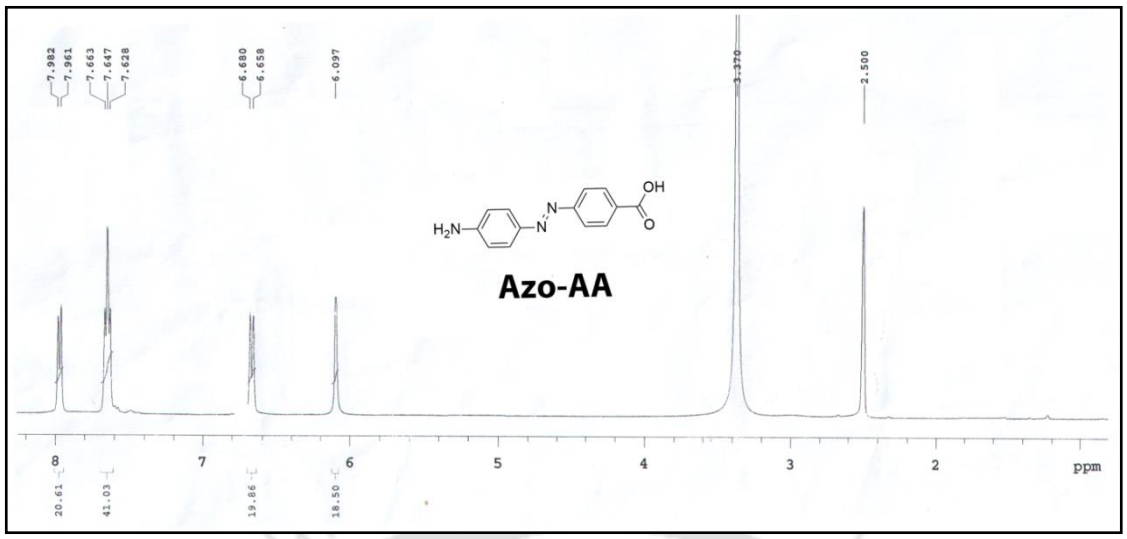

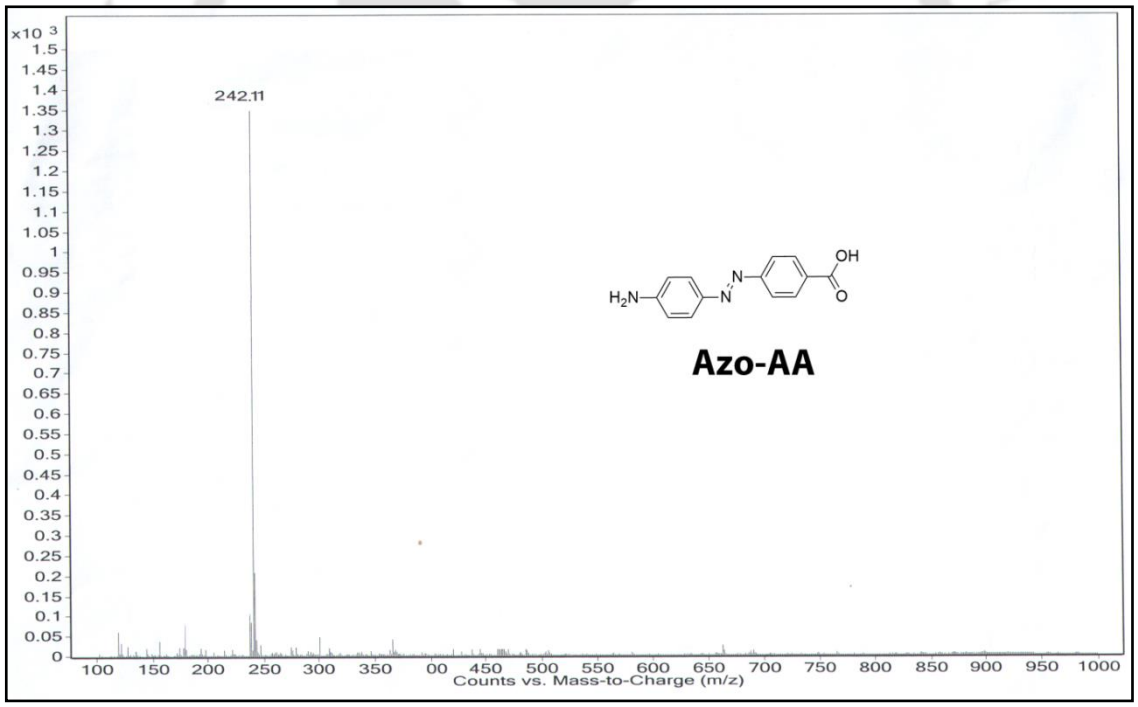

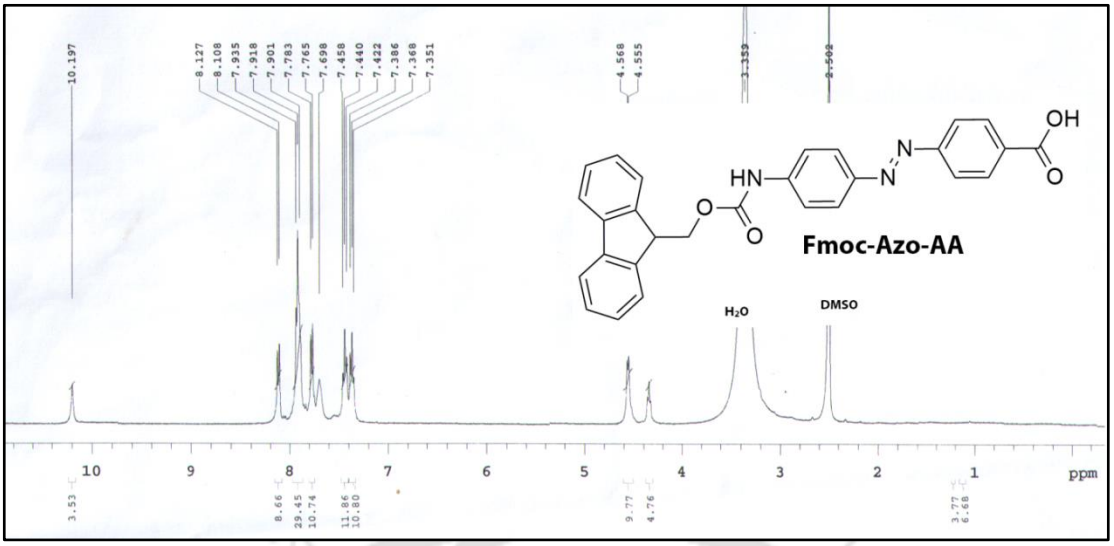

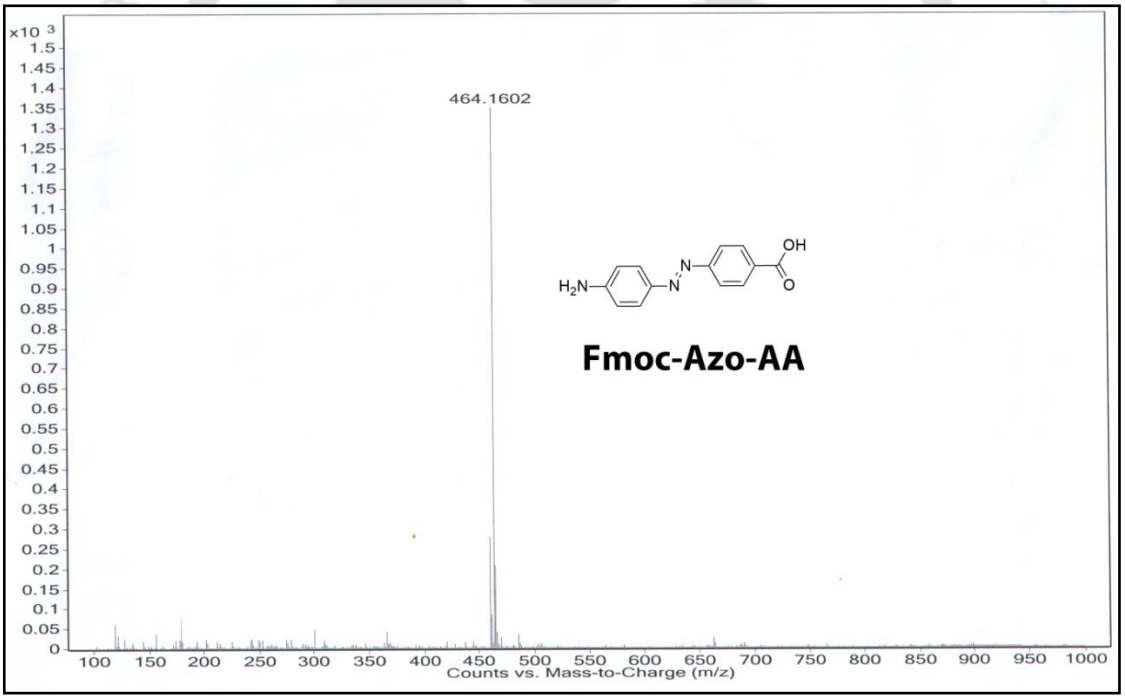

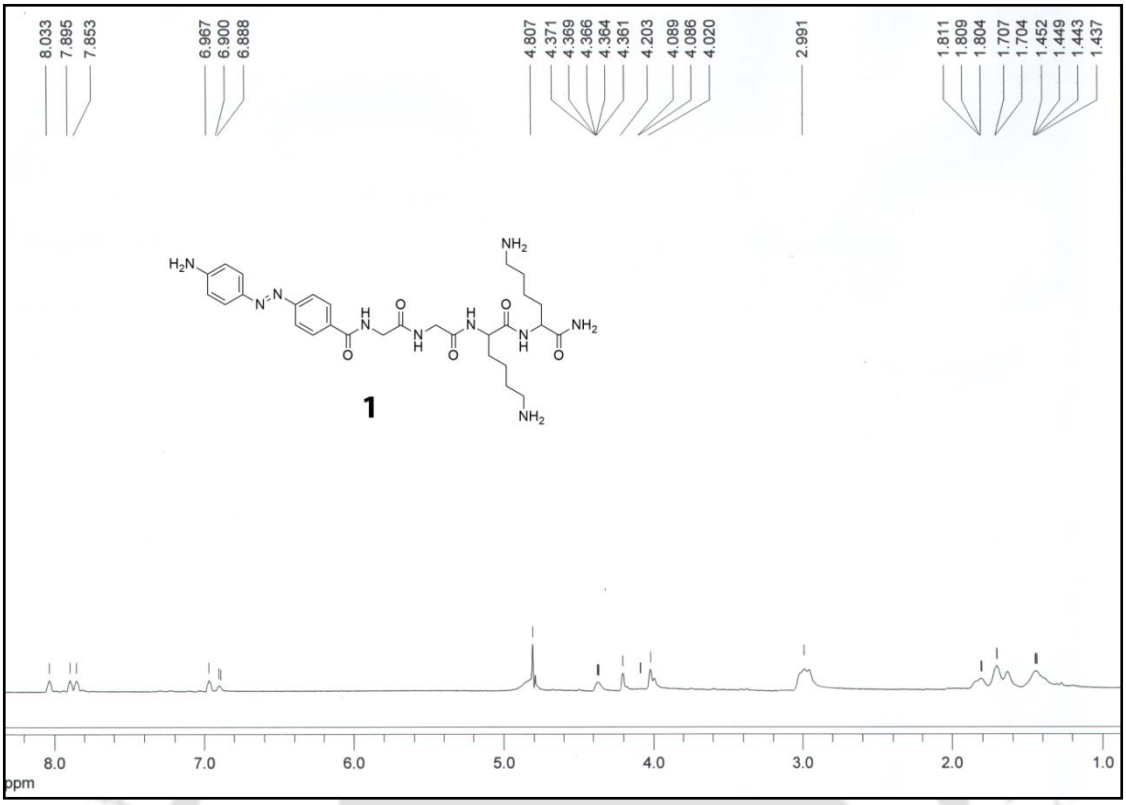

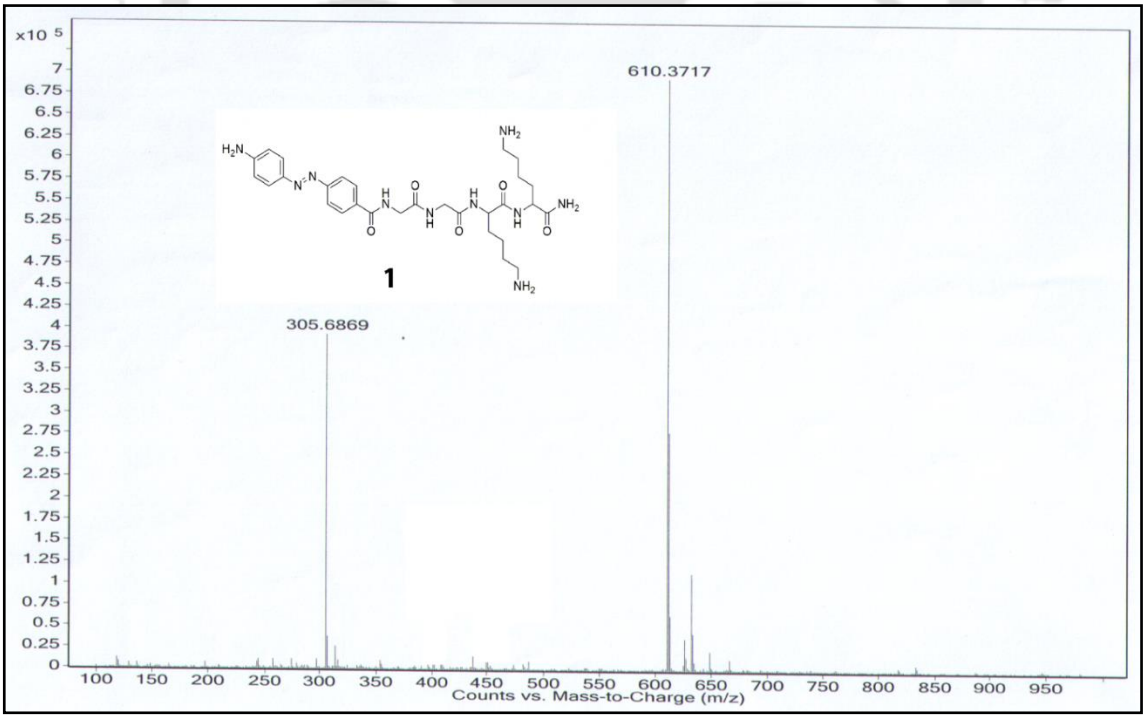

Postlude

"In literature and in life we ultimately pursue, not conclusions, but beginnings."
— Sam Tanenhaus

The research reported in this thesis started with a small question. The transformation of the aqueous viologen amphiphile solution to vesicles by CB[8] amazed us and we did ask "how and why?". The exploration began and in this long process many of the underlying un-answer questions found their answers. Though the mechanistic detail is still not revealed in detail, in the process we could interpret it partially. The studies depicted here helped us to understand and use this phenomenon to construct newer efficient systems which may find applications in the coming years.

As the quotation of Sam Tanenhaus says, this is not the conclusion but just the beginning. Our group at IIT Guwahati is devoted to the development of new insights to provide a better understanding of the supramolecular chemistry. The work depicted in this thesis is the result of our consistent effort toward contributing to the scientific advancement and ends with an optimistic note to content the reader.

REFERENCES

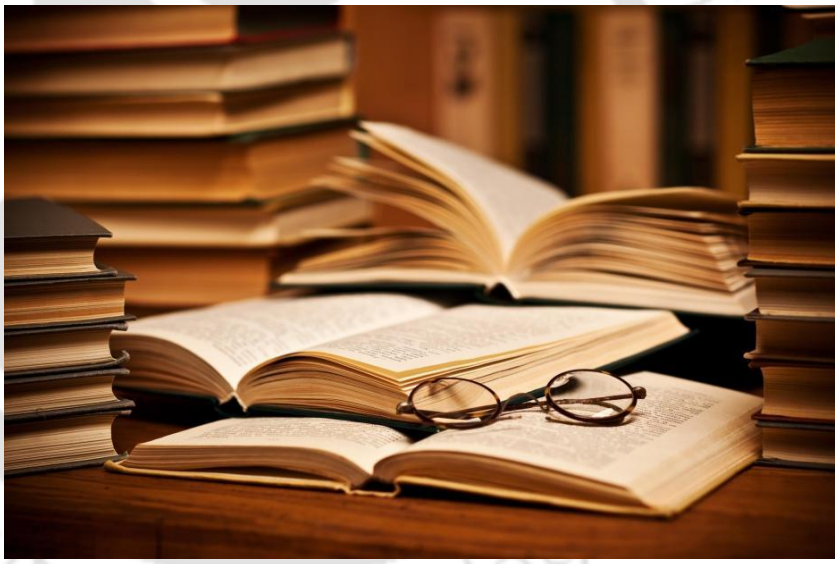

1. van der Waals, J. D. (1873) *Over de Continuiteit van den Gas-en Vloeistoftoestand (on the continuity of the gas and liquid state)*. PhD thesis (excerpt), Leiden, The Netherlands.
2. Fischer, E. *Berichte der deutschen chemischen Gesellschaft* **1894**, *27*, 2985–2993.
3. Watson, J. D.; Crick, F. H. C. Molecular structure of nucleic acid. *Nature* **1953**, *171*, 737-738.
4. Pederson, C. J. Cyclic polyethers and their complexes with metal salts**.** *J. Am. Chem. Soc.* **1967**, *89*, 7017–7036.
5. Pedersen, C. J. The Discovery of Crown Ethers (Noble Lecture). *Angew. Chem., Int. Ed.* **1988**, 27, 1021-1027.
6. Cram, D. J. The Design of Molecular Hosts, Guests, and Their Complexes (Nobel Lecture). *Angew. Chem., Int. Ed.* **1988**, 27, 1009-1020.
7. Lehn, J.-M. Supramolecular Chemistry—Scope and Perspectives Molecules, Supermolecules, and Molecular Devices (Nobel Lecture). *Angew. Chem., Int. Ed.* **1988**, 27, 89-112.
8. Gale, P. A. Supramolecular Chemistry Anniversary. *J. Chem. Soc. Rev.* **2007**, *36*, 141-142.
9. Gokel, G. W. Comprehensive Supramolecular Chemistry, Vol. 1: Molecular Recognition: Receptors for Cationic Guests, Pergamon, Oxford, **1996**.
10. Vögtle, F. Comprehensive Supramolecular Chemistry, Vol. 2: Molecular Recognition: Receptors for Molecular Guests, Pergamon, Oxford, **1996**.
11. Szejtli, J.; Osa, T. Comprehensive Supramolecular Chemistry, Vol. 3: Cyclodextrins, Pergamon, Oxford, **1996**.
12. Lagona, J.; Mukhopadhyay, P.; Chakrabarti, S.; Isaacs, L. The Cucurbit[n]uril Family. *Angew. Chem., Int. Ed.* **2005**, *44*, 4844−4870.
13. Lee, J. W.; Samal, S.; Selvapalam, N.; Kim, H.-J.; Kim, K. Cucurbituril Homologues and Derivatives: New Opportunities in Supramolecular Chemistry. *Acc. Chem. Res.* **2003**, *36*, 621-630.
14. Das, D.; Scherman, O. Cucurbituril: At the Interface of Small Molecule Host−Guest Chemistry and Dynamic Aggregates. *Isr. J. Chem.* **2011**, *51*, 537−550.
15. Rekharsky, M. V.; Mori, T.; Yang, C.; Ko, Y. H.; Selvapalam, N.; Kim, H.; Sobransingh, D.; Kaifer, A. E.; Liu, S.; Isaacs, L.; Chen, W;. Moghaddam, S.; Gilson, M. K.; Kim, K.; Inoue, Y. A synthetic host-guest system achieves avidin-biotin affinity by overcoming enthalpy–entropy compensation.*Proc. Natl. Acad. Sci. USA* **2007**, *104*, 20737–20742.
16. Freeman, W. A.; Mock, W. L.; Shih, N.-Y. Cucurbituril. *J. Am. Chem. Soc*. **1981**, *103*, 7367–7368.
17. Behrend, R.; Meyer, E.; Rusche, F. Liebigs F. *Justus Liebigs Ann. Chem*. **1905**, *339*, 1–37.
18. Kim, J.; Jung, I.-S.; Kim, S.-Y.; Lee, E.; Kang, J.-K.; Sakamoto, S.; Yamaguchi, K.; Kim, K. New Cucurbituril Homologues: Syntheses, Isolation, Characterization, and X-ray Crystal Structures of Cucurbit[*n*]uril (*n* = 5, 7, and 8). *J. Am. Chem. Soc*. **2000**, *122*, 540–541.
19. Day, A. I.; Arnold, A. P.; Blanch, R. J.; Snushall, B. Controlling Factors in the Synthesis of Cucurbituril and Its Homologues. *J. Org. Chem*. **2001**, *66*, 8094 –8100.
20. Day, A. I. Blanch, R. J. Arnold, A. P. Lorenzo, S. Lewis, G. R. Dance, I. A Cucurbituril-Based Gyroscane: A New Supramolecular Form. *Angew. Chem., Int. Ed.* **2002**, 41, 275–277.
21. Liu, S.; Zavalij, P. Y.; Isaacs, L. Cucurbit[10]uril. *J. Am. Chem. Soc.* **2005**, *127*, 16798 –16799.
22. Buschmann, H.-J.; Cleve, E.; Jansen, K.; Wego, A.; Schollmeyer, E. The determination of complex stabilities between different cyclodextrins and dibenzo-18-crown-6, cucurbit[6]uril, decamethylcucurbit[5]uril, cucurbit[5]uril, p-tert-butylcalix[4]arene and p-tert-butylcalix[6]arene in aqueous solutions using a spectrophotometric method. *Mater. Sci. Eng. C* **2001**, *14*, 35 – 39.
23. Germain, P.; Letoffe, J. M.; Merlin, M. P.; Buschmann, H.-J. Thermal behaviour of hydrated and anhydrous Cucurbituril: A DSC, T.G. and calorimetric study in temperature range from 100 to 800 K. *Thermochim. Acta* **1998**, *315*, 87 – 92.
24. Buschmann, H.-J.; Cleve, E.; Schollmeyer, E. *Inorg. Chim. Acta*. Cucurbituril as a ligand for the complexation of cations in aqueous solutions. **1992**, *193*, 93 – 97.
25. Mårquez, C.; Hudgins, R. R.; Nau, W. M. Mechanism of Host−Guest Complexation by Cucurbituril. *J. Am. Chem. Soc.* **2004**, *126*, 5806 – 5816.
26. Buschmann, H.-J.; Jansen, K.; Meschke, C.; Schollmeyer, E. *J. Solution Chem.* **1998**, *27*, 135 – 140.
27. Zhang, G.-L.; Xu, Z.-Q.; Xue, S.-F.; Zhu, Q.-J.; Tao, Z. *Wuji Huaxue Xuebao* **2003**, *19*, 655 – 659.
28. Jansen, K.; Buschmann, H.-J.; Wego, A.; DWpp, D.; Mayer, C.; Drexler, H. J;. Holdt, H. J.; Schollmeyer, E. *J. Inclusion Phenom. Macrocyclic Chem.* **2001**, *39*, 357 – 363.
29. Uzunova, V. D.; Cullinane, C.; Brix, K.; Nau W. M.; Day, A. I. *Org. Biomol. Chem*. **2010**, *8*, 2037-2042.
30. Hettiarachchi, G.; Nguyen, D.; Wu, J.; Lucas, D.; Ma, D.; Isaacs, L.; Briken, V. *PLoS One*, **2010**, *5*, e10514.
31. Jeon, Y. J.; Kim, S.-Y.; Ko, Y. H.; Sakamoto, S.; Yamaguchi, K.; Kim, K. *Org. Biomol. Chem*. **2005**, *3*, 2122-2125.
32. Masson, E.; Ling, X.; Joseph, R.; Kyeremeh-Mensah, L.; Lu, X. Cucurbituril chemistry: a tale of supramolecular success. *RSC Advances* **2012**, *2,* 1213–1247.

33. Urbach A. R.; Ramalingam, V. Molecular Recognition of Amino Acids, Peptides, and Proteins by Cucurbit[n]uril Receptors. *Isr. J. Chem.* **2011**, *51*, 537–550.
34. Kaifer, A. E.; Li, W.; Yi, S. Cucurbiturils as Versatile Receptors for Redox Active Substrates. *Isr. J. Chem.* **2011**, *51*, 496–505.
35. Zhang, X. X.; Krakowiak, K. E.; Xue, G.; Bradshaw, J. S.; Izatt, R. M. A Highly Selective Compound for Lead: Complexation Studies of Decamethylcucurbit[5]uril with Metal Ions. *Ind. Eng. Chem. Res.* **2000**, *39*, 3516-3520.
36. Heo, J.; Kim, J.; Whang, D.; Kim, K. Columnar One-Dimensional Coordination Polymer Formed with a Metal ion and a Host-Guest complex as Building Blocks: Potassium Ion Complexed Cucurbituril. *Inorg. Chim. Acta* **2000**, *279*, 307-312.
37. Sokolov, M. N.; Virovets, A. V.; Dybtsev, D. N.; Gerasko, O. A.; Fedin, V. P.; Hernandez-Molina, R.; Clegg, W.; Sykes, A. G. Metal Incorporation into and Dimerization of M_3E_4 Clusters (M=Mo, W; E=S, Se) in Supramolecular Assemblies with Cucurbituril: A Molecular Model of Intercalation *Angew. Chem., Int. Ed.* **2000**, *39*, 1659-1661.
38. Jeon, Y.-M.; Kim, J.; Whang, D.; Kim, K. Molecular Container Assembly Capable of Controlling Binding and Release of Its Guest Molecules: Reversible Encapsulation of Organic Molecules in Sodium Ion Complexed Cucurbituril. J. *Am. Chem. Soc.* **1996***, 118,* 9790-9791.
39. Whang, D.; Heo, J.; Park, J. H.; Kim, K. A Molecular Bowl with Metal Ion as Bottom:Reversible Inclusion of Organic Molecules in Cesium Ion Complexed Cucurbituril. *Angew. Chem., Int. Ed.* **1998***, 37*, 78-80.
40. Jeon, W. S.; Moon, K.; Park , S. H.; Chun , H.; Ko , Y. H.; Lee, J. Y.; Lee, E. S.; Samal, S.; Selvapalam, N.; Rekharsky, M. V.; Sindelar. V.; Sobransingh, D.; Inoue,Y.; Kaifer, A. E.; Kim, K. Complexation of Ferrocene Derivatives by the Cucurbit[7]uril Host: A Comparative Study of the Cucurbituril and Cyclodextrin Host Families. *J. Am. Chem. Soc.* **2005**, *127*, 12984–12989.
41. Jeon, W. S.; Kim, H.-J.; Lee, C.; K. Kim, Control of the Stoichiometry in Host-guest Complexation by Redox Chemistry of Guests: Inclusion of Methyl-viologen in Cucurbit[8]uril. *Chem. Commun*. **2002**, 1828-1829.
42. Kim, H-J.; Heo, J.; Jeon, W. S.; Lee, E.; Kim, J.; Sakamoto, S.; Yamaguchi, K.; Kim, K. Selective Inclusion of a Hetero-Guest Pair in a Molecular Host: Formation of Stable Charge-Transfer Complexes in Cucurbit[8]uril. *Angew. Chem., Int. Ed.* **2001,** *40*, 1526-1529.
43. Rauwald, U.; Biedermann, F.; Deroo, S.; Robinson, C. V.; Schermann, O. A. Correlating Solution Binding and ESI-MS stabilities by Incorporating Solvation Effects in a Confined Cucurbit[8]uril System. *J. Phys. Chem. B* **2010,** *114,* 8606–8615.
44. U.S. Patent: Kim, K.; Kim, J.; Jung, I.-S.; Kim, S.-Y.; Lee, E.; Kang, J.-K. Pohang University of Science and Technology Foundation, 2000.
45. Bush, M, E.; Bouley, N. D.; Urbach, A. R. Charge-Mediated Recognition of N- Terminal Tryptophan in Aqueous Solution by a Synthetic Host. *J. Am. Chem. Soc.* **2005***, 127,* 14511-14517.
46. Heitmann, L. M.; Taylor, A. B.; Hart, P. J.; Urbach, A. R. Sequence-Specific Recognition and Cooperative Dimerization of N-Terminal Aromatic Peptides in Aqueous Solution by a Synthetic Host. *J. Am. Chem. Soc.* **2006**, *128*, 12574-12581.
47. Nguyen, H. D.; Dang, D. T.; van Dongen, J. L. J.; Brunsveld, L. Protein Dimerization Induced by Supramolecular Interactions with Cucurbit[8]uril. *Angew. Chem., Int. Ed.* **2010**, *49*, 895–898.
48. Uhlenheuer, D. A.; Young, J. F.; Nguyen, H. D.; Scheepstraa, M.; Brunsveld, L. Cucurbit[8]uril induced heterodimerization of methylviologen and naphthalene functionalized proteins. *Chem. Commun.* **2011**, *47*, 6798–6800.
49. Biedermann, F.; Rauwald, U.; Zayed, J. M.; Scherman, O. A. A supramolecular route for reversible protein-polymer conjugation. *Chem. Sci.* **2011**, *2*, 279–286.
50. Rauwald, U.; Scherman, O. A.; Supramolecular Block Copolymers with Cucurbit[8]uril in Water. *Angew. Chem., Int. Ed.* **2008**, *47*, 3950–3953.
51. Appel, E. A.; Biedermann, F.; Rauwald, U.; Jones, S. T.; Zayed, J. M.; Schermann, O. A. Supramolecular Cross-Linked Networks *via* Host-Guest Complexation with Cucurbit[8]uril. *J. Am. Chem. Soc.* **2010***, 132,* 14251-14260.
52. Coulston, R. J.; Jones, S. T.; Lee, T. C.; Schermann, O. A. Supramolecular gold nanoparticle–polymer composites formed in water with cucurbit[8]uril. Chem. Commun. **2010**, *47*, 164–166.
53. Loh, X. J.; Barrio, J. d.; Toh, P. P. C.; Lee, T. C.; Jiao, D.; Rauwald, U.; Appel, E. A.; Schermann, O. A. Triply Triggered Doxorubicin Release From Supramolecular Nanocontainers. *Biomacromolecules* **2012**, *13*, 84–91.
54. Tian, F.; Cziferszky, M.; Jiao, D.; Wahlström, K.; Geng, J.; Scherman, O. A. Peptide Separation through a CB[8]-Mediated Supramolecular Trap-and-Release Process. *Langmuir* **2011**, 27, 1387–1390.
55. Lan, Y.; Wu, Y.; Karas, A.; Scherman, O. A. Photoresponsive Hybrid Raspberry-Like Colloids Based on Cucurbit[8]uril Host–Guest Interactions. *Angew. Chem., Int. Ed.* **2014**, *53*, 2166–2169.
56. Barooah, N.; Pemberton, B. C.; Sivaguru, J. Manipulating Photochemical Reactivity of Coumarins within Cucurbituril Nanocavities. *Org. Lett.* **2008**, *10*, 3339-3342.
57. Ko, Y. H.; Kim, E.; Hwang, I.; Kim, K. Supramolecular assemblies built with host-stabilized charge-transfer interactions. *Chem. Commun*. **2007**, 1305–1315.

58. Fendler, J. H. *Membrane mimetic chemistry*; Wiley & Sons: New York. **1982**.
59. Zana, R.; Lang, J.; Mittal, K. L.; Fendler, E. J. *Solution Behavior of Surfactants*; Plenum: New York. **1982**. Vol. 2.
60. Stenius, P. *Reverse Micelles*, Luisi, P. L.; Straub, E.; Eds.; Plenum, New York, **1984**, 1.
61. Eicke, H. F.; Kvita, P. *Reverse Micelles*; Luisi, P. L.; Straub, B. E.; Eds.; Plenum: New York, **1984**, 21.
62. Luisi, P. L.; Magid, L. J. *CRC Crit. Rev. Biochem.* **1986***, 20,* 409.
63. Luisi, P. L. Enzymes hosted in reverse micelles in hydrocarbon solution. *Angew. Chem., Int. Ed.* **1985**, *24*, 439-450.
64. Eicke, H. F.; Rehak, J. *Helv. Chim. Acta* **1976**, *59*, 2883.
65. Eicke, H. F.; Shepherd, T. C.; Steinmann, A. *J. Colloid Interface Sci.* **1976**, *56*, 168.
66. Fendler, J. H. Interactions and reactions in reversed micellar systems. *Acc. Chem. Res.* **1976**, *9*, 153-161.
67. Holmberg, K.; Jonsson, B.; Kronberg, B.; Lindman, B. *Surfactants and Polymers in Aqueous Solution*, Wiley & Sons: New York. **2003**; 2nd ed.
68. Menger, F. M. Groups of organic molecules that operate collectively. *Angew. Chem., Int. Ed.* **1991**, *30*, 1086-1099.
69. Voet, D.; Voet, J. G.; Pratt, C. W. *Fundamentals of Biochemistry*; Wiley & Sons: New York. **1999**.
70. Nelson, D. L.; Cox, M. M. *Lehninger Principles of Biochemistry*; Worth Publishers: New York. **2003**; 3rd ed.
71. IUPAC, *Compendium of Chemical Terminology*, 2nd ed. (the "Gold Book") (1997). Online corrected version: (2006–).
72. Bird, C. L.; Kuhn, A. T. Electrochemistry of the viologens. *Chem. Soc. Rev.* **1981**, *10*, 49-82.
73. Ito, M.; Kuwana, T. Spectroelectrochemical study of indirect reduction of triphosphopyridine nucleotide: I. Methyl viologen, ferredoxin-TPN-reductase and TPN. *J. Electroanal. Chem*. *Interfacial Electrochem.* **1971**, *32*, 415-425.
74. Szentrimay, P.Y.; Kuwana, T. *Electrochemical Studies of Biological Systems*; Swayer, D. Ed. American Chemical Society: Washington, DC, **1977**, p. 143.
75. Whitten, D. G. Photoinduced Electron-Transfer Reactions of Metal Complexes in Solution. *Acc. Chem. Res.* **1980**, *13,* 83-90.
76. *Photogeneration of Hydrogen*; Harriman, A., West, M. A. Eds. Academic Press:New York, **1982**.
77. Kalyanasundaram, K. Photochemistry and solar energy conversion with tris(bipyridyl)ruthenium(II) and its analogues. *Coord. Chem. Rev.* **1982**, *46,* 159-244.
78. M. Gratzel, *Energy Resources through Photochemistry and Catalysis*; Academic Press: New York, **1983**.
79. Bruink, J.; Kregting, C.G.A.; Ponjee, J.J. Modified Viologens with Improved Electrochemical Properties for Display Applications. *J. Electrochem. Soc.* **1977**, *124*, 1854-58.
80. Yasuda, A.; Kondo, H.; Itabashi, M.; Seto, J. Structure changes of viologen + β-cyclodextrin inclusion complex corresponding to the redox state of viologen. *J. Electroanal. Chem.* **1986**, *210,* 265-275.
81. Yasuda, A.; Mori, H.; Seto, J. Electrochromic properties of alkylviologen-cyclodextrin systems. *J. Appl. Electrochem*. **1987**, *17*, 567-573.
82. Nomura, K.; Hirayama, K.; Ohsaka, T.; Nakanishi, M.; Hatozaki, O.; Oyama, N. Electrochemical and Electrochromic Properties of Conductive Powder Containing Polymer Complex Films Composed of Poly-(tetramethylene viologen)and Poly(p-styrenesulfonic acid). J. *Macromol. Sci. Chem. A* **1989**, *26*, 593-608.
83. Park, J. W.; Lee, B. A.; Lee, S. Y. Linkage Length Dependence of Intramolecular Photoinduced Electron Transfer Reactions in Aromatic Donor−Viologen Acceptor Molecules Linked by Polymethylene Bridges. *J. Phys. Chem. B*, **1998**, *102*, 8209-8215.
84. Hariharan, M.; Joseph, J.; Ramaiah, D. Novel Bifunctional Viologen-Linked Pyrene Conjugates: Synthesis and Study of Their Interactions with Nucleosides and DNA. *J. Phys. Chem. B* **2006**, *110*, 24678-24686.
85. Mogera, U.; Sagade, A. A.; George S. J.; Kulkarni, G. U. Ultrafast response humidity sensor using supramolecular nanofibre and its application in monitoring breath humidity and flow. *Sci. Reports* **2014**, *4*, 4103.
86. Yonemura,H.; Nakamura, H.; Matsuo, T. External magnetic field effects on photoinduced electron transfer reactions in phenothiazine-viologen-linked systems complexed with cyclodextrins. *Chem. Phys. Lett*., **1989**, *155*, 157-161.
87. Kunkely, H.; Vogler, A. Optical Charge Transfer in the Ion Pairs Methyl Viologen (2+) Guanosine-5′-monophosphate(2−) and Adenosine-5′-triphosphate(2−). *Chem. Phys. Lett.* **2001**, *345*, 309−311.
88. Jalilov, A. S.; Patwardhan, S.; Singh, A.; Simeon, T.; Sarjeant, A. A.; Schatz, G. C.; Lewis, F. D. Structure and Electronic Spectra of Purine−Methyl Viologen Charge Transfer Complexes. *J. Phys. Chem. B* **2014**, *118*, 125−133.
89. Fromherz, P.; Rieger, B. Photoinduced Electron-Transfer in DNA Matrix from Intercalated Ethidium to Condensed Methylviologen. *J. Am. Chem. Soc*. **1986**, *108*, 5361−5362.
90. Gomez, M. E.; Li, J.; Kaifer, A. E. Interfacial Stabilization of Amphiphilic Viologen Monolayers Induced by Poly(styrenesu1fonate). *Langmuir* **1991**, *7*, 1571-1575.
91. Kostela, J.; Elmgren, M.; Hansson, P.; Almgren, M. Electrochemical properties of an amphiphilic viologen in differently charged micelles. *J. Electroanal. Chem.* **2002**, *536*, 97-107.

92. Lee, C. W.; Oh, M. K.; Jang, J-M. Reduction Potentials of N-Hexadecyl-N'-methyl Viologen(2+/+) Solubilized in Cationic, Nonionic, and Anionic Micelles. *Langmuir* **1993**, *9*, 1934-1936.
93. Fu, Y. R.; Zhang, S.; Chen, M.; Qian, D-J. Morphology and electrochemical properties of amphiphilic viologen functionalized multiwalled carbon nanotube hybrids in Langmuir–Blodgett films. *Thin Solid Films* **2012**, *520,* 6994–7001.
94. Rao, K. V.; Jayaramulu, K.; Maji, T. K.; George, S. J. Supramolecular Hydrogels and High-Aspect-Ratio Nanofibers through Charge-Transfer-Induced Alternate Coassembly. *Angew. Chem., Int. Ed.* **2010**, *49*, 4218-4222.
95. Sagade, A. A.;Rao, K. V.; Mogera, U.; George, S.J.; Datta, A.; Kulkarni, G.U. High-Mobility Field Effect Transistors Based on Supramolecular Charge Transfer Nanofibres. *Adv. Mater.* **2013**, *25,* 559-564.
96. Ko, Y. H.; Kim, H.; Kim, Y.; Kim, K. U-Shaped Conformation of Alkyl Chains Bound to a Synthetic Host. *Angew. Chem., Int. Ed.* **2008**, *47*, 4106–4109.
97. Baek, K.; Kim, Y.; Kim, H.; Yoon, M.; Hwang, I.; Ko, Y. H.; Kim, K. Unconventional U-shaped conformation of a bolaamphiphile embedded in a synthetic host. *Chem. Commun*. **2010**, *46*, 4091–4093.
98. Choudhury, S. D.; Barooah, N.; Aswal, V. K.; Pal, H.; Bhasikuttan, A. C.; Mohanty, J. Stimuli-responsive supramolecular micellar assemblies of cetylpyridinium chloride with cucurbit[5/7]urils. *Soft Matter*, **2014**, *10*, 3485-3493.
99. Pessêgo, M.; Basilio, N.; Moreira, J. A.; Garcia-Rio, L. Cucurbit[7]uril: Surfactant Host–Guest Complexes in Equilibrium with Micellar Aggregates. *ChemPhysChem* **2011**, *12*, 1342-1350.
100. Pessêgo, M.; Moreira, J. A.; Garcia-Rio, L. Evidence of Higher Complexes Between Cucurbit[7]uril and Cationic Surfactants. *Chem. Eur.J.* **2012**, *18*, 7931-7940.
101. Jeon, Y. J.; Bharadwaj, P. K.; Choi, S. W.; Lee, J-W.; Kim, K. Supramolecular amphiphiles: Spontaneous formation of vesicles triggered by formation of a charge-transfer complex in a host. *Angew. Chem., Int. Ed.* **2002,** *41,* 4474-4476.
102. Jiao, D.; Geng, J.; Loh, X. J.; Das, D.; Lee, T-C.; Scherman, O. A. Supramolecular peptide amphiphile vesicles through host–guest complexation. *Angew. Chem., Int. Ed.* **2012,** *51,* 9633-9637.
103. Loh, X, J.; Barrio, J. d.; Lee, T. C.; Scherman, O. A. Supramolecular polymeric peptide amphiphile vesicles for the encapsulation of basic fibroblast growth factor. *Chem. Commun.* **2014**, *50*, 3033-3035.
104. Yang, L.; Yang, H.; Li, F.; Zhang, X. Supramolecular Glycolipid Based on Host-Enhanced Charge Transfer Interaction. *Langmuir* **2013**, *29*, 12375-12379.
105. Krieg, M.; Pileni, M-P.; Braun, A. M.; Gratzel. M. Micelle formation and surface activity of functional redox relays: viologens substituted by a long alkyl chain. *J. Colloid Interface Sci.* **1981**, *83*, 209-213.
106. Bae, I. T.; Huang, H.E.; Yeager, B.; Scherson, D. A. In situ infrared spectroscopic studies of redox active self-assembled monolayers on gold electrode surfaces. *Langmuir* **1991**, *7*, 1558-1562.
107. Li, J.; Kaifer, A. E.Surfactant monolayers on electrode surfaces: self-assembly of a viologen derivative having a cholesteryl hydrophobic residue. *Langmuir* **1993**, *9*, 591-596.
108. Lei, Y.; Hurst, J. K. Reduction potentials of vesicle-bound viologens. *J. Phys. Chem.* **1991,** *95,* 7918-7925.
109. Moulik, S. P.; Haque, Md. E.; Jana, A. R.; Das, P. K.; Micellar Properties of Cationic Surfactants in Pure and Mixed States. *J. Phys. Chem.* **1996**, *100*, 701-708.
110. McGrath, K. M. Phase Behavior of Dodecyltrimethylammonium Bromide/Water Mixtures. *Langmuir* **1995**, *11*, 1835-1839.
111. Rosen, M. J.; Dahanayake, M. *Industrial Utilization of Surfactants, Principles and Practice*; AOCS Press: Champaign, IL, 2000; pp 28-29.
112. Clint, J. H. Micellization of mixed nonionic surface active agents. *J. Chem. Soc., Faraday Trans.* **1975**, *171,* 1327-1334.
113. Rubingh, D. N. *Solution Chemistry of Surfactants*; *Vol. 1*; Mittal, K. L. Ed. Plenum: New York, **1979**, p 337.
114. Motomura, K.; Yamanku, M.; Aratono, M. Thermodynamic consideration of the mixed micelle of surfactants. *Colloid Polym. Sci.* **1984**, *262*, 948-955.
115. Sarmoria, C.; Puvvada, S.; Blankschtein, D. Prediction of critical micelle concentrations of nonideal binary surfactant mixtures. *Langmuir* **1992**, *8*, 2690-2697.
116. Puvvada, S.; Blankschtein, D. Theoretical and experimental investigations of micellar properties of aqueous solutions containing binary mixtures of nonionic surfactants. *J. Phys. Chem*. **1992**, *96*, 5579-5592.
117. Haque, M. E.; Das, A. R.; Rakshit, A. K.; Moulik, S. P. Properties of Mixed Micelles of Binary Surfactant Combinations. *Langmuir* **1996**, *12,* 4084-4089.
118. D'Errico, G.; Ortona, O.; Paduano, L.; Tedeschi, A.; Vitagliano, V. Mixed micellar aggregates of cationic and nonionic surfactants with short hydrophobic tails. An intra diffusion study. *Phys. Chem. Chem. Phys.* **2002***, 4,* 5317-5324.
119. Chakraborty, T.; Ghosh, S.; Moulik, S. P. Micellization and Related Behavior of Binary and Ternary Surfactant Mixtures in Aqueous Medium: CetylPyridinium Chloride (CPC), CetylTrimethyl Ammonium Bromide (CTAB), and Polyoxyethylene (10) Cetyl Ether (Brij-56) Derived System *J. Phys. Chem. B* **2005**, *109*, 14813-14823.

120. Alami, E.; Beinert, G.; Marie, P.; Zana, R. Alkanediyl-.alpha, omega.-bis(dimethylalkylammonium bromide) surfactants. Behavior at the air-water interface. *Langmiur* **1993**, *9*, 1465-1467.
121. Moulik, S. P.; Ghosh, S. Surface Chemical and micellization behaviours of binary and ternary mixtures of amphiphiles (Triton X-100, Tween-80 and CTAB) in aqueous medium. *J. Mol. Liq*. **1997**, *72*, 145-161.
122. Zana, R.; Yiv, S.; Strazielle, C.; Lianos, P. Effect of alcohol on the properties of micellar systems: I. Critical micellization concentration, micelle molecular weight and ionization degree, and solubility of alcohols in micellar solutions. *J. Colloid Interface Sci.* **1981**, *80*, 208-223.
123. Israelachvili, J. N. *Intermolecular and Surface Forces, 2nd ed;* Academic Press: London, **1991**; Chapter 17, p 370.
124. Tanford, C. *The Hydrophobic Effect: Formation of Micelles and Biological Membranes*; Wiley and Sons: New York, **1980**.
125. Mahajan, S.; Sharma, R.; Mahajan, R. K. An Investigation of Drug Binding Ability of a Surface Active Ionic Liquid: Micellization, Electrochemical, and Spectroscopic Studies. *Langmuir* **2012**, *28*, 17238-17246.
126. Das, D.; Roy, S.; Mitra, R. N.; Dasgupta, A.; Das, P. K. Head-Group Size or Hydrophilicity of Surfactants: The Major Regulator of Lipase Activity in Cationic Water-in-Oil Microemulsions. *Chem. Eur. J.* **2005**, *11,* 4881-4889.
127. Kim, H.-J.; Woo, S. J.; Young, H. K.; Kim, K. Inclusion of methylviologen in cucurbit[7]uril. *Proc. Nat. Acad. Sci. USA* **2002**, *99*, 5007-5011.
128. Diaz, A.; Quintela, P. A.; Schuette, J. M.; Kaifer, A. E. Complexation of redox-active surfactants by cyclodextrins. *J. Phys. Chem.* **1988,** *92,* 3537-3542.
129. J. H. Fendler, Interactions and reactions in reversed micellar systems. *Acc. Chem. Res.* **1976**, *9*, 153-161.
130. Correa, N. M.; Silber, J. J.; Riter, R. E.; Levinger, N. E. Nonaqueous Polar Solvents in Reverse Micelle Systems. *Chem. Rev*. **2012,** *112,* 4569–4602.
131. de Borba, E. B.; Amaral, C. L. C.; Politi, M. J.; Villalobos, R.; Baptista, M. S. Photophysical and Photochemical Properties of Pyranine/Methyl Viologen Complexes in Solution and in Supramolecular Aggregates: A Switchable Complex. *Langmuir* **2000**, *16*, 5900-5907.
132. Harris, C.; Kamat, P. V. Photocatalytic Events of CdSe Quantum Dots in Confined Media. Electrodic Behavior of Coupled Platinum Nanoparticles. *ACS Nano* **2010**, *4*, 7321-7330.
133. Dasgupta, A.; Das, D.; Mitra, R. N.; Das, P. K. Surfactant tail length-dependent lipase activity profile in cationic water-in-oil microemulsions. *J. Colloid Interface Sci.* **2005**, *289,* 566–573.
134. Mondal, J. H.; Ahmed, S.; Das, D. Physicochemical Analysis of Mixed Micelles of a Viologen Surfactant: Extended to Water-in-Oil (w/o) Microemulsion, and Cucurbit[8]uril Assisted Vesicle Formation. Langmuir 2014, 30, 8290−8299.
135. Zayed, J. M.; Biedermann, F.; Rauwald, U.; Scherman, O. A. Probing Cucurbit[8]uril-Mediated Supramolecular Block Copolymer Assembly in Water Using Diffusion NMR. Polym. Chem. 2010, 1, 1434−1436.
136. Zana, R.; Kaler, E. Giant Micelles: Properties and Applications; Taylor & Francis: London, 2007.
137. Rodrigues, R. K.; Ito, T. H.; Sabadini, E. Thermal-Stability of Mixed Giant Micelles of Alkyltrimethylammonium Surfactants and Salicylate. J. Colloid Interface Sci. 2011, 364, 407−412.
138. Mukhopadhyay, P.; Wu, A.-X.; Isaacs, L. Social Self-Sorting in Aqueous Solution. *J. Org. Chem*. **2004**, *69*, 6157 – 6164.
139. Jiang, W.; Wang, Q.; Linder, I.; Klautzsch, F.; Schalley, C. A. Self-Sorting of Water-Soluble Cucurbituril Pseudorotaxane. Chem. Eur. J. 2011, 17, 2344 – 2348.
140. Zhou, S.; Burger, C.; Chu, B.; Sawamura, M.; Nagahama, N.; Toganoh, M.; Hackler, U. E.; Isobe, H.; Nakamura, E. Spherical Bilayer Vesicles of Fullerene-Based Surfactants in Water: A Laser Light Scattering Study. *Science*, **2001**, *291*, 1944-1947.
141. Zhang, X.; Rehm, S.; Safont-Sempere, M. M.; Wurthner, F. Vesicular perylene dye nanocapsules as supramolecular fluorescent pH sensor systems. *Nat. Chem*., **2009**, *1*, 623-629.
142. Vriezema, D. M.; M. Aragones, C.; Elemans, J. A. A. W.; J. J. L. M. Cornelissen, Rowan, A. E.; Nolte, R. J. M. Self-Assembled Nanoreactors. *Chem. Rev*., **2005**, *105*, 1445-1490.
143. Checot, F.; Lecommandoux, S.; Gnanou, Y.; Klok, H.-A. Water-Soluble Stimuli-Responsive Vesicles from Peptide-Based Diblock Copolymers. *Angew. Chem., Int. Ed*., **2002**, *41*, 1339-1343.
144. Zhu, J.; Munn, R. J.; Nantz, M. H. Self-Cleaving Ortho Ester Lipids: A New Class of pH-Vulnerable Amphiphiles. *J. Am. Chem. Soc*., **2000**, *122*, 2645-2646.
145. Guo, X.; Szoka, F. C. Chemical Approaches to Triggerable Lipid Vesicles for Drug and Gene Delivery *Acc. Chem. Res*., **2003**, *36*, 335-341.
146. Johnsson, M.; Wagenaar, A.; Engberts, J. B. F. N. Sugar-Based Gemini Surfactant with a Vesicle-to-Micelle Transition at Acidic pH and a Reversible Vesicle Flocculation near Neutral pH. *J. Am. Chem. Soc*., **2003**, *125*, 757-760.

147. Lee, M.; Lee, S.-J.; Jiang, L.-H. Stimuli-Responsive Supramolecular Nanocapsules from Amphiphilic Calixarene Assembly. *J. Am. Chem. Soc*., **2004**, *126*, 12724-12725.
148. Wang, K.; Guo, D-S.; Wang, X.; Liu, Y. Multistimuli Responsive Supramolecular Vesicles Based on the Recognition of p-Sulfonatocalixarene and its Controllable Release of Doxorubicin. *ACS Nano*, **2011**, *5*, 2880-2894.
149. Bigot, J.; Charleux, B.; Cooke, G.; Delattre, F.; Fournier, D.; Lyskawa, J.; Sambe, L.; Stoffelbach, F.; Woisel, P. J. Tetrathiafulvalene End-Functionalized Poly(N-isopropylacrylamide): A New Class of Amphiphilic Polymer for the Creation of Multistimuli Responsive Micelles. *J. Am. Chem. Soc*., **2010**, *132*, 10796-10801.
150. Deng, Y.; Wang, C.; Shen, X.; Yang, W.; Jin, L.; Gao, H.; Fu, S. Preparation, Characterization, and Application of Multistimuli-Responsive Microspheres with Fluorescence-Labeled Magnetic Cores and Thermoresponsive Shells. *Chem.—Eur. J*., **2005**, *11*, 6006-6013.

List of Publication

05. Julfikar Hassan Mondal, Sahnawaz Ahmed, Titli Ghosh, Debapratim Das, Multistimuli Responsive Vesicle of a Supramolecular Peptide Amphiphile using Cucurbit[8]uril. *(Communicated)*

04. Julfikar Hassan Mondal, Titli Ghosh, Sahnawaz Ahmed, Debapratim Das, *Dual Self-sorting by Cucurbit[8]uril to Transform a Mixed Micelle to Vesicle*. *Langmuir* **2014**, *30, 11528-11534.*

03. Julfikar Hassan Mondal, Sahnawaz Ahmed, Debapratim Das, *Physicochemical Analysis of Mixed Micelles of a Viologen Surfactant: Extended to Water-in-oil (w/o) Microemulsion, and Cucurbit[8]uril Assisted Vesicle Formation*. *Langmuir* **2014**, *30*, 8290-8299.

02. Sahnawaz Ahmed, Julfikar Hassan Mondal, Nibedita Behera, Debapratim Das, *Self-assembly of a Peptide-Amphiphile Forming Helical Nano-fibres and in-situ Template Synthesis of Uniform Mesoporous Single Wall Silica Nano-tubes*. *Langmuir* **2013**, *29*, 14274–14283.

01. Antara Dasgupta, Julfikar Hassan Mondal, Debapratim Das, *Peptide Hydrogels*. *RSC Advances* **2013**, *3*, 9117-9149.